THE ANALYSIS OF ALBEDO ON BIOENERGY CROPS: ASSESSMENT FOR CLIMATE AND GLOBAL WARMING IMPACT

By

Cheyenne India Lei

A DISSERTATION

Submitted to
Michigan State University
in partial fulfillment of the requirements
for the degree of

Geography—Doctor of Philosophy

2022

ABSTRACT

THE ANALYSIS OF ALBEDO ON BIOENERGY CROPS: ASSESSMENT FOR CLIMATE AND GLOBAL WARMING IMPACT

By

Cheyenne India Lei

What if the production and expansion of bioenergy crops was realized? What bioenergy crops would be planted? Which crops would be sustainable? How would bioenergy affect landscape dynamics, surface reflectivity and global warming impact? These core questions are investigated in this dissertation by investigating the effects of agronomic practices, climate and crop-species on albedo in southwest Michigan.

Albedo changes can be quantified in terms of global radiative forcing (RF), which can be positive or negative, correlating to carbon emissions or sequestrations in biofuel ecosystems respectively. With an overarching hypothesis which aims to understand how albedo is dependent on the landscape (i.e., crop-species type), climate variables (i.e., micrometeorological, temporal, and seasonal) and agricultural practices (i.e., fertilization, stover retention), which in turn affect its global warming impact and the ability to reflect more sunlight back into the atmosphere and sequester carbon. As a result, the Kellogg Biological Station was selected as the study site.

This research analyzes changes in albedo over seven different biofuel crops at the Biofuel Cropping System Experiment (BCSE), situated at the Great Lakes Bioenergy Research Center (GLBRC). This dissertation investigates the radiative forcing associated with each one of the bioenergy scenarios, in order to model the conversion of a landscape into a relatable carbon dioxide equivalent. This CO_2 equivalent – called global warming impact (GWI) – allows for a climate impact comparison of potential global warming impact of CO_2 emissions from biofuels relative to

a reference gas to investigate potential climate warming/cool impacts. This research examined annual row crops of maize and energy sorghum, monoculture perennial grasses of switchgrass and miscanthus, and polyculture perennials of native grasses, early successional grassland and restored prairie bioenergy systems. Each chapter provides a deeper analysis into the spatiotemporal effects of surface reflectivity on biofuel ecosystems and provides an understanding of the total global warming impact of different croplands and their contribution to the energy budget and carbon production.

Results of this research include: 1) a long-term network of towers which effectively measure albedo continuously over multiple biofuel ecosystems, and 2) regionalized instantaneous data from landscapes of candidate bioenergy crops to significantly advance knowledge and understanding in how surface reflectivity affects GWI.

Major findings indicated that albedo observations are an invaluable tool in order to calculate and improve climate models, in order to understand how land use and land cover affects albedo and climate cooling. Perennial grasses provided a sustainable form of climate mitigation by reflecting more solar radiation back into the atmosphere, and can sustainability provide localized cooling while reducing the need for fertilizer input. Finally, an overall cooling effect from modeling the conversion of historical landscape forest and modern landscapes of maize over a three-year study period to candidate different bioenergy crops was found, which indicated a climate warming mitigation from long-term increased surface albedo reflectance.

ACKNOWLEDGEMENTS

My academic journey has been full of people who have helped me achieve this momentous occasion. Firstly, I must thank my advisor Jiquan Chen who took a chance on an unconventional scholar. Jiquan was tough, rigorous and demanding, but also supportive, encouraging and trusting, allowing me to venture out on my own and create a network of sites dedicated to measuring climate, and with strong mentorship, helped me mature into a strong scientist and academic scholar. I also thank Philip Robertson, Lifeng Luo and Joseph Messina for serving on my dissertation committee. I am thankful to them for ensuring the quality of my Ph.D. education through expanding my knowledge in ecology, geography, atmospheric physics, modeling and being available for Zoom meetings when the pandemic pressed everyone to new spaces.

I would also like to thank the department of Department of Geography, Environment & Spatial Sciences and Center for Global Change & Earth Observations for their support during my academic career. I also give a special thanks to Sharon Ruggles and Jean Lepard, who have both been integral in kept the cogs turning smoothly and guided me on my track within my program.

I am incredibly grateful for my colleagues who have stood by me this entire period. I am appreciative of the friendships from Cristina Gauthier, Shengpan Lin, Gabriela Shirkey, Piero Sciusco, Michael Abraha, Jing Yuan, Dong Liu, Shenghua Gao, Maowei Liang, William Baule, and Amanda Kreuze. We spent much time collaborating, problem solving, and engaging in scholarly research, but I will not forget the days we played basketball, swam at IM West Fitness Center, went camping, gathered around a hotpot but most importantly, kept each other accountable to ensure we all moved forward in our careers. I also thank my colleagues from the Landscape Ecology & Ecosystem Science Lab, and the research personnel and technicians at the W.K.

Kellogg Biological Station whose presence have been essential in helping ensure my research went efficiently. I also acknowledge the Dahlin Lab who allowed easy cross collaborations and great scientific discussions.

Many thanks to the departments at Michigan State University including the Graduate College, College of Social Science, Department of Geography, Environment & Spatial Sciences and the W.K. Kellogg Biological Station for providing me with funding to complete my research. Without the help from fellowships, assistantships, grants, research awards and dissertation completion fellowships, my work would have been much more difficult.

Zero Alliance in State 189 from State of Survival, I see you. Thanks for your support during this time, the friendships made I hope last a lifetime.

Finally, there have been many adversities which I have struggled through in my journey. My inmost moment came when I tore my shoulder in November 2020. During this critical time in my Ph.D. career, I found myself struggling to perform basic tasks, and many times doubted if I would ever reach the end of my journey. I thank my husband Ming Lei who kept me grounded through my frustrations and pushed me to do what I could in small steps. You worked as volunteer during my fieldwork within the LEES Lab, I can’t thank you enough for being tall enough to help raise the towers or haul an extra car battery. You kept me in high spirits when the days were long. I cannot convey how much it has meant to me having your love, patience, and support during this journey.

TABLE OF CONTENTS

LIST OF TABLES

LIST OF FIGURES

KEY TO ABBREVIATIONS

α_s	Albedo
Δ_α	delta Albedo
T_a	Upwelling Transmittance
AFOLU	Fossil fuel and industry, Agriculture, Forestry and Other Land use
ANOVA	Analysis of Variance
asl	above sea level
DOY	Day of Year
BECCS	Bioenergy with Carbon Capture and Storage
BCSE	Biofuel Cropping System Experiment
CCS	Carbon Capture and Storage
CO_2	Carbon Dioxide
CO_2e	Carbon Dioxide equivalent
CSI	Campbell Scientific Inc
ES	Early Successional grassland
F	Fertilized treatment
ft	feet
GS	Growing Season
GLBRC	Great Lakes Bioenergy Research Center
GWI	Global Warming Impact
IPCC	Intergovernmental Panel on Climate Change
IQR	Interquartile Range

KBS	W.K. Kellogg Biological Station
KEF	W.K. Kellogg Experimental Forest
kg/ha	kilogram per hectare
LPR	local polynomial regression
MAI	Maize
MIS	Miscanthus
m	meter
Mg/ha	Mega grams per hectare
N	Nitrogen
NF	Non-fertilized treatment
NG	Native Grasses
NGS	Non-Growing Season
NOAA	National Oceanic and Atmospheric Administration
NS	Stover removal treatment
PR	Restored Prairie
R	R Development Team Software
RF	Radiative Forcing
S	Stover retention treatment
SCS	Soil Carbon Storage
SD	Standard Deviation
SE	Standard Error
SOR	Sorghum
SW	Switchgrass

TH	Time Horizon
TOA	Top of Atmosphere
W/m^2	watts per meter square

CHAPTER 1. INTRODUCTION

General Introduction

Changes in surface reflectivity can affect the atmosphere's ability to warm or cool itself efficiently (Bonan, 2008; Burakowski et al., 2018). These changes are often the result of complex with biogeophysical (e.g., temperature, plant phenology, land dynamics, climate) and biogeochemical (e.g., GHG emissions of CO_2, N_2O, CH_4, water availability, field operation emissions, radiation) factors.

One important biogeophysical factor is albedo. Defined as surface reflectance, albedo has been closely analyzed in current policy as potentially increasing the solar reflectivity of different land surfaces can impact the amount of solar radiation being reflected back to space, thus altering the energy balance at the top-of-atmosphere (TOA). It is theorized that surface reflectance of incoming radiation can change the Earth's radiative balance, with positive radiative forcings (induced by a decrease in albedo) corresponding to carbon emissions, while negative radiative forcings correspond to carbon accrual and sequestration within an ecosystem (Caiazzo et al., 2014).

Albedo can be affected by multiple factors, including type of vegetation (e.g., perennial crops, annual row crops, forest, arid grasslands), type of agronomic management practices (e.g., tillage, fertilization, cover crops, residue retention), as well as human disturbances (e.g., urban expansion) where increasing albedo can reduce summertime temperatures, create better air quality, and reduce fossil fuel demand (Akbari, 2009; Robertson et al., 2015, Lei et al., 2021). Studies have found that a global increase of just 0.01 in albedo can create an average radiative forcing change of -1.27 W m^{-2} (Akbari, 2009), which can provide cooling effects by increasing the total outgoing radiation. While efforts have been made to understand the climate impacts of albedo, results from existing studies are limited.

Humans altered surface reflectivity through anthropogenic activities including population growth, globalization, deforestation, agriculture, and the greater need for food and fuels (Vitousek et al., 1997). The consumption of fossil fuels adds carbon to the atmosphere, while livestock rearing and production have led to higher releases methane into the atmosphere. These can both affect the amount of incoming solar radiation received at the surface, and the amount of radiation trapped by greenhouse gases. In the United States Midwest, conversions from native perennial grasses into annual row crops such as maize have occurred in vast quantities since the 1800s (Bonan, 1997; Ramankutty et al., 2008). Between 1982 and 1997, there was a 34% increase in the amount of rural landscapes (e.g., marginal lands, forested regions, grasslands) transformed into (Alig et al., 2004). Forests have been the largest source of land converted into another landscape in recent decades, which has impacted forest cover and ecological diversity. This has become a critical point, as forests have higher albedo than bare ground soil and urban areas, where afforestation can increase planetary albedo and provide a cooling effect on the planet (Duveiller et al., 2021). As such, changes in surface albedo can drastically affect all components and partitions of the energy balance. Vegetation plays a key role in the exchange of latent heat fluxes, as well as the energy and water balances of the Earth. Vegetation and forests are efficient at intercepting incoming radiation by absorption for photosynthesis or reflection back into the atmosphere. Plant vegetative factors including leaf area index, vegetative growth, plant texture, leaf canopies, leaf texture, leaf age, and root dynamics (e.g., root depth, CO_2 uptake capacity) (Betts, 2001; Monteith, 1959; Hartmann, 1994; Henderson-Sellers & Wilson, 1983) can vary between different crop ecosystems (i.e., forest, perennial crops, annual crops, grassland), and can consequently affect changes in surface reflectivity. This change in radiative forcing affects the amount of energy available at the surface for non-radiative fluxes such as evaporation, transpiration, and evapotranspiration to occur (Robertson et al., 2013; Sellers et al., 1997; Senay et al., 2015; Waring, 2007). Canopies with high concentrations of nitrogen in leaves, stems and roots absorb more incoming shortwave radiation (Ollinger et al., 2008) compared to low-nitrogen plants. Vegetative leaves also have complex geometries and textures, which affect how radiation is absorbed or reflected, and subsequently the amount of albedo of single stalks and leaves. Climatic and temporal changes in the vegetation-dependent parameters of croplands over growing seasons (i.e., bare-ground, seeding, vegetative, senescence and harvest) can also alter surface-induced albedo over local to regional scales. Agricultural regions are subject to substantial local to global climate changes, as agricultural land management can alter the surface energy balance and influence temperatures. For example, the 'Dust Bowl' of the 1930's was created by inappropriate management of agricultural lands within the United States that altered the hydrology, climate, and vegetation. Cover crop adaptation can also change the land-induced albedo by providing a localized warming/cooling climate effect (i.e., changes in cloud formation, precipitation, and evapotranspiration), breaking up snowpack and providing opportunity for increased organic carbon accumulation within the soil (Lugato et al., 2020). As the type of land cover can alter surface reflectivity, diversification of the agricultural sector may help balance the effects of vegetation on local to regional climate. In the United States, the most prominent biofuel crops have been lignocellulosic perennial grasses, such as *Panicum Virgatum* (switchgrass) and *Miscanthus × Giganteus* (miscanthus) (Heaton, 2004; 2010), though annual row crops of *Zea mays L*. (maize) is still commonplace. Annual row crops such as maize require substantial fertilizer, herbicides, and pesticides to thrive, which can be detrimental to the environment. As a result, recent studies have exampled how other native, sustainable biofuel crops such as switchgrass, early successional grasses, and native grasses can generate bioenergy and sustainable biofuel crop production without the negative impacts to the economy or the environment.

The Intergovernmental Panel on Climate Change (IPCC) AR4 and AR5 reports have acknowledged the necessity in developing sustainable agronomic practices which can mitigate GHG emissions (Flato et al., 2013). Some major land-based strategies have included afforestation/reforestation, soil carbon sequestration (Caiazzo et al., 2014), biochar addition (Meyer et al., 2012) and upgraded agricultural practices (Robertson & Hamilton, 2015), which take key components of carbon capture and storage (CCS), soil carbon storage (SCS) fossil fuel and industry, agriculture, forestry and other land use (AFOLU), and bioenergy with carbon capture and storage (BECCS) into primary consideration (Haszeldine et al., 2018; Smith, 2016). BCCES has been widely viewed as offering the most promise for sequestering CO_2 from the atmosphere. Biomass is converted into heat, electricity, or fuels, while the carbon emissions from this bioenergy conversion are captured and stored in the plants, roots and soil. However, it is crucial that carbon emissions from the agronomic practices that grow, harvest, transport, and process the biomass do not offset the carbon that is sequestered. Research has shown that converting farming practices from conventional tilling to conservational no-tilling can improve carbon sequestration in soils (Robertson et al., 2017), allowing for deeper and more comprehensive root growth structures in perennial crops (Betts et al., 2001), and reducing soil and nutrient erosion (Odum, 1984). This can affect surface-induced albedo through the use of cover crops and residue management, which cover bare ground topsoil and reflects more radiation (Luyssaert et al., 2014; Odum, 1984). Soil moisture and stover from tilling practices can also affect the amount of albedo reflected from different grasslands and croplands (Campbell & Norman, 2012; Davin et al., 2014).

The purpose of this research was to investigate how surface reflectivity affects the global warming impact of biofuel ecosystems. The goal was to develop an understanding of how albedo is related to landscape (e.g., crop species), climate variables (e.g., micrometeorological, temporal, and seasonal) and agronomic practices (e.g., tilling, fertilization, stover removal, planting density, seeding dates), and to better understand how these factors affect the ability to reflect more sunlight back into the atmosphere and mitigate climate warming.

Study Area

The W.K. Kellogg Biological Station (KBS) is Michigan State University's largest off-campus field research station (42° 24′ N 85° 24′ W, 288 m asl). This site is sixty-five miles from the main campus in Augusta, Michigan. KBS encompasses approximately 1600 hectares of cropping systems, small lakes, wetlands and includes sites such as the W.K. Kellogg Bird Sanctuary, W.K. Kellogg Farm, KBS Academic and Research Facilities, W.K. Kellogg Conference Center and Manor House, and Lux Arbor Reserve. The nearby W.K. Kellogg Experimental Forest is also closely affiliated with KBS. The climate consists of humid continental temperate with a 30-year (1981–2010) average annual air temperature of 9.9°C and average annual precipitation of 1027 mm (NCDC, 2013).

Land surveys taken from the United States Survey Field Notes ranging back to the 1900’s suggest that the area surrounding the Kellogg Biological Station comprised predominantly of oak savanna, described as a lightly forested grassland. However, forest cover has declined since then to its current acreage due to the increasing use of wood as a fuel source during the 1930’s. Land usage around the Kellogg Biological Station consists of rural farmlands, to forested regions, to two urban regions (Battle Creek: population of 51,000; Kalamazoo: population of 335,000) (Bolter et al., 2019; Dickason et al., 1995). The physical geography on which KBS resides is made up of a mature glacial outwash plain and moraine complex, which consists of fine-loamy, mixed, mesic Typic Hapludalfs soils (Muñoz & Kravchenko, 2011; Thoen, 1990).

The Kellogg Biological Station is home to one of the National Science Foundation's Long-Term Ecological Research (LTER) programs. Established in 1988, the program focuses on the conservation of natural resources and sustainable agriculture research through the integration of long-term scientific research, education, and public engagement. As part of one of the long-term research initiatives, the Great Lakes Bioenergy Research Center (GLBRC) Biofuel Cropping System Experiment (BCSE, http://glbrc.org/) was established in 2008 to establish a research site for investigating the performance of potential bioenergy cropping systems, comparing alternative agronomic practices, and modeling changes in climate-environmental interactions such as climate, greenhouse gases and biodiversity.

Measurements & Methodology

Overview

Data collection was conducted at the Great Lakes Bioenergy Research Center (GLBRC) Biofuel Cropping System Experiment (BCSE) from May 2018 to December 2020. Current cropping systems at the study site include three annual row crops: continuous maize with stover removal (*Zea mays L*, G1), continuous energy sorghum (*photoperiod-sensitive hybrid ES5200*, G2), energy sorghum (*photoperiod insensitive hybrid TAM 17900*, G3), and six perennial crops: switchgrass (*Panicum virgatum* variety Cave-in-rock, G5), miscanthus (*Miscanthus x giganteus*, G6), native grasses (a mix of 4 species; G7), hybrid poplar ("NM-6" *Populus nigra x Populus maximowiczii*, G8), early successional grassland (G9), and restored prairie (G10). These crops were cultivated at KBS as candidate crops for future bioenergy research and expansion.

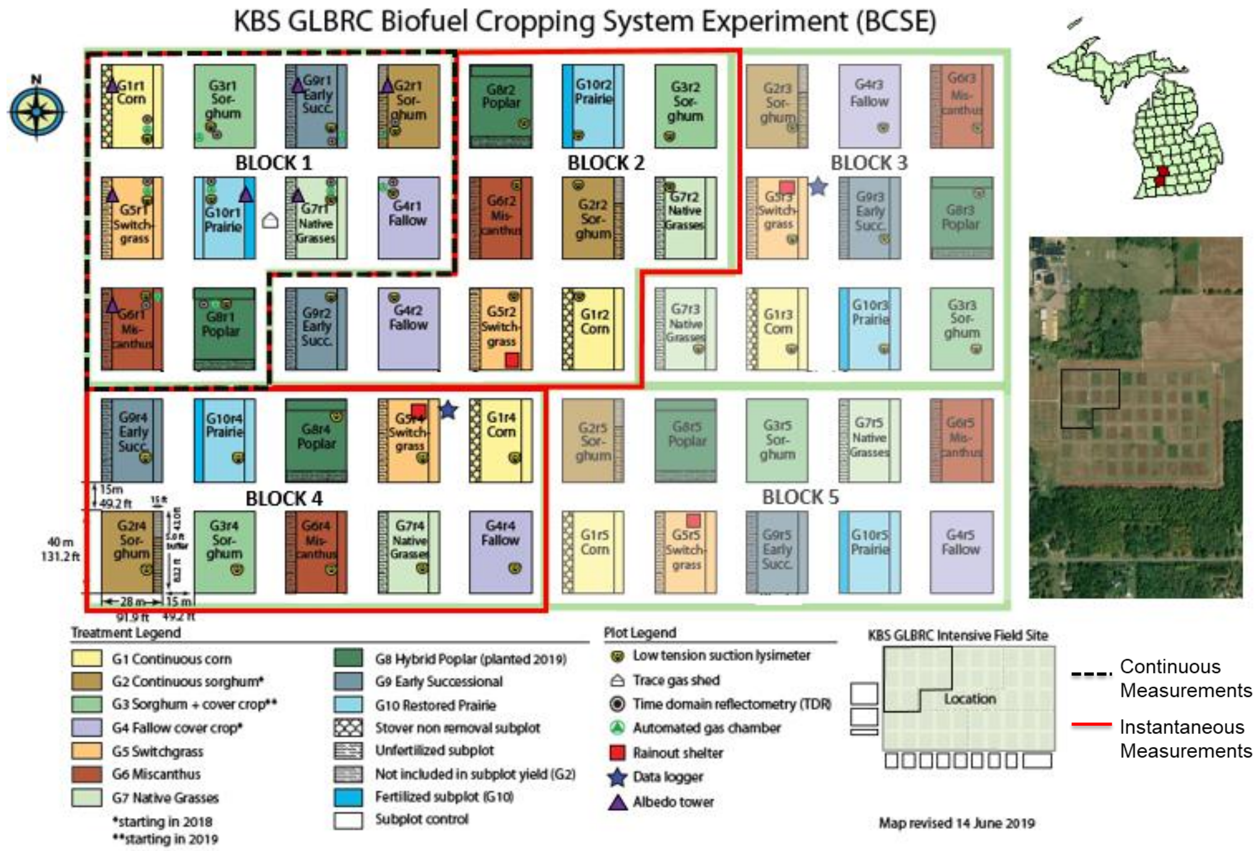

Figure 1.1: Current KBS GLBRC Biofuel Cropping System Experiment Map. Albedo towers are labelled with a purple triangle and situated in Block 1. Instantaneous measurements are taken from Block 1, 2 and 4. Continuous measurements are shown in a black dotted line, while instantaneous measurements are shown in a solid red line. See https://lter.kbs.msu.edu for more information on its long-term experiment.

This experiment was designed to quantify, through direct measurements at the land surface, the temporal changes of albedo in six biofuel crops: as well as reference sites of maize and forest. Thus, this research focused on the following crops: annual row crops of maize (G1) and energy sorghum (G3), monoculture perennials of switchgrass (G5) and miscanthus (G6), and polyculture perennials of native grasses (G7), early successional grasses (G9), and restored prairie (G10) at Blocks 1, 2 and 4 respectively (Figure 1.1). Values for growing season (GS), non-growing season (NGS), and annually were calculated each year. The growing season was defined as May through

October (DOY of 121-304) following previous studies completed at the University of Illinois Energy Farm and Southwest Michigan on the similar biofuel species (Sciusco et al., 2020; Zeri et al., 2011), while non-growing season included winter periods, and all other days not defined as a growing period. Measurements were performed using sensors mounted on a micrometeorological tower to gather continuous data upon the surface, and survey measurements were formed to collect instantaneous data observations using handheld sensors and devices.

Continuous measurements

The installation of micrometeorological climate towers on seven different bioenergy crops was completed late April 2018 and is currently ongoing at the Biofuel Cropping System Experiment (BCSE) site (Figure 1.2; Figure A1). Each tower was installed in perennials crops of switchgrass, miscanthus, native grasses, early successional and restored prairie, and annual row crops of maize and sorghum. All towers used a tripod design to ensure minimum footprint and allow the crops to grow uninhibited around the tower, anchored to the ground using 12-inch ground screwed and three bungie cables. Each tower was grounded using an antenna and grounding rod, and powered using a Duracell Ultra 12V 14AH Deep Cycle AGM SLA Battery (summer) or Duralast 29DP-DL Deep Cycle Marine Battery (winter), as well as a Solartech Power 10Watt Polycrystalline Solar Panel.

Each tripod was equipped with the following sensors: a single four-component net radiometer (SN-500, Apogee Instruments, Utah, USA) to measure shortwave and longwave incoming and outgoing radiation, two net radiometers (Q.7.1, REBS, USA) to measure net radiation of different treatments, a single soil water content reflectometer (CS616, Campbell Scientific Inc., Logan, UT, USA) to measure soil moisture content. One tower was also equipped with a precipitation gauge (TE525, CSI) to measure rainfall events, and a temperature sensor to measure air temperature and relative humidity (HMP 60, CSI). All sensors were attached to a 10-foot-long horizontal bar, with the exception of the CS616, which was installed vertically into the soil profile. In the case of maize and restored prairie, an additional a four-component net radiometer (CNR4, Kipp & Zonen, Netherlands) to measure solar and infrared radiation, and a ClimaVUE50: Compact Digital Weather Sensor meteorological sensor to measure air temperature, relative humidity, vapor pressure, baro-metric pressure, wind (speed, gust, and direction), solar radiation, precipitation were installed.

All data were logged at 10-Hz using a datalogger (Campbell Scientific Inc., Logan, UT, USA) at 5-minute intervals during the summer, and 30-minute intervals during the winter months (November-March). The height of the towers in each plot were changed over the course of the growing season and study period in order to maintain a consistent footprint (Figure A2).

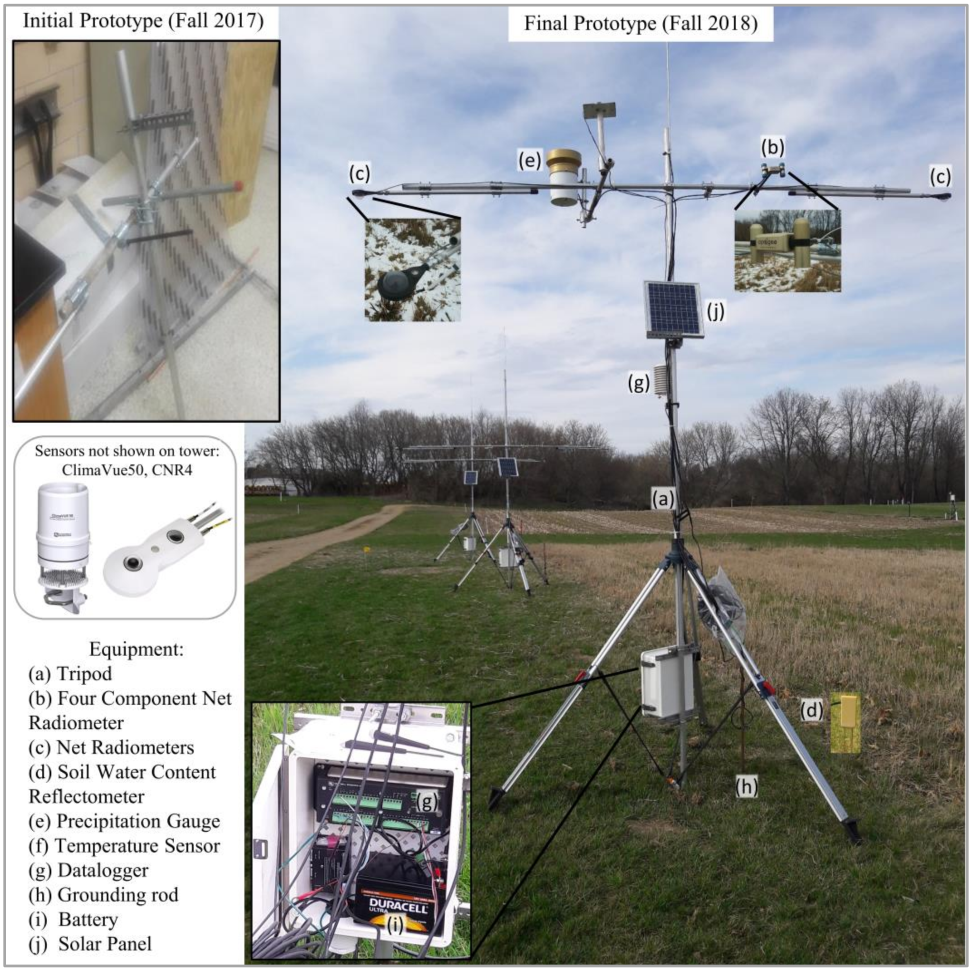

Figure 1.2: Images depicting the research prototype from October 2017 to April 2018 (left) and final tower installation for continuous measurements in late April 2018 (right). Towers shown here are for miscanthus, switchgrass and maize sites at the Biofuel Cropping System Experiment. Image inset shows the waterproof fiberglass enclosure with a datalogger powered by a solar controller and battery.

An additional eddy covariance tower was also installed at the Kellogg Experimental Forest (KEF) (42.365961°N, 85.352615°W) in the summer of 2018 and used as a reference landscape (Figure 1.3). The data collected by this tower was intended to fill the gap in the prior research of climate assessments that overlook forests, which represent the historical landscape of Michigan. Established on abandoned agricultural land, the Kellogg Experimental Forest is comprised of spruce, maples, pine and oak trees as the current dominant species. At the Kellogg Experimental Forest, the eddy covariance tower, the site was located 33 meters (110 feet) above the ground surface, 6 meters (20 feet) above the forest canopy and is equipped with similar sensors as the BCSE sites, including a four-component net radiometer (CNR4, Kipp & Zonen, Netherlands), two precipitation gauges (TE525), one soil water content reflectometer (CS616, Campbell Scientific Inc., Logan, UT, USA), two temperature sensors to measure air temperature and relative humidity (HMP 60, CSI), three Soil Heat Flux plates (HTF3, REBS, USA), and an IRGASON (Campbell Scientific Inc., Logan, UT, USA). All data were logged at 10-Hz using a datalogger (CSI) and stored as 30-minute averages.

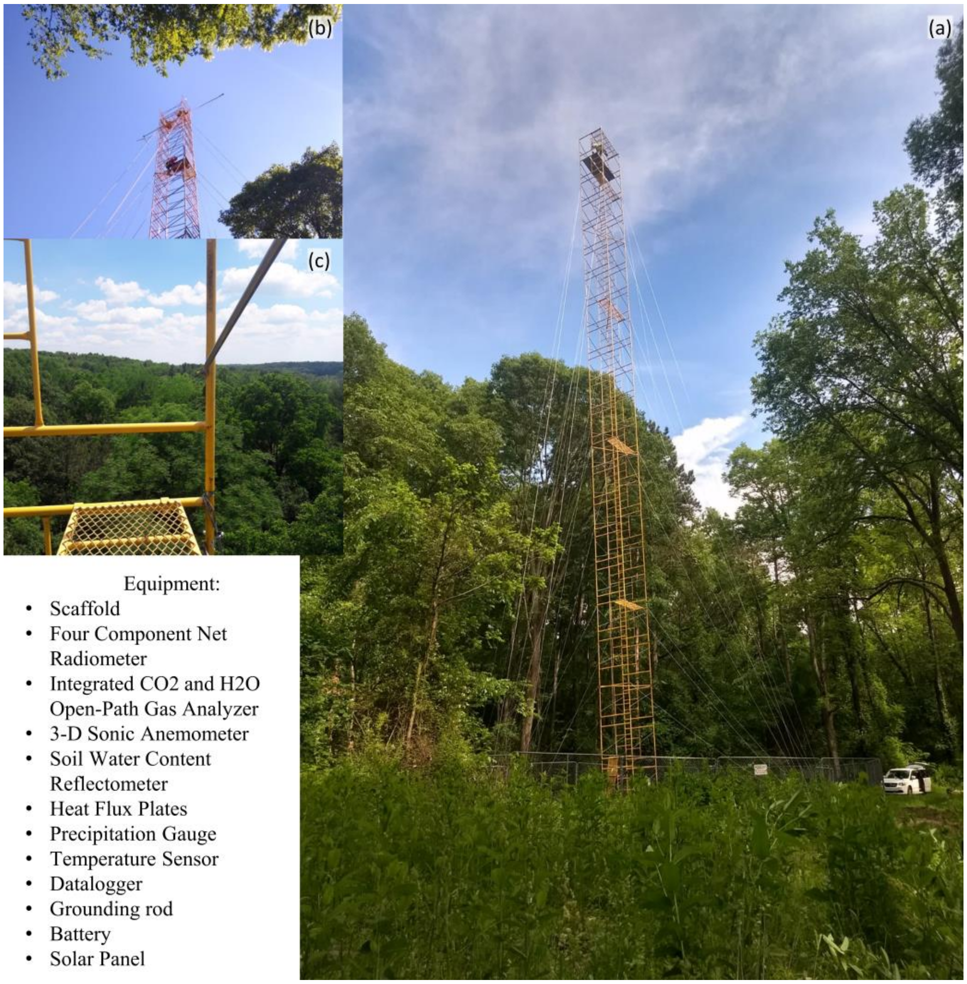

Figure 1.3: (a) Kellogg Experimental Forest eddy covariance tower installed June 2018. (b) Sensors installed at the 110ft section of the tower, with (c) view of sensors overlooking the forest canopy.

Throughout the year, the towers at the Biofuel Cropping System Experiment were maintained, which included changing batteries, adjustments to tower heights, as well as cleaning sensors and solar panels. Each tower was also removed within each agricultural site due to agronomic practices including seeding, pesticide application, fertilizer application, stover removal, and harvest. Once completed, each tower was replaced and level after the allowable Re-entry Interval stated by the U.S. Environmental Protection Agency. Final coverage of each site consists of quality control protocols which involved checking the data for values that were outside a reasonable range, and removing data potentially subjected to errors (i.e., instrument tilt; snow cover on upfacing dome, tower removal from plots). Gap-filling was completed as needed. Accounting for 2018 mid-year pilot study, tower removal, quality control analyses and the goals of the research project, the research period coverage was well over 80% annually for statistical analyses and robustness (Anderson & Gough, 2018; World Meteorological Organization, 1989) (Table 1.1).

Table 1.1: Coverage of continuous measurements from 2018 to 2020 at the KBS GLBRC Biofuel Cropping System Experiment for each unique crop and the entire study period.

Crop	Year	# Days	Coverage
Maize	2018	182	75%
	2019	315	86%
	2020	278	76%
Sorghum	2018	120	49%
	2019	220	60%
	2020	306	84%
Switchgrass	2018	194	80%
	2019	316	87%
	2020	296	81%
Miscanthus	2018	113	46%
	2019	303	83%
	2020	283	78%
Native Grasses	2018	198	81%
	2019	355	97%
	2020	330	90%
Early Successional	2018	131	54%
	2019	335	92%
	2020	292	80%
Restored Prairie	2018	131	54%
	2019	262	72%
	2020	319	87%
Study Period	**2018**		**63%**
	2019		**82%**
	2020		**82%**

Instantaneous measurements

Survey measurements were used to collect data on the changes on albedo and its determinants based on real ground measurements of different biofuel crops, which offer higher spatial and temporal resolution over existing agroecosystems in determining accurate albedo (Figure 1.4). A portable unit was utilized in BCSE plots to perform field measurements. This portable unit consisted of a movable survey tower, attached to a golf cart. The 10-foot pole is replicated from the tower to reach over each unique crop and provide measurements of shortwave and longwave incoming and outgoing radiation using a portable four-component net radiometer (CNR4). The height of the mobile measurements in each plot was adjusted according to the current plant height in order to maintain optimal sensor field of view to the vegetation. Data were logged at 10-Hz using a Campbell 1000X datalogger to produce 1-minute data of shortwave incoming and outgoing radiation, in order to determine albedo. Measurements were completed in both the mainplot and subplot in within each site, as subplots within treatment plots provided a means for comparing alternative agronomic practices such as stover removal vs. leaving the stover on the landscape, and fertilization vs. no N fertilization. To mark each measurement site for consistent data locations over the study period, each stop was marked with a red marker flag using global positioning coordinates (GPS) from a Garmin Oregon 700. Observations were taken between 10:00 and 14:00 hours UTC-5 on each day of data collect to coincide with MODIS satellite imaging trajectories, as well as to ensure that data measurements were consistent around solar noon to reduce bias. During this period, measurements of chlorophyll content using a Soil Plant Analysis Development (SPAD). A healthy crop representing the majority of the treatment plot was selected, the leaf being measured was kept under shade of the body to avoid color variance caused by sun's angle and sunlight intensity, and was measured three times to gain the average chlorophyll content of the crop at that current temporal period.

Figure 1.4: Image depicting instantaneous measurements of miscanthus using mobile surveying at its fertilized mainplot at the BCSE site July 26th, 2018. Inset, above view of the CNR4 sensor over a sorghum canopy during the growing season.

Measurements were completed weekly during the summer season from May to September, then biweekly until senescence, with one measurement during the winter season during bare ground (Figure A3). In total, 21 crops were measured over three replications (Block 1, 2 and 4), and each crop measured its current agronomic practice: stover vs non stover in the case of maize, and fertilization vs non-fertilization in all other crops. The number of measurements taken for each replicate during the study period is shown in Table 1.2. Also see Supplementary Tables A1 and A2 on survey sheet used within the field, as well as physical coordinates, replicate and treatments IDs for each crop-species. Supplementary Figure A4 provides a brief overview of instructions during survey field measurements.

Table 1.2: Number of instantaneous measurements in 2018, 2019 and 2020 at the KBS GLBRC Biofuel Cropping System Experiment for each unique crop, each block replicate, and the entire study period.

Crop	Observations
Maize	170
Sorghum	248
Switchgrass	252
Miscanthus	156
Native Grasses	256
Early	156
Restored Prairie	156
Block 1	478
Block 2	471
Block 4	445
Total Site	**1394**

Purpose & Research Objectives

This dissertation examines how surface energy and its reflectivity (e.g., albedo) are associated with landscape conversion from forest and corn to unique biofuel annual and perennial crops. This research also links these temporal changes with climate scenarios through the conversion of radiative reflectance to carbon dioxide equivalences using global warming potential. This research focuses on three overarching questions:

1. What is the albedo of different types of bioenergy crops at the Kellogg Biological Station?
2. How does agronomic practices (i.e., fertilization, stover removal, planting density) and climate contribute to difference in albedo between different biofuel croplands?
3. How does surface induced albedo contribute to climate warming/cooling and GWI in biofuel croplands?

To answer these research questions, this research aimed to achieve the following goals:

- Establish a long-term network of towers which would effectively measure albedo continuously over multiple biofuel ecosystems

- Identify which biofuel crops were more sustainable at reflecting solar radiation throughout multiple timescales using instantaneous survey measurements.
- Evaluate the effectiveness of climate warming and/or cooling of unique bioenergy crops through modeling global warming impact (Figure 1.5).

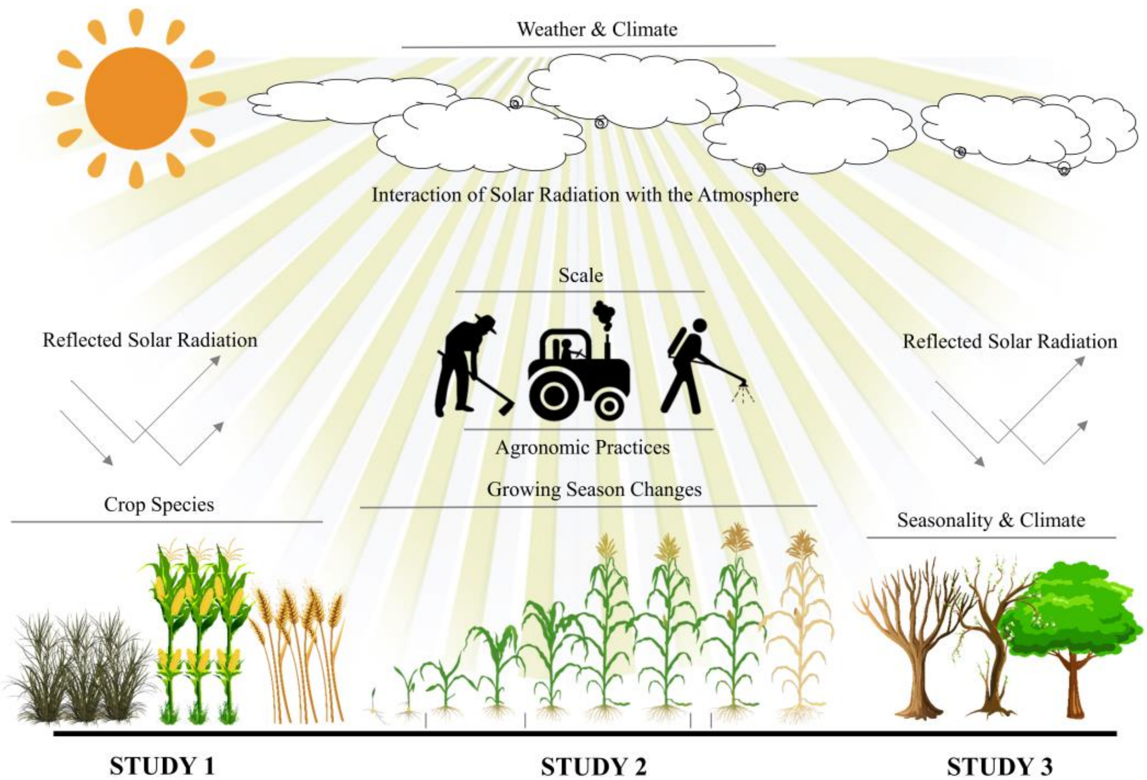

Figure 1.5: Conceptual framework linking the relationship between solar radiation, the impact of albedo on climate, and global warming potential using three studies. Study 1: Cooling Effects of Perennial Bioenergy Croplands due to Elevated Albedo. Study 2: Temporal Variations of Albedo on Bioenergy Crops: Effects of Agronomic Practices during Three Cultivation Seasons. Study 3: Global Warming Impacts of Converting Forest into Bioenergy Croplands in Southwest Michigan.

Overview of Chapters

In Chapter 1, the magnitudes and temporal changes of albedo in bioenergy crops over a 3-year study period were investigated. The seasonal changes in albedo ranging from growing seasons to non-growing season variations were quantified. Albedo aggregated from half hourly timesteps into daily values was used to determine seasonal and annual analyses. These means were plotted using linear time series. An ANOVA with a Tukey HSD was utilized to analyze the significance between crops and temporal periods. Lastly, albedo-induced radiative forcing ($RF_{\Delta\alpha}$) for the warming/cooling impacts on the climate was quantified

Chapter 2 discusses a study conducted to understand the local, crop-specific and management-specific characterization of surface albedo. This study delved deeper into the growing season, looking at each specific month, as well as the early growing season, which consisted of the month of May, the peak growing season which consisted of June to August, and September as the period of Senescence. Field measurements of albedo were utilized specifically to analyze differences of agronomic practices. The spatiotemporal changes of albedo across managed bioenergy crop systems by using instantaneous measurements at field level were quantified, through the intra and inter-annual changes of albedo during three growing seasons. Albedo was also analyzed for variances over the growing season for different croplands, sites which were fertilized versus which were not and those which had stover on the landscape in the case of Maize. Ancillary data including chlorophyll content, precipitation and air temperature were presented as additional analysis. Finally, ANOVA and Tukey HSD were used to estimate the effects of climate and chlorophyll with albedo, as well as the effects of seasonality.

Chapter describes the work that built upon the study described in Chapter 1, utilizing the albedo measured and observed over the past three years to assess the potential global warming impact of each biofuel crop presented in the study. Continuous measurements from installed albedo towers from 2018-2020 were used to calculate radiative measurements, albedo and GWI using the growing season, non-growing season and annually as a baseline. Changes in albedo fluctuations were estimated seasonally and temporally, as well as variations of RF and GWI at daily, monthly, and seasonal time scales. Estimated carbon cooling effects of albedo-induced GWI when converted from a reference forest to another bioenergy crop were analyzed (Figure 1.6).

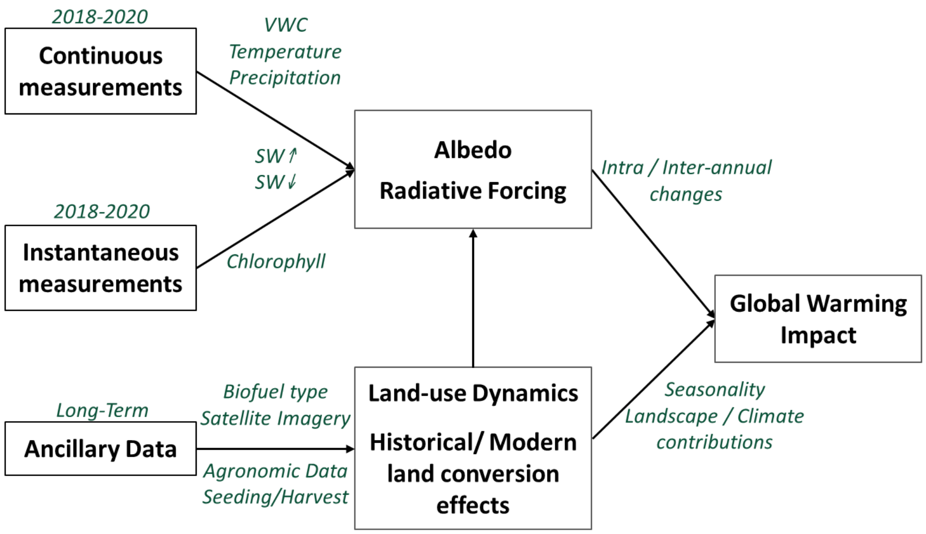

Figure 1.6: Research framework which includes continuous tower measurements, instantaneous survey measurements and ancillary long-term data from the W.K. Kellogg Biological Station to determine albedo, radiative forcing, and global warming impacts.

The concluding chapter of this dissertation summarizes all lessons learned at the Kellogg Biological Station, which includes the most effective methods of measuring albedo, calculating global warming impact and determining the most efficient biofuel crop which would be the most sustainable to mitigating climate change as well as providing maximum ecosystem services.

APPENDIX

Table A1: All GPS coordinates for measurements taken at the BCSE site, KBS, Michigan, USA. Measurements taken with a Garmin Oregon 700. G'*X*' stands for the crop species ID, R depicts the block replicate, F/NF/S/NS stands for the plot agronomic treatment.

ID	Latitude	Longitude	Name, Replicate and
1	42.39597	-85.3752	G10R1/F
2	42.39597	-85.375	G10R1/NF
3	42.39635	-85.3733	G10R2/F
4	42.39633	-85.3731	G10R2/NF
5	42.39487	-85.372	G10R4/F
6	42.39487	-85.3752	G10R4/NF
7	42.39633	-85.3759	G1R1/S
8	42.39633	-85.3757	G1R1/NS
9	42.39535	-85.373	G1R2/S
10	42.39483	-85.3736	G1R4/S
11	42.39635	-85.3742	G2R1/F
12	42.39635	-85.3743	G2R1/NF
13	42.39587	-85.3732	G2R2/F
14	42.39585	-85.373	G2R2/NF
15	42.39437	-85.3757	G2R4/F
16	42.39437	-85.3756	G2R4/NF
17	42.39585	-85.3757	G5R1/F
18	42.39585	-85.3758	G5R1/NF
19	42.39535	-85.3737	G5R2/F
20	42.39535	-85.3736	G5R2/NF
21	42.39485	-85.3743	G5R4/F
22	42.39487	-85.3742	G5R4/NF
23	42.39533	-85.3757	G6R1/F
24	42.39533	-85.3759	G6R1/NF
25	42.39583	-85.3737	G6R2/F
26	42.39583	-85.3738	G6R2/NF
27	42.39435	-85.3746	G6R4/F
28	42.39435	-85.3748	G6R4/NF
29	42.39587	-85.3748	G7R1
30	42.39585	-85.3747	G7R1/F
31	42.39583	-85.3725	G7R2/F
32	42.39583	-85.3727	G7R2/NF
33	42.39435	-85.3741	G7R4/F
34	42.39435	-85.3743	G7R4/NF
35	42.39633	-85.3748	G9R1/F
36	42.39635	-85.3746	G9R1/NF
37	42.39535	-85.3746	G9R2/F
38	42.39535	-85.3748	G9R2/NF
39	42.39487	-85.3757	G9R4/F
40	42.39487	-85.3759	G9R4/NF

Table A2: Survey sheet of variables taken during instantaneous measurements at BCSE, KBS, Michigan, USA. G‘X’ stands for the crop species ID, R depicts the block replicate, F/NF/S/NS stands for the plot agronomic treatment.

PLOT	CROP	F/NF	SPAD			CNR4		SW Rad		LW Rad		Albedo
			1	2	3	Time	Time	In	Out	In	Out	
G1R1	Corn	S										
G1R1	Corn	NS										
G1R2	Corn	S										
G1R2	Corn	NS										
G1R4	Corn	NS										
G5R1	Switchgrass	F										
G5R1	Switchgrass	NF										
G5R2	Switchgrass	F										
G5R2	Switchgrass	NF										
G5R4	Switchgrass	F										
G5R4	Switchgrass	NF										
G2R1	Sorghum	F										
G2R1	Sorghum	NF										
G2R2	Sorghum	F										
G2R2	Sorghum	NF										
G2R4	Sorghum	F										
G2R4	Sorghum	NF										
G7R1	Native Grasses	F										
G7R1	Native Grasses	NF										
G7R2	Native Grasses	F										
G7R2	Native Grasses	NF										
G7R4	Native Grasses	F										
G7R4	Native Grasses	NF										
G6R1	Miscanthus	F										
G6R1	Miscanthus	NF										
G6R2	Miscanthus	F										
G6R2	Miscanthus	NF										
G6R4	Miscanthus	F										
G6R4	Miscanthus	NF										
G10R1	Prairie	F										
G10R1	Prairie	NF										
G10R2	Prairie	F										
G10R2	Prairie	NF										
G10R4	Prairie	F										
G10R4	Prairie	NF										
G9R1	EarlySuccess	F										
G9R1	EarlySuccess	NF										
G9R2	EarlySuccess	F										
G9R2	EarlySuccess	NF										
G9R4	EarlySuccess	F										
G9R4	EarlySuccess	NF										

Figure A1. Tower prototype (left) and final instrumentation (right) placed in BCSE study sites May 2018.

Figure A2. Examples of micrometeorological tower during different climate and seasonal periods. Top left: early spring; Top right: peak growing period; Bottom left: harvest; Bottom right: early winter.

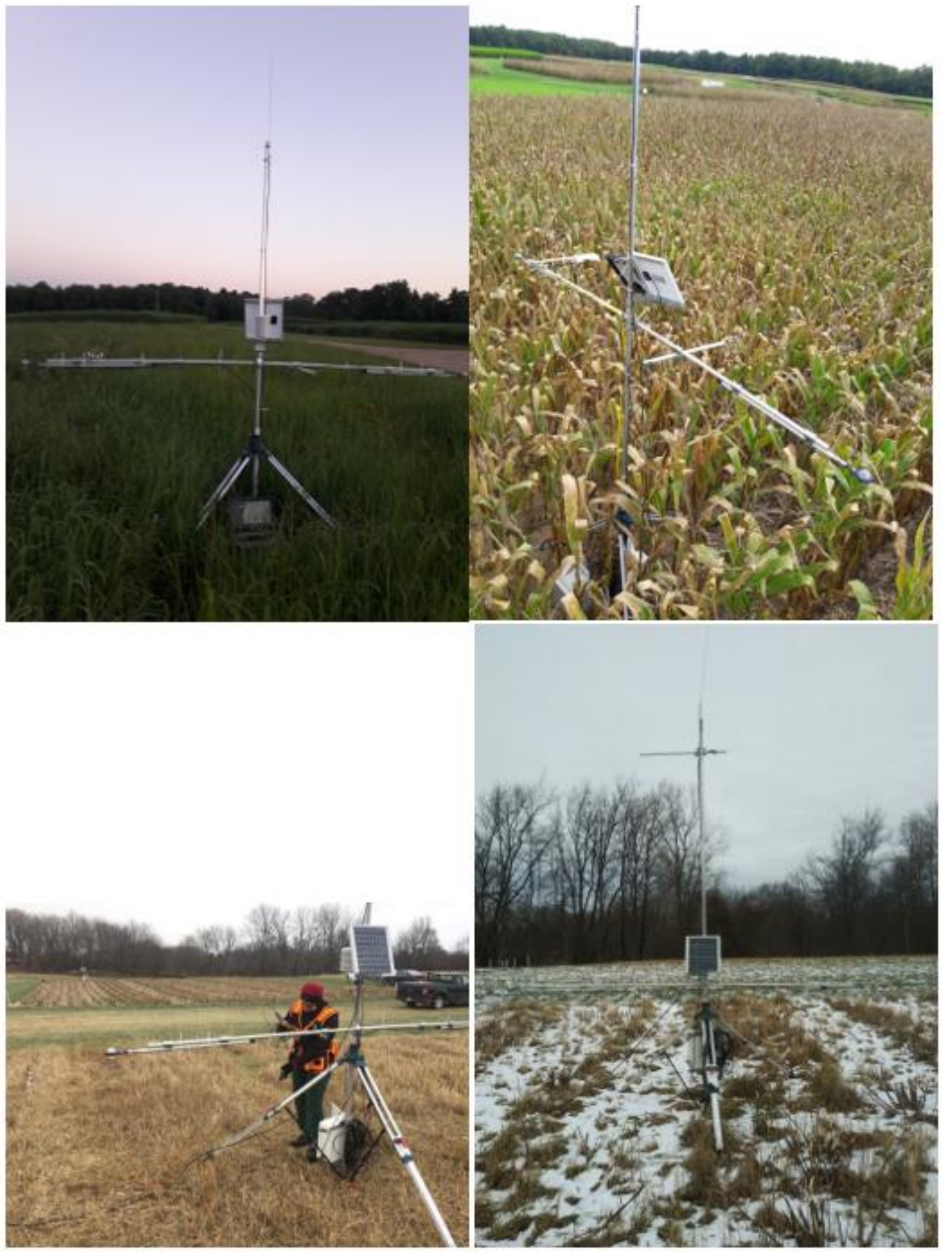

Figure A3. Visual demonstration of instantaneous survey measurements completed at BCSE from May 2018 to 2020. Left: early growing season; Right: peak growing season.

Figure A4: Instructions for instantaneous measurements at the BCSE site, Kellogg Biological Station. Observations were completed following the protocol listed below.

Make a note of the weather (i.e., clear, cloudy, sunny), the date and time of the field measurement on the right side of the paper.

Carefully connect the CNR4 to the Survey Pole. Take care that your hands do not touch the glass domes. If there are any smudges, take a clean cloth and gently wipe them off.

Make sure that the sensor is straight and level.

Connect the cable from the backpack to the **S** (Solar) portion of the CNR4.

Use electrical tape to tape the excess cable along the pole.

Connect the battery within the backpack: Red cable to red terminal / Black cable to black terminal.

Connect the USB to the computer. The other end of the cable should be connected to the datalogger.

Turn on computer, open LoggerNet, and navigate to **'Main' -> 'Connect'**

In the "**Connect Page**", Click on these in the following order:

1. Click on **CR10XLTER** in the Stations Tab
2. Then on "**Connect**" in the Menu Tab
3. Click on "**Set**" to ensure the datalogger time is to the date/time of the laptop
4. Click on "**Num Display**" to view the data from the datalogger in real time.

In the "Num Display" new page, please view the following variables:

- RecNum- The record number of the variable the datalogger is taking. It is done every second.
- Timestamp- The date/time of the datalogger. Please make sure this is correct
- BattV- Battery Voltage of the battery.
- ProgSig- Signature from datalogger reading the program, please ignore this.
- Sw_In- Incoming Shortwave Radiation
- Sw-Out- Outgoing Shortwave Radiation
- Lw_In- Incoming Longwave Radiation
- Lw-Out- Outgoing Longwave Radiation
- Albedo- Ratio of SW_Out/Sw_In

Start at the correct area for the first measurement. Please refer to BCSE maps for correct orientation.

- Make sure you are at the correct area. Double check the map for the **PLOT Name, Mainplot, Subplot and the Replicate.**
- Fertilized vs non-fertilized treatments.
- Fill in the **SPAD measurement**.
    - Measure three different plants.
    - The plants measured should represent the majority of the area being measured.

Figure A4 (cont'd)

Troubleshooting:

Issue	Solution
Cannot connect to the datalogger	• Check battery voltage • Check the laptop cable is in the computer • Check the Datalogger cable is connected to the datalogger • Check the intermediary cables are still connected to each other
Values from the Num Display table are not showing in real time	• Check that you have connected to the sensor using the "Connect" function • Check that you have clicked on the CORRECT sensor in the Station tab. The logger should read CR10XLTER • Check that the laptop cables are connected to the computer
Albedo measurements do not seem accurate	• Check that the CNR4 sensor is properly levelled • Check that the CNR4 cable is properly attached to the CNR4 SOLAR (S) section • Check that you are connected to the correct Datalogger in the Station tab. The sensor should read CR10XLTER • Albedo values should read between 0.2 – crops, 0.4 – bare, 0.5-0.8 - snow
Battery Voltage is low	• Battery was not disconnected from datalogger, will need to be charged. • Battery voltage should read between 11.2V – 12.8V for good values.
Date/Time on data and Timestamp is incorrect	• Press "Set" in the Connect tab before starting measurements.
I am not sure where I am, if I am measuring Fertilized or Non-fertilized	• Refer to the maps/legend located in the blue binder • Refer to the maps/legend located in document.
What direction should I be holding the sensor?	• The sensor should be held in a southern orientation.
I wrote the data in the wrong section	• Be sure to make a note of any changes where errors might have been made so that they can be placed correctly in the primary spreadsheet at a later date • If the error is large, discard the sheet and carefully rewrite accurate data to a new sheet.
I disconnected the sensor and laptop before retrieving the data from the datalogger using the "Collect Now" function	• The sensor does not need to be reconnected, simply reconnect the laptop to the datalogger using the cable and reconnect to the Datalogger. Once connected, press "Collect Now", then rename the file appropriately.
I am measuring a plot and a cloud passes over at the same time	• If the cloud passing is short (1-2minutes), redo the measurement. • If the cloud passing is longer than 2 minutes, restart once cloud has passed.

REFERENCES

REFERENCES

Alig, R. J., Kline, J. D., & Lichtenstein, M. (2004). Urbanization on the US landscape: Looking ahead in the 21st century. *Landscape and Urban Planning*, *69*(2-3), 219-234. https://doi.org/10.1016/j.landurbplan.2003.07.004

Akbari, H., Menon, S., & Rosenfeld, A. (2009). Global cooling: increasing world-wide urban albedos to offset CO 2. *Climatic Change*, *94*(3-4), 275-286. https://doi.org/10.1007/s10584-008-9515-9

Anderson, C. I., & Gough, W. A. (2018). Accounting for missing data in monthly temperature series: Testing rule-of-thumb omission of months with missing values. *International Journal of Climatology*, *38*(13), 4990-5002. https://doi.org/10.1002/joc.5801

Baveye, P. C., Rangel, D., Jacobson, A. R., Laba, M., Darnault, C., Otten, W., et al. (2011). From Dust Bowl to Dust Bowl: Soils are still very much a frontier of science. *Soil Science Society of America Journal*, *75*(6), 2037–12. http://doi.org/10.2136/sssaj2011.0145

Betts, R. A. (2001). Biogeophysical impacts of land use on present-day climate: Near-surface temperature change and radiative forcing. *Atmospheric Science Letters*, *2*(1-4), 39-51. https://doi.org/10.1006/asle.2001.0037

Bonan, G.B. (1997). Effects of land use on the climate of the United States. *Climatic Change, 37*, 449–486. https://doi.org/10.1023/A:1005305708775

Bonan, G. B. (2008). Forests and climate change: forcings, feedbacks, and the climate benefits of forests. *Science*, *320*(5882), 1444-1449. https://doi.org/10.1126/science.1155121

Bolter, K., Robey, J., & Anderson, G. (2019). *An Assessment of the Economic Conditions in the City of Battle Creek*. Prepared for the W.K. Kellogg Foundation.

Bright, R. M., Zhao, K., Jackson, R. B., & Cherubini, F. (2015). Quantifying surface albedo and other direct biogeophysical climate forcings of forestry activities. *Global Change Biology*, *21*(9), 3246–3266. https://doi.org/10.1111/gcb.12951

Burakowski, E., Tawfik, A., Ouimette, A., Lepine, L., Novick, K., Ollinger, S. ... & Bonan, G. (2018). The role of surface roughness, albedo, and Bowen ratio on ecosystem energy balance in the Eastern United States. *Agricultural and Forest Meteorology*, *249*, 367-376. https://doi.org/10.1016/j.agrformet.2017.11.030

Caiazzo, F., Malina, R., Staples, M. D., Wolfe, P. J., Yim, S. H., & Barrett, S. R. (2014). Quantifying the climate impacts of albedo changes due to biofuel production: a comparison with biogeochemical effects. *Environmental Research Letters*, *9*(2), 024015. https://doi.org/10.1088/1748-9326/9/2/024015

Campbell, G. S., & Norman, J. (2012). *An Introduction to Environmental Biophysics*. Second Edition, Springer Science & Business Media, New York, NY, USA.

Davin, E. L., Seneviratne, S. I., Ciais, P., Olioso, A., & Wang, T. (2014). Preferential cooling of hot extremes from cropland albedo management. *Proceedings of the National Academy of Sciences*, 201317323.

Dickason, D. G., Anderson, G. P., Faul, J. M., & Sandburg, C. (1995). Urban sprawl in the Kalamazoo metropolitan region: Land use change, 1938-L978. In M.Wyckoff (Ed.), *Michigan Trend Futures Study: The Built Environment.* Lansing, MI. pp. 4-47-52, 4-66-75. Publisher: Michigan Society of Planning Officials Editors: M. Wyckoff

Flato, G., Marotzke, J., Abiodun, B., Braconnot, P., Chou, S.C., Collins, W., Cox, P., Driouech, F., Emori, S., Eyring, V., Forest, C., Gleckler, P., Guilyardi, E., Jakob, C., Kattsov, V., Reason, C... & Rummukainen, M. (2013). Evaluation of Climate Models. In: *Climate Change 2013: The Physical Science Basis*. Contribution of Working Group I to the Fifth Assessment Report of the Intergovernmental Panel on Climate Change. Cambridge University Press, Cambridge, United Kingdom and New York, NY, USA.

Hartmann, D. L. (1994). *Global Physical Climatology*. (Vol. 103), Second Edition. Elsevier, Waltham, MA, USA.

Haszeldine, R. S., Flude, S., Johnson, G., & Scott, V. (2018). Negative emissions technologies and carbon capture and storage to achieve the Paris Agreement commitments. *Philosophical Transactions of the Royal Society.* A, *376*(2119), 20160447

Heaton, E., Voigt, T., & Long, S. P. (2004). A quantitative review comparing the yields of two candidate C4 perennial biomass crops in relation to nitrogen, temperature and water. *Biomass and Bioenergy*, *27*(1), 21-30. https://doi.org/10.1016/j.biombioe.2003.10.005

Heaton, E. A., Dohleman, F. G., Miguez, A. F., Juvik, J. A., Lozovaya, V., Widholm, J., ... & Long, S. P. (2010). Miscanthus: a promising biomass crop. *Advances in Botanical Research, 56*, 75-137. https://doi.org/10.1016/B978-0-12-381518-7.00003-0

Henderson-Sellers, A., & Wilson, M. (1983). Surface albedo data for climatic modeling. *Reviews of Geophysics*, *21*(8), 1743–1778. https://doi.org/10.1029/RG021i008p01743

Luyssaert, S., Jammet, M., Stoy, P. C., Estel, S., Pongratz, J., Ceschia, E. ... nnnnnnb Gielen, B. (2014). Land management and land-cover change have impacts of similar magnitude on surface temperature. *Nature Climate Change*, *4*(5), 389–393. https://doi.org/10.1038/nclimate2196

Meyer, S., Bright, R. M., Fischer, D., Schulz, H., & Glaser, B. (2012). Albedo impact on the suitability of biochar systems to mitigate global warming. *Environmental Science & Technology*, *46*(22), 12726-12734. https://doi.org/10.1021/es302302g

Miller, J. N., VanLoocke, A., Gomez-Casanovas, N., & Bernacchi, C. J. (2016). Candidate perennial bioenergy grasses have a higher albedo than annual row crops. *Global Change Biology: Bioenergy*, *8*(4), 818-825. https://doi.org/10.1111/gcbb.12291

Monteith, J. L. (1959). The reflection of short‐wave radiation by vegetation. *Quarterly Journal of the Royal Meteorological Society*, *85*(366), 386-392. https://doi.org/10.1002/qj.49708536607

Mueller, N. D., Butler, E. E., McKinnon, K. A., Rhines, A., Tingley, M., Holbrook, N. M., & Huybers, P. (2016). Cooling of US Midwest summer temperature extremes from cropland intensification. *Nature Climate Change*, *6*(3), 317-322. https://doi.org/10.1038/nclimate2825

Muñoz, J. D., Kravchenko, A. (2011). Soil carbon mapping using on-the-go near infrared spectroscopy, topography and aerial photographs. *Geoderma*, *166*, 102–110. https://doi.org/10.1016/j.geoderma.2011.07.017

NCDC (National Climate Data Center). (2013). Summary of Monthly Normal 1981–2010 (MI, USA: Gull Lake Biology Station) (www.ncdc.noaa.gov/cdo-web/search)

Odum, E.P. (1984). Properties of agroecosystems. Pages 5-11 in R. Lowrance, B.R. Stinner, and G.J. House, editors. *Agricultural Ecosystems: Unifying Concepts*. John Wiley, New York, USA.

Ollinger, S. V., Richardson, A. D., Martin, M. E., Hollinger, D. Y., Frolking, S. E., Reich, P. B., ... & Smith, M. L. (2008). Canopy nitrogen, carbon assimilation, and albedo in temperate and boreal forests: Functional relations and potential climate feedbacks. *Proceedings of the National Academy of Sciences*. https://doi.org/10.1073/pnas.0810021105

Ramankutty, N., Evan, A. T., Monfreda, C., & Foley, J. A. (2008). Farming the planet: 1. Geographic distribution of global agricultural lands in the year 2000. *Global Biogeochemical Cycles*, *22*(1). https://doi.org/10.1029/2007GB002952

Robertson, G. P., Bruulsema, T. W., Gehl, R. J., Kanter, D., Mauzerall, D. L., Rotz, C. A., & Williams, C. O. (2013). Nitrogen–climate interactions in US agriculture. *Biogeochemistry*, *114*(1-3), 41-70. https://doi.org/10.1007/s10533-012-9802-4.

Robertson, G. P., & Hamilton, S. K. (2015). Long-Term ecological research at the Kellogg Biological Station LTER Site. In: *The Ecology of Agricultural Landscapes: Long-term Research on the Path to Sustainability*, 1-32. Oxford University Press, New York, NY, USA.

Robertson, G. P., Hamilton, S. K., Barham, B. L., Dale, B. E., Izaurralde, R. C., Jackson, R. D., ... & Tiedje, J. M. (2017). Cellulosic biofuel contributions to a sustainable energy future: Choices and outcomes. *Science*, *356*(6345), http://dx.doi.org/10.1126/science.aal2324

Russell, H. N. (1916). On the albedo of the planets and their satellites. *The Astrophysical Journal*, *43*, 173-196. http://adsabs.harvard.edu/full/1916ApJ....43...173R

Senay, G. B., Velpuri, N. M., Bohms, S., Budde, M., Young, C., Rowland, J., & Verdin, J. P. (2015). Drought monitoring and assessment: remote sensing and modeling approaches for the famine early warning systems network. *Hydro-Meteorological Hazards*, *Risks and Disasters* (pp. 233-262). https://doi.org/10.1016/B978-0-12-394846-5.00009-6

Sellers, P. J., Dickinson, R. E., Randall, D. A., Betts, A. K., Hall, F. G., Berry, J. A., ... & Sato, N. (1997). Modeling the exchanges of energy, water, and carbon between continents and the atmosphere. *Science*, *275*(5299), 502-509. https://doi.org/10.1126/science.275.5299.502

Smith, P. (2016). Soil carbon sequestration and biochar as negative emission technologies. *Global Change Biology*, *22*(3), 1315-1324. https://doi.org/10.1111/gcb.13178

Thoen, G. F. (1990). *Soil Survey of Barry County, Michigan*. (USDA Soil Conservation Service, Michigan Agricultural Experiment Station, and Michigan Technological University, Washington DC), pp. 187, 286.

Vitousek, P. M., Mooney, H. A., Lubchenco, J., & Melillo, J. M. (1997). Human domination of Earth's ecosystems. *Science*, *277*(5325), 494-499. https://doi.org/10.1126/277.5325.494

Waring, R. H. (2007). Advances in eddy-flux analyses, remote sensing, and evidence of climate change. *Forest Ecosystems*. 317-344. https://doi.org/10.1016/B978-012370605-8.50017-7

World Meteorological Organization. (1989) Calculation of monthly and annual 30-year standard normals. Washington, DC: World Meteorological Organization. Technical report: WMO-TD No. 341, WCDP-10.

CHAPTER 2. CLIMATE COOLING BENEFITS OF CELLULOSIC BIOENERGY CROPS DUE TO ELEVATED ALBEDO

Abstract

Changes in albedo can alter ecosystem energy balance and potentially influence climate warming. This chapter describes the analysis of temporal changes of albedo in managed biofuel systems by measuring albedo-induced radiative forcing at monthly, seasonal, and annual timescales. Direct field measurements of surface albedo (α_s) at high temporal resolution were conducted to quantify the magnitudes and intra- and inter-annual differences in albedo (Δ_α) and albedo-induced radiative forcing ($RF_{\Delta\alpha}$) in seven bioenergy crops in southwest Michigan from May 2018 through December 2020. A nearby forest was used as a historical reference to calculate albedo differences and the corresponding $RF_{\Delta\alpha}$. Albedo differences among crops during the growing season and annually were statistically significant ($p < 0.05$). During the growing season (GS), albedo was stable in perennial croplands, with α_s ~20% higher (0.206±0.003SE, on average) than in no-till maize (0.184±0.002). Throughout the non-growing season (NGS), α_s was much higher compared to that of the GS (0.340±0.02) but showed insignificant differences among crops ($p > 0.05$). Annually, α_s differed among crops in the following order of early successional (0.268) > miscanthus (0.266) > restored prairie (0.264) > native grasses (0.254) > sorghum (0.248) > switchgrass (0.245) > maize (0.223). Overall, transitioning a crop field to early successional, miscanthus and native grasses yielded the highest cooling annual cooling effects when modeling the conversion from either forest or maize, while restored prairie exhibited the least efficient cooling. As perennials have higher albedo than the reference crops they are replacing, they reflect more radiation than conversion from annual row crop/forest to perennial cropland. The decreased annual energy absorption would lead to an overall potential cooling effect.

Introduction

Surface albedo (α_s), defined as the ratio of outgoing radiation to incoming shortwave radiation, (Henderson-Sellers, 1980; Henderson-Sellers & Hughes, 1982; Russel, 1916), is one of the most important measures in radiation and energy budgets (Bright, 2015). Albedo is a vital indicator of energy partitioning because it reflects the amount of energy being absorbed by a land surface (e.g., grasslands, forest, or urban lands) and converted to heat, versus the amount reflected back into outer space with no warming impact (Ollinger et al., 2008). Spatial and temporal changes in albedo have been closely explored as albedo not only reflect direct warming and cooling processes (Campbell & Norman, 2012), but also indirectly reflects changes in evaporation and transpiration, land surface properties, and local climate through its impact on surface energy fluxes and the hydrologic cycle (Akbari et al., 2009; Cherubini et al., 2012; Pachauri et al., 2014).

Although large-scale bioenergy plays a key role in climate change mitigation scenarios, Substantially less attention and effort have been focused on albedo compared to greenhouse gas (GHG) research in terrestrial ecosystems and across different spatial scales (IPCC, 2008). A key measure of global warming impact (GWI) is its radiative efficiency, in this case, through albedo-induced warming/cooling (Chen et al., 2021). Methods on calculating GWI is actively debated in the literature currently due to nonlinear effects, large uncertainties for multi-century processes and strong assumptions of changing atmospheric conditions, but most scientists agree that a metric to quantify the contributions of climate change to different GHG emissions is vitally needed. Thus, determining the total energy added to a climate system by a GHG relative to that added by CO_2 is one of the most important applications of GWI.

Agricultural practices can influence climate through altered biogeochemical processes and albedo (Davin et al., 2014), which can differ by crop type and be very different from the albedo of native, pre-conversion cover types such as forest. Forests, for example, have lower albedos due to a complex canopy structure that traps radiation, compared to annual cropland that reflects more incoming radiation during the growing season and can also greatly accentuate wintertime albedo in northern latitude climates due to snow cover (Betts, 2001; Forster et al., 2007). A lower forest albedo can potentially cause warming effects on the climate (Davin et al., 2014; Hartmann, 1994). In Michigan, forest was the dominant pre-conversion land cover type prior to European settlement (Brown, 2000); however, today croplands dominate with higher elevated albedo, producing net cooling effects (Bonan, 2008; Chen et al., 2019; Fu et al., 2021; Sciusco et al., 2020). As albedo can be attributed to either climatic conditions (i.e., cloud cover, temperature, humidity), surface emissivity (i.e., fluxes of moisture through evaporation and transpiration, the ratio of latent to sensible heat fluxes), land transformations (i.e., abandoned, agriculture, forested), plant phenology (i.e., plant height, leaf area index, plant density, plant species), or natural disturbances (Henderson-Sellers & Wilson, 1983; Wang et al., 2004), the albedo of short vegetation such as grasslands is likely to be more variable than that of forests. The biogeophysical effects of agronomic management practices such as tillage, harvesting, fertilization, pesticide, and cover crops on GHG fluxes have also been studied extensively (Pielke et al., 2011), but research on albedo is still severely lacking (Henderson-Sellers & Wilson, 1983; Flato et al., 2013).

The effects of cellulosic bioenergy crops on albedo are unclear, specifically relative to the systems they might replace – e.g., row crops of maize, soybean and wheat currently grown for grain-based ethanol. The impacts of large-scale bioenergy production on the land surface could be significant, as perennial bioenergy grasses have a higher albedo than annual row crops, and if conventional arable agriculture are replaced, could lead to significant regional cooling and slower snowmelt. Previous studies on albedo-induced warming effects are mostly based on satellite data

(Sciusco et al., 2020; Fang et al., 2007; Zhang et al., 2010), biophysical models (Cherubini et al., 2012), or statistical partitioning of land surface energy fluxes (e.g., Bowen ratio) (Bright, 2015). Very few studies are based on ground measurements, which offer higher spatial and temporal resolutions. The drawbacks of studies using satellite imagery include a limited temporal resolution and restriction to cloudless periods (Jonsell et al., 2003). However, some studies completed emphasize the importance of landscape change due to the emergence of bioenergy cropping as a major climate mitigation strategy. Miller et al., (2016) who found that perennials switchgrass and miscanthus had a daily cooling potential of -5 W m^{-2}, and -8 W m^{-2} respectively, similar to Sciusco et al. (2020, 2021), who integrated spatial and temporal changes of albedo and showed that croplands had higher albedo and intra-annual variabilities. Abraha et al. (2021) also observed that cellulosic bioenergy crop of switchgrass and restored prairie fields provided albedo-induced cooling climate benefits from greenhouse gas (GHG) emissions, while Robertson et al. (2000) and Gelfand et al. (2013) discussed how perennials including early successional, poplar and alfalfa can provide net global warming potential cooling benefits based on soil carbon sequestration, agronomic inputs, and trace gas fluxes. Finally, IPCC (2014) acknowledges the importance of bioenergy with carbon dioxide capture and storage (BECCS) for providing reductions in the GHG emissions by switching to low-carbon energy sources. Thus, albedo is becoming more conventional for inclusion in climate modeling, and useful for deriving different mechanisms to model the climate by potentially increasing the reflectance of radiation back into the atmosphere, rather than being stored within the Earth (Lenton & Vaughn, 2009).

This study hypothesized that perennial crops have a higher albedo compared to annual row crops. Previous research has shown that stand density, canopy height and leaf phenology are critical factors affecting albedo. This project aimed to understand how changes vary between each biofuel crop. Secondly, it was hypothesized that the albedo of different crops are significantly different due to plant seasonality (i.e., growing season, winter, monthly, annually). Within this study I focus the priority on plant seasonality temporally from short to longer terms and how land management affects albedo. Finally, it was hypothesized that albedo of different biofuel crops are time dependent as each species and ecosystem are affected by climate, plant green-up to plant senescence (i.e., phenological changes), seasonality, and human disturbances (i.e., agronomic practices). To test these hypotheses, an experiment was designed to quantify, through direct measurements at the land surface, the temporal changes of albedo of seven candidate bioenergy crops. The crops used in this study included annual row crops of energy sorghum, perennial monocultures of switchgrass, and miscanthus, and perennial polycultures of native grasses, early successional vegetation, and restored prairie. Conventional maize and forest were selected as contemporary and historical reference sites, respectively. The objectives were to: (a) estimate the magnitudes and temporal changes of albedo in different cellulosic bioenergy crops over a 3-year period, (b) compare these albedos to those of continuous maize and forest reference systems, and (c) quantify albedo-induced radiative forcing ($RF_{\Delta\alpha}$) by the bioenergy crops to evaluate warming/cooling impacts on the climate.

Materials & Methods

Study site

This study was conducted at the Department of Energy Great Lakes Bioenergy Research Center's (GLBRC) Biofuel Cropping Systems Experiments (BCSE, http://glbrc.org/) located in southwest Michigan at the W.K. Kellogg Biological Station. The Biofuel Cropping System Experiment (42° 24' N, 85° 24' W, 288 m asl) is located in a diverse, rural- to-semirural landscapes and cropping system appear typical of the U.S. Great Lakes and upper Midwest regions. The climate is humid continental temperate with a 30-year (1981–2010) average annual air temperature of 9.9°C, ranging from a monthly mean of −4 °C in January to 23 °C in July, and average annual precipitation of 1027 mm (NCDC, 2013). The predominant soil characteristics within the study site consists of Kalamazoo and Oshtemo soil series, which are classified as Fine-Loamy, Mixed, Semiactive, and Mesic Typic Hapludalfs soils, which formed under the dominant historical forested landscape in loamy outwash overlaying sand and gravel (Sanford et al., 2016; Thoen, 2011). Our study sites were established as a randomized complete block design, replicated in five 30 m × 40 m plots with a subplot (4.6 m × 13.1 m) (Gelfand et al., 2020).

At BCSE, six candidate bioenergy crops were chosen, alongside two reference sites depicting the historical and modern landscape. Cropping systems measured included energy sorghum (*photoperiod insensitive hybrid TAM 17900*), switchgrass (*Panicum virgatum L.*), a prairie grass native to North America, giant miscanthus (*Miscanthus x giganteus*), a sterile perennial hybrid crossed between two grasses (*Miscanthus sinensis* and *Miscanthus sacchariflorus*), native grasses (a mix of 4-6 species), early successional vegetation, a landscape which consist of grasses which grow naturally following land removed from agriculture use, and restored prairie. Each crop was planted and managed according to standard agricultural practices for the region (Table 2.1). A continuous no-till maize (*Zea mays L.*) was chosen at the BCSE site to represent the modern agricultural landscape of the Midwest while an 87-year-old managed hybrid-spruce forest located at the Kellogg Experimental Forest (KEF, 42° 21' N, 85° 21'W) was used as a historical landscape reference site. Established in 1932, the 716-acre forest was once abandoned agricultural land, but now focuses its research on tree breeding, tree genetics, forest carbon and the development of Spartan Spruce.

Table 2.1: Management dates (month/day) for all sites at the BCSE site, KBS, MI, USA, which include planting (P) and harvesting (H). Initial plantings of perennials were also included.

Year	Maize		Sorghum		Switchgrass		Miscanthus		Native Grasses		Early Succesional		Restored Prairie	
	P	H	P	H	P	H	P	H	P	H	P	H	P	H
2008					6/19		5/23		6/17		5/05		6/17	
2018	5/01	10/04	6/02	11/07	-	10/24	-	11/07	-	10/24	-	10/24	-	10/24
2019	5/19	10/29	6/07	11/20	-	11/08	-	11/05	-	10/24	-	10/23	-	10/23
2020	5/13	10/29	5/27	11/17	-	11/03	-	11/14	-	11/03	-	11/03	-	11/03

Data collection and instrumentation

Continuous measurements of albedo at the BCSE and KEF were completed from May 2018 to December 2020. Albedo measurement stations at the BCSE (Figure 2.1) consisted of towers, each equipped with a four-component net radiometer (SN-500, Apogee Instruments, UT, USA), two net radiometers (Q.7.1, REBS, USA), and one soil water content reflectometer (CS616, Campbell Scientific Inc., UT, USA). One tower was also equipped with a precipitation gauge (TE525, CSI) and temperature sensor to measure air temperature and relative humidity (HMP 60, CSI). Maize and restored prairie both maintained an extra four-component net radiometer in 2018 and 2019 respectively. All data were logged at 10-Hz using a datalogger (CSI) at 5-minute intervals during the summer, and 30-minute intervals during the winter months (November-March). The heights of the towers in each plot were adjusted over the study period in order to maintain a field of view above the canopy layer. Sensors were placed at about 30-40 cm above the canopies, consistent with other studies in agricultural landscapes (Raupach, 1994; Zeri et al., 2011). Each tower was removed for approximately 5-14 days in the spring and fall to allow for agronomic operations including fertilization, seeding and harvest. At the KEF site, the eddy covariance tower (42.365961°N, 85.352615°W) was 34 meters tall and equipped with a four-component net radiometer (CNR4, Kipp & Zonen, Netherlands), precipitation gauge (TE525), and an IRGASON (CSI). Data were logged at 10-Hz using a datalogger (CSI) and stored as 30-minute averages (Poe et al., 2020).

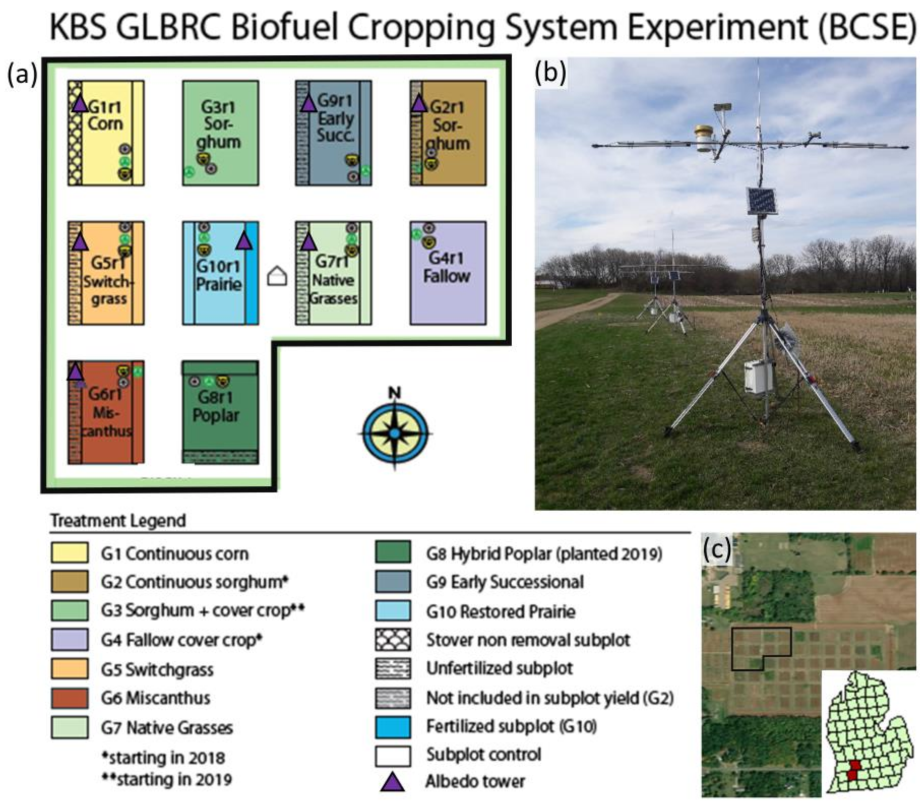

Figure 2.1: Map showing (a) plot layout of the study sites at the GLBRC BCSE of the KBS, MI, USA; (b) photo of albedo towers outside each crop site; and (c) inset of entire study site, with towers located in Block 1 (top left, black outline) of the study area in southwest Michigan. Albedo towers are indicated by a purple triangle. Map modified from https://lter.kbs.msu.edu/research/

Statistical analysis

Expressed in dimensionless terms, all radiation absorbed by a surface represents zero while all radiation onto a surface is reflected is expressed as one. Albedo (α_s) was calculated as the ratio of outgoing shortwave radiation ($SW_\uparrow$) to incident shortwave radiation ($SW_\downarrow$):

$$\alpha_s \frac{SW_\uparrow}{SW_\downarrow} \qquad (1)$$

Our quality control protocols consisted of checking the data for values within expected range, e.g., $0 < \alpha_s < 1$; $0 < SW_{\downarrow} < 1500$ W m^{-2}. Data potentially subject to errors (i.e., instrument tilt; snow cover on an upfacing radiometer dome, temporary tower removal) were eliminated. In the case of maize and restored prairie, where two net radiometers existed on the albedo tower, gap-filling was completed where needed. Otherwise, discarded observations were treated as gaps for both incoming and outgoing irradiance at the same interval for all sites. Larger gaps of several hours to up to 30 consecutive days existed due to instrument failure, see Supplementary Table A3 for complete tower coverage throughout the study period. Statistical analysis of albedo was limited to sunlit hours of day, based on sun angles and daylength for each day (Campbell & Norman, 2012):

$$\boldsymbol{t_{r/s}} \frac{\boldsymbol{A\cos(-\tan(\phi)*\tan(\delta))*(180/\pi())}}{\mathbf{15}} \tag{2}$$

where $t_{r/s}$ is the time of sunrise/sunset, t_o is the solar noon, determined from longitude and the equation of time, ϕ is latitude, and δ is the solar declination at each calendar day. As the Earth turns at a rate of 360 degrees per 24 hours, a factor of 15 is used to convert hours to degrees. Change in albedo (Δ_α) in this study is determined by the albedo of a specific crop less the albedo from a reference crop:

$$\Delta\boldsymbol{\alpha} = \Delta\boldsymbol{s_{crop}} - \Delta\boldsymbol{s_{ref}} \tag{3}$$

where Δ_α is the local change in albedo at a specific time, Δs_{crop} is the crop albedo, and Δs_{ref} is the reference crop albedo. For annual and seasonal analysis, I calculated values for growing season (GS), non-growing season (NGS), and annually. The growing season for sites was defined as May through October (DOY of 121-304) following previous studies similar biofuel species (Sciusco et al., 2020; Zeri et al., 2011), where plant emergence occurs in early May, and harvesting at KBS BCSE is completed in November. In this study, the non-growing season included winter periods and all other days not defined as a growing period. The daily mean albedo for each site was computed by aggregating 5-minute data into half hourly timesteps. Differences in annual and seasonal albedo were analyzed by mixed models analysis of variance (ANOVA) using the statistical package R (R Development Team, 2013), with crop type as fixed effects and years as random effects. For all tests, the statistical significance using Tukey HSD was evaluated at $p < 0.05$. To investigate the intra-annual variances of albedo, monthly albedo averages for all sites were also compared using boxplots with outlying ranges determined at ±1.5 Interquartile Ranges (IQRs).

Radiative forcing caused by changes in albedo at the top-of-atmosphere ($RF_{\Delta\alpha}$, W m^{-2}) is calculated as:

$$\boldsymbol{RF_{\Delta\alpha} = -\frac{1}{N}\sum_{N=1}^{N} SW_{\downarrow} * \Delta_{\alpha} * T_{a}} \tag{4}$$

where $RF_{\Delta\alpha}$ is the albedo-induced radiative forcing at the top-of-atmosphere, Δ_{α} is the mean albedo difference caused by altered albedo from a reference over a specific season, $SW_{\downarrow}$ is local incoming solar radiation, N is the number of days for each season (i.e., GS, NGS, annual), and T_a is the upward atmospheric transmittance. By multiplying both SW↓ and by T_a, the calculation of the instantaneous amount of radiation that leaves the atmosphere was derived. Negative values of $RF_{\Delta\alpha}$ indicated a cooling effect due to increased albedo at cropland compared with the albedo of the forest. Radiative forcing provides a basis for comparing surface albedo with other climate forcing variables. T_a is usually considered a constant average of 0.854 for clear sky conditions (Chen et al., 2013; Cheribuni et al., 2012; Lenton & Vaughn, 2009). However, to reduce bias caused by day-to-day differences in cloud cover calculated, T_a was manually calculated as the ratio of incoming solar radiation at the top of the atmosphere (SW_{TOA}) to that at the surface ($SW_{\downarrow}$), assuming a same value of upward and downward atmospheric transmittances (Carrer et al., 2018; Sciusco et al., 2020). $SW_{\downarrow}$ was obtained from each tower daily, while SW_{TOA} was calculated as:

$$Sw_{TOA} = I_{sc} * I_{\theta} * d_r \tag{5}$$

where I_{sc} is the solar constant (1367 W m^{-2}), I_{θ} is the extraterrestrial irradiance intensity using the cosine of the solar zenith angle, and d_r is the average Earth-Sun distance calculated for each day of the year (see Chen et al., 2021 for a detailed model). The daily zenith angle was derived from NOAA Earth System Research Laboratories for calculating solar radiation (NOAA, 2005). To understand how albedo drives radiative forcing from land use conversion, and to investigate the cooling/warming effects of conversions from both a forested landscape and a renowned monoculture crop, such as maize, into other biofuel crops, the diurnal changes in Δ_{α} for each site were explored by analyzing the averages of days. Each site was modeled using local polynomial regression (LPR). This nonparametric technique is used to plot local weighted regressions, in order to fit a smooth curve between two variables (Cleveland et al., 1990). Local polynomial regression is more computationally complex than standard regression techniques, as a model must be fitted for each data point (Cleveland, 1979; Fan & Gijbels, 2018). Loess curves can reveal trends and cycles in data, combined the simplicity of linear least squares regression and the flexibility of non-linear regression (Cleveland et al., 1988).

Results

Annual row crops

Annual crops of sorghum (mean±SE:0.266±0.01) and maize (0.247±0.01) had lower albedo throughout the study period. Average annual albedo ranged from 0.212±0.005 in 2018, to 0.270±0.01 in 2019, to 0.268±0.01 in 2020. During the GS, average albedo for maize (0.184±0.002) was lower than sorghum (0.208±0.004), while during the NGS both crops had an albedo of approximately 0.361±0.016.

Perennial crops

Perennial crops had consistently higher annual and GS α_s compared to annual row crops (Figure 2). Annual average albedo was 0.252±0.001, with early successional (0.268±0.01) and miscanthus (0.266±0.01) having the highest albedo, followed by restored prairie (0.264 ± 0.01) and switchgrass (0.245±0.01), while restored prairie and native grasses were lowest at 0.244±0.01 and 0.254±0.01 respectively.

Among the crop types, Miscanthus had the highest mean α_s during the GS 2018 (0.251±0.003) and 2019 (0.227±0.002), while native grasses had the lowest average GS α_s (0.186±0.002). Albedo was observed to be more variable during the NGS, with ranges between 0.22 up to 0.85. Albedo during the NGS was much higher compared to that of the GS but showed insignificant differences among crops ($p > 0.05$). Restored prairie and switchgrass averaged similar NGS α_s in all three years (0.373±0.021), while miscanthus and early successional had their highest NGS α_s during 2018/2019 (0.531±0.054) and 2019/2020 (0.419±0.009), respectively (Figure 2.2c).

Differences

Overall, the annual mean albedo for all crops ranged from 0.135 for the reference forest, 0.223 for reference crop maize, to 0.245-0.268 for the six biofuel crops (Figure 2.2, Table 2.2). The reference forest had consistently lower albedo than the biofuel croplands during the GS (0.122±0.002) and NGS (0.155±0.005), as well as annually (0.135±0.003). The differences between crops during the GS and annually were statistically significant ($p<0.05$), between forest and perennial crops, as well as between perennials and annual croplands (Figure 2.2a, b). The intra-annual changes in albedo was similar during the GS, with the GS exhibiting slightly lower values.

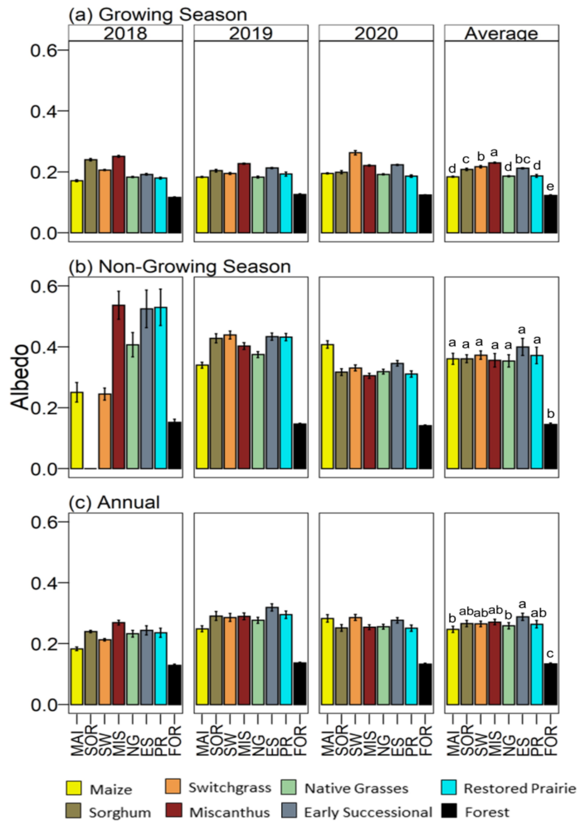

Figure 2.2: Mean albedo of the growing season (GS) (a), non-growing season (NGS) (b), and the entire year (c) for the seven crop types: including a reference forest at KEF. Groupings of different letters indicate statistical differences at p=0.05. Average was calculated over the three-year study period; error bars represent ±1SE.

Table 2.2: Average and ±1SE of the growing season, non-growing season, and the entire year for the six crop types including reference maize and reference forest at KEF, at the BCSE of KBS in Southwest Michigan.

Crop	Growing Season		Non-Growing Season		Annual	
	Mean	SE	Mean	SE	Mean	SE
Maize	0.184	0.002	0.336	0.018	0.223	0.010
Sorghum	0.206	0.004	0.337	0.013	0.248	0.010
Switchgrass	0.223	0.004	0.338	0.014	0.245	0.009
Miscanthus	0.235	0.002	0.368	0.022	0.266	0.009
Native Grasses	0.193	0.002	0.377	0.020	0.254	0.010
Early Successional	0.207	0.002	0.405	0.028	0.268	0.012
Restored Prairie	0.215	0.005	0.361	0.027	0.264	0.012
Forest	0.122	0.002	0.155	0.005	0.135	0.003
Study Period	0.209	0.003	0.360	0.018	0.252	0.009

Seasonality

Monthly changes of albedo in the reference forest showed the lowest α_s of all study sites, which also changed little throughout the year (Figure 2.3). Early in the spring (February-April), showed perennial grasses having consistently higher albedo than annual croplands (noted also by largest differences in surface reflectivity and IQRs). However, at the peak of the GS, all biofuel crops had similar α_s values and low IQRs. After harvest (November-December), α_s was elevated at all biofuel croplands. In winter months (January- March), temporal variations among all biofuel crops appeared quite high, especially when snow was present on the ground.

Mean diurnal variation of α_s during different seasons and growing conditions is visible throughout the day for all sites, but with varying degrees and by crop type (Figure 2.4). During the GS, most biofuel crops have much lower albedo values, with switchgrass showing larger diurnal differences while forest and maize had smaller differences during the day. The reference forest maintained a consistent low diurnal α_s in all periods, depicting a much lower albedo (0.125) throughout the day, and a slightly higher reflectivity closer to sunrise and sunset (0.246).

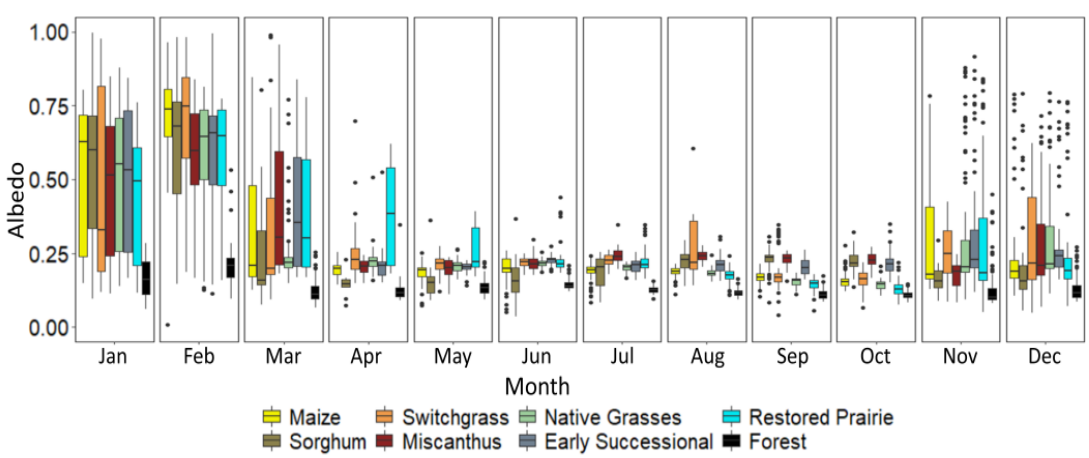

Figure 2.3: Monthly changes of mean albedo at KBS in Southwest Michigan for six biofuel crops, reference maize and reference forest. Error bars indicate ±1.5 IQR.

Solar irradiance averaged around 630 W m^{-2} during the GS, 270 W m^{-2} during the NGS, and 480

W m^{-2} annually. Variations in Δ_{α} among crops were similar between GSs and years for biofuel crops when using either forest or maize as the reference in Eq. 3 (Figure 2.5). Perennial crops showed an average $\Delta_{\alpha FOREST}$ of 0.07 and $\Delta_{\alpha MAIZE}$ of 0.02 during the GS, and a $\Delta_{\alpha FOREST}$ of 0.16 and $\Delta_{\alpha MAIZE}$ of 0.02 during the NGS months. The candidate annual row sorghum had a similar average of $\Delta_{\alpha FOREST}$ of 0.07 and $\Delta_{\alpha MAIZE}$ of 0.02 during the GS, while slightly higher mean Δα were noted during the NGS months ($\Delta_{\alpha FOREST}$ of 0.18; $\Delta_{\alpha MAIZE}$ of 0.04). Annually, albedo change from a historical forest reference to a bioenergy crop was larger (average $\Delta_{\alpha} = 0.10$) (Figure 2.6) compared to albedo changes from reference maize to another bioenergy crop (average $\Delta_{\alpha} = 0.03$).

The forest–perennial crop differences were greater than the forest–annual row crop difference, as indicated by $RF\Delta_{\alpha}$. Average cooling effects from modeling the conversion of maize to another biofuel crop yielded -1.52±1.00 W m^{-2}, while modeled conversions from forest to another biofuel crop showed a -16.75±2.93 W m^{-2} cooling effect (Table A4). Were my forest site was not included in conversion assessments from maize, then annual cooling would have increased from -1.52 ± 1.00 W m^{-2} to -3.83 ± 0.779 W m^{-2}. Highest daily averages in mean growing season RF were observed in miscanthus ($RF\Delta_{\alpha FOREST}$: -20.99 ± 3.45 W m^{-2}; $RF\Delta_{\alpha MAIZE}$: -9.49 ± 1.66 W m^{-2}) and switchgrass ($RF\Delta_{\alpha FOREST}$: -17.37 ± 2.68 W m^{-2}; $RF\Delta_{\alpha MAIZE}$: -6.07 ± 0.96 W m^{-2}). There was also a clear seasonality in RF when modeling the conversion from annual row crop maize to another candidate crop. During the NGS, average cooling effects from planting maize were small, on the order of -0.95 W m^{-2} for all perennials crops versus a -4.54 W m^{-2} during the GS. Overall, changing a stand to early successional, miscanthus and native grasses would yield the highest average annual cooling effects.

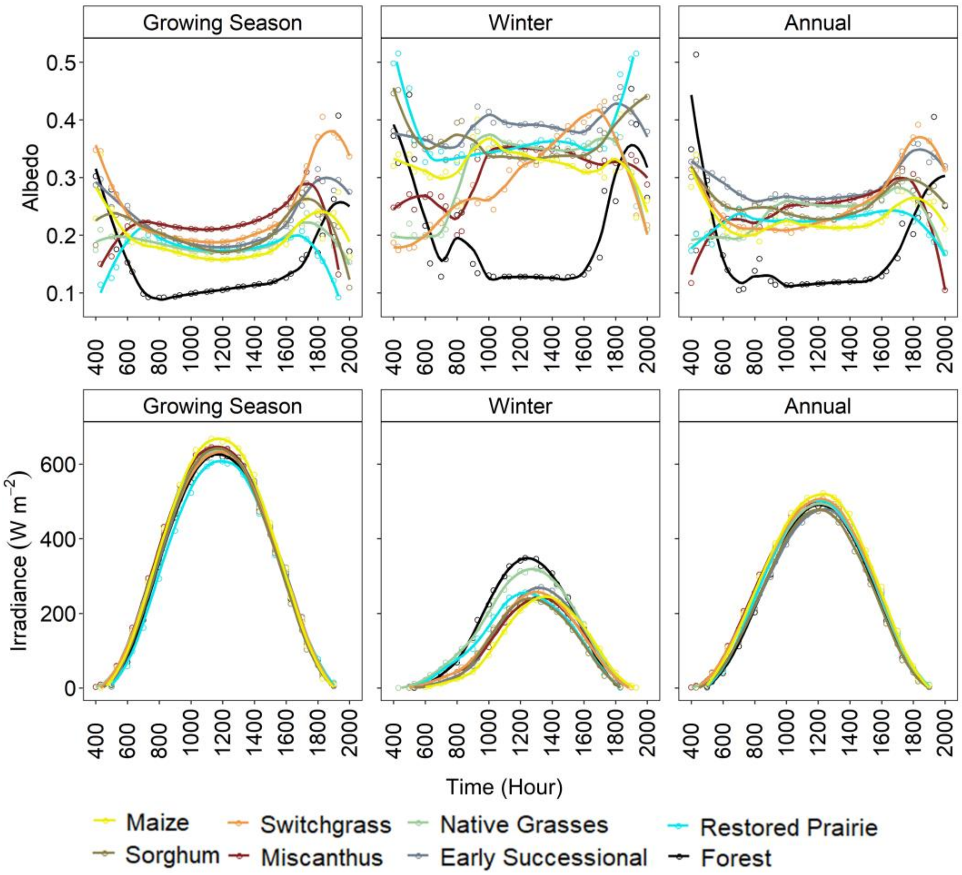

Figure 2.4: Averaged albedo and solar irradiance diurnal variations over the growing season, winter, and annual scale at a reference forest and seven biofuel cropping system in KBS in MI, USA. All sites are averaged with each point representing a 30-minute timestep.

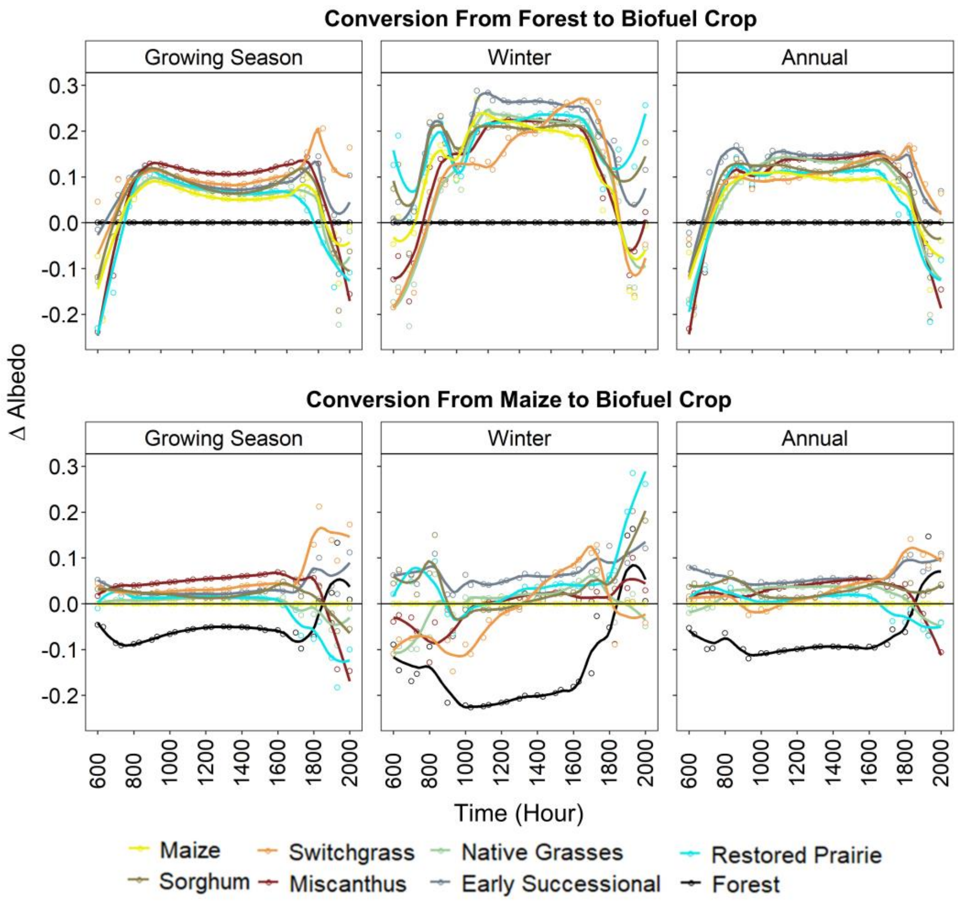

Figure 2.5: Difference in change of albedo (Δ_{α}) between conversion of landscapes of forest (top row) and annual maize crops (bottom row) compared to another biofuel crop albedo for all sites over the growing season, winter, and annually at biofuel cropping system experiment, KBS, MI, USA.

Discussion

Investigations have been made on development of potential biofuel crops, including maize, switchgrass and miscanthus (Abraha et al., 2018; Sanford et al., 2016; Sprunger et al., 2017; Wang et al., 2020). Building upon these previous work at these well-studied biofuel crops, this study focused on changes of albedo at eight ecosystem types in southwest Michigan, USA (i.e., maize, sorghum, switchgrass, miscanthus, native grasses, early successional grassland, restored prairie, and forest) and, for the first time, explored their contributions to the climate due to elevated albedo when compared with either native forest, or dominant maize in the Midwest of USA.

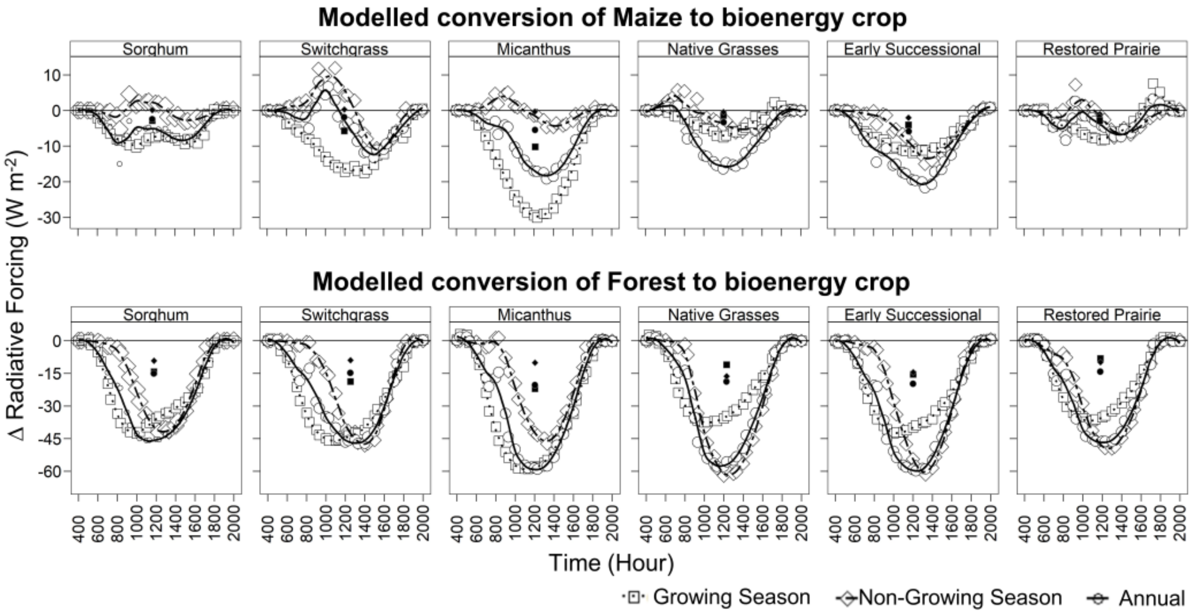

Figure 2.6: Diurnal changes in radiative forcing (RF) due to conversion of forest to biofuel croplands, or from annual row crops of maize to biofuel croplands (including early successional, native grasses, switchgrass, miscanthus, restored prairie, sorghum, maize, and forest). All sites are averaged for the growing season (squares), non-growing season (diamond) and year-round (circles), with each point representing a 30-min mean value. Daily mean values are also computed. Error bars represent ±1SE.

Perennial crops have a higher albedo compared to annual row crops.

Overall, the annual mean albedo for all bioenergy crops in this study ranged between 0.135 (reference forest), 0.223 (reference maize) to 0.245-0.268 for candidate perennials (Figure 2.2), which is consistent with previously reported albedo values for similar perennial grasses and annual row crops (Fritschen, 1967; Krishnan et al., 2012; Kuhn & Suomi, 1958). These values are also comparable to albedo in unmanaged prairies at around 0.240 and 0.260 (Campbell & Norman, 2012). Because these sites were managed agricultural fields, albedo values appeared slightly higher than natural grasslands. Minor changes in surface albedo can result in substantial climate change impact. In general, the differences among crop species were maximal during the early in the growing season, with the perennial grasses having consistently higher albedo. However, at the peak of the GS all biofuel crops had closed canopies, resulting in an elevated interception of irradiance (Figure 2.3). This caused differences in albedo to drop significantly among the biofuel crops.

The reference forest was a mix of both coniferous and deciduous forest, which is advantageous as coniferous forest retain their leaves throughout the winter. Bonan (2008) showed that forests have lower surface albedo than other cover types which contributes to climate warming. The field data indicated a similar conclusion: forest had consistently lower albedo than both perennial and annual row croplands (Figure 2.4, α_s: 0.135). Sciusco et al., (2020) also showed that α_s within forest landscapes in southwest Michigan were almost 3% lower than for their biofuel counterparts. The effect of tree canopy shading on albedo within forests during winter periods and its climatological significance has been researched over the past few decades. Interestingly, the mixed forest landscape at the Kellogg Experimental Forest allowed snow during the winter periods to persist. This occurred due to the tree stand dynamics around the eddy covariance tower, which consisted of both coniferous and deciduous trees. Within northern forested sites such as the one in this study, high solar zenith angles during the winter periods can produce a large canopy shading effect, affecting albedo. Reforestation and afforestation (both prominent in this research forest) can also cause phenology effects, as lichen, understory and younger trees with significant leaf cover can affect the amount of radiation absorbed or reflected. These results were also replicated in other studies as well (Betts & Ball, 1997; Robinson & Kukla, 1984), where albedo in winter mixed forests were estimated to be around 0.11 to 0.15.

Differences in crop albedo from plant seasonality

The GS albedo at my study site indicated a good representation of what the annual albedo of a cropland would be (Figures 2.3, 2.4). Diurnally, incoming solar radiation during the growing season was observed to reach an average of 680 W m^{-2}, while during the winter it was much lower

(279 W m^{-2}). This is due mostly to the changes in solar zenith angles, where the solar radiation in Michigan is much lower during the winter months. Diurnal variations of albedo during the winter period are highly asymmetrical from the early morning to around just after 11:00 hours. This is most likely due to a lack of solar irradiance reaching the surface strongly and consistently, along with inconsistencies in water vapor and other meteorological conditions. This is noted by Grant et al., (2000) who stated that the solar zenith angle makes up a strong component of albedo measurements. Thus, changes in albedo observed during the GSs and NGSs emphasize the importance of understanding landscape dynamics and climate, as albedo can vary during periods of high snow, snowmelt, winter thaws and sunlight intensity.

Land cover dynamics can influence local climate through radiative forcings due to varied biophysical surface properties. Observed differences in α_s associated with different biofuel crops have indicated direct changes in energy budget (Figure 2.5). The study sites had a negative $RF_{\Delta\alpha}$ representing a cooling effect. There was also a strong RF seasonality between NGSs and GSs, averaging -13 W m^{-2} to -1 W m^{-2} in the winter and -16 W m^{-2} to -5 W m^{-2} in the summer (Figure 2.6), depending on the biofuel cropland. Perennials were shown to provide albedo-induced cooling during the summer months, especially for crops having long, dense, green leafy phenology, such as of switchgrass, miscanthus and sorghum. This can have a significant effect on growing season temperatures. As negative RFs correspond to carbon accrual and sequestrations, these crop ecosystems are actively mitigating global warming (Caiazzo et al., 2014).

Climate, agronomic practices and plant species on albedo

Agronomic management also contributed significantly to the surface reflectivity at my study site. Agronomic farming practices, such as conservational tillage, can improve carbon sequestration in soils (Abraha et al., 2021; Robertson et al., 2017), allow for deeper and more comprehensive root growth structures in perennial crops, and reduce soil and nutrient erosion (Odum, 1984). These contributions are coupled with albedo which is generally higher than that of forest (Odum, 1984; Luyssaert et al., 2014; Robertson et al., 2017).

Maize was observed to have much lower albedo during the GS than that of the perennials (Figures 2.2, 2.4). The leaf area index (LAI) of perennials, such as switchgrass, early successional and restored prairie, increased at a much faster rate compared to maize at the beginning of each GS (April/May). This was due to the immediate growth of perennials at the start of the last frost in March. As maize was planted at the sites around early May, this suggests that the land surface was still moderately exposed due to late seeding and small seedlings during the same period. In combination with the tillage performed by many farmers, the dark, bare earth was left exposed to the atmosphere during the first few weeks of the GS when maize absorbs more solar radiation than vegetated fields until their canopies fully develop; hence their overall albedo remains much lower (Figure 2.3). Planting density at the study site for maize was completed in much wider rows at the Kellogg Biological Station, which also affects the amount of radiation through the canopy, i.e., higher warming effect.

Although sorghum is an annual row crop, its planting density at BCSE was much higher than that of maize, which caused it to perform more like a perennial, i.e., a closed canopy during the GS, and thus reflecting more energy back into the atmosphere instead of allowing radiation to filter through its leaves and warm the surface. Sorghum takes approximately six weeks to fully establish a closed canopy, but once it has reached its peak, it remains green until harvest due to its long growing season. Consequently, its average albedo was much more comparable to perennials (0.266) and resembled prior research in the region (Moore et al., 2021). Zeri et al. (2011) and Miller et al. (2016) noted the differences in albedo were highly influenced by planting density, plant morphology, and canopy architecture. Similar variables such as phenology, cover crops and crop residue management also play an integrative role in affecting albedo (Campbell & Norman, 2012; Luyssaert et al., 2014; Odum, 1984).

Albedo during the NGS periods was markedly higher when the landscape was completely or partially covered with snow. Previous research has shown that planting cover crops before the onset of the winter season can aid in the restoration of degraded lands and can be a key method in the expansion of bioenergy crops. Cover crops can also induce a localized cooling effect by reflecting more incoming radiation back into the atmosphere (Lugato et al., 2020). During the winter periods, stover upon the landscape in maize, miscanthus and sorghum at the BCSE sites likely aided in how much snow accumulated and subsequent energy reflected. This is important as management practices of stover residue can alter microclimates, aid in slowing soil erosion, break up snowpack on the surface for much of the winter, subsequently changing surface albedo (Ojekanmi & Johnson, 2021).

These results also show that modeling large scale conversions of landscape by expanding bioenergy crops can significantly affect local climate in the Midwest U.S. (Georgescu et al., 2009; Mykleby et al., 2017). Although annual $RF_{\Delta\alpha}$ were mostly similar among biofuel crops, RFs have strong seasonal variations. The results of modeling the conversion of a forested landscape into another bioenergy crop presented a climate cooling ($RF_{\Delta\alpha}$: -16.75 Wm^{-2}), due to perennial crops having much higher albedo. However, harvesting large forests and planting biofuel crops can inhibit carbon stores within the crop and soil itself (Chen et al., 2004; Noormets, 2016), which could potentially cause higher emission of GHG, i.e., warming effects. As Field et al. (2020) reported, conversions of non-agricultural land with high initial carbon stocks to the cultivation of another biofuel crop could result in large, direct carbon debts that must be overcome via other means of fossil fuel displacement or carbon sequestration before net mitigation is achieved (approximately 70 years) and atmosphere cooling can commence. Meanwhile, Fu et al. (2021) observed that negative $RF_{\Delta\alpha}$ was due to albedo-induced GWP by deforestation, while Bastable et al. (1993) also noted that the widespread deforestation for croplands could lead to positive feedback effects dampening the cooling effects from elevated albedo. At KBS, the models have shown the conversion of maize to another biofuel energy crop tends to avoid the carbon debt, resulting in immediate atmosphere cooling potential. For example, modeling the conversion of a landscape from reference maize to miscanthus within this study resulted in a GS average cooling effect of -9.5 W m^{-2}, while a lack of cover crop with residue stover created a winter neutral effect of -0.2 W m^{-2}. The peak difference in annual mean $RF_{\Delta\alpha}$ between maize and other biofuel croplands (except forest) averaged -3.83±0.779 W m^{-2}, with early successional, miscanthus and native grasses having the highest cooling potentials at -6.77±1.16 W m^{-2}, -5.13±1.02 W m^{-2} and -4.26 ± 0.91 W m^{-2}, respectively. This was similar to prior research, like Miller et al. (2016), who found that switchgrass had a daily cooling potential of -5 W m^{-2}, and miscanthus of -8 W m^{-2}. Sciusco et al. (2020, 2021), who integrated spatial and temporal changes as main drivers of albedo variations showed that cropland had higher albedo and intra-annual variabilities, with an average RF between -5.6 W m^{-2} to -1.2 W m^{-2} when compared to forested regions. However, these values can also vary over time and by years (Bastable et al., 1993). Thus, altering the Earth’s surface properties, including albedo, through agronomic practices (i.e., seeding times, planting density, perenniality) which in turn will produce warming or cooling effects on local to regional climate (Perkins, 2019).

Assumptions and uncertainty

Change in albedo is highly correlated with other land surface properties, where soil moisture (Ahmad & Lockwood, 1979; Weidong et al., 2002) and climate/weather as important variables (Bright et al., 2012). Modifying surface albedo through different avenues, such as crop residue management, may enhance cooling influences (Davin et al., 2014). Vegetative leaves also have complex geometries and textures, which affects radiation absorption and reflectance, and can create lower albedos than that of single stalks and leaves. Changes in the vegetation-dependent parameters of croplands over growing seasons from bare-ground to seeding, to vegetative states, and finally senescence and harvest can also change surface albedo over temporal scales through crop height, crop cover, root dynamics (root depth, CO_2 uptake capacity), leaf texture and leaf age (Henderson-Sellers & Wilson; 1983; Monteith, 1959). Native perennials such as switchgrass and prairie are well-established in the Midwest and continue to prove their benefits in providing alternate fuels as well as mitigating against climate change (Heaton et al., 2008; Lei et al., 2021). However, crops such as miscanthus are relatively new to the U.S., and its nascency makes its viability as a biofuel crop uncertain, especially in its suitability to replace large landscapes such as forests, maize or marginal lands as a potential biofuel crop (Jørgensen et al., 2014; Mishra et al., 2013). Results show that although albedo can potentially drive a localized cooling effect, tradeoffs between climate and biodiversity upon the landscape will be large (Gelfand et al., 2013, 2015).

Accurate quantification of RF from a specific land surface depends not only reliable measurements of albedo, but also on atmospheric transmittance (T_a). Following Muñoz and Kravchenko (2011) and Cherubini et al. (2012), the upward atmospheric transmittance was assumed to be a global constant of 0.854 with a zenith angle of 60° denoting the solar radiation from clear sky conditions. However, I employed a manual daily calculation of T_a as the ratio of

$SW_{\downarrow} / SW_{TOA}$, with calculations of T_a obtained from measurements from towers within each biofuel site. By calculating T_a manually, I reduced my bias in regions of highly variable weather and clouds, and therefore reduced error estimates in radiative forcing by up to 30% (Sciusco et al., 2020).

Finally, the KEF forest was used as the historical reference in this study as there is an established eddy covariance flux tower, which otherwise would prove difficult for calculation of albedo-induced RF. Models suggested that the land conversion from forests to perennial crops, such as switchgrass and miscanthus, provide substantial climate cooling compared to potentially converting from annual maize. However, forests are known to acquire large initial carbon debts requiring long payback periods before substantial gains in albedo-induced cooling are achieved (Mykleby et al., 2017). Changing forest cover can further affect climate change through complex forest-atmosphere dynamics including plant phenology, land changes and climate (Duveiller et al., 2021). As forests, particularly coniferous or mixed- hybrid stands, are known to have lower albedo, increased amounts of radiation can enter the canopy which can lead to higher warming effects and may even offset ecosystem carbon sequestration. However, current afforestation agendas have been considered to effectively sequester carbon as well as provide a benefit to biofuel croplands, with hybrid poplar being an ideal candidate as a biofuel crop, especially in places where landscapes have been deemed marginal and not suited for other biofuel production (Bagley et al., 2014; Zumkehr & Campbell, 2013). Finally, forests are also known to aid in generating cloud cover, which can affect precipitation, and reflect more radiation back into the atmosphere, thus providing a net cooling effect in the long term.

Conclusion

Modifying surface albedo through alternative avenues, such as crop residue management, shifts through conversion of landscapes and seasonality from climate and agronomic practices, may add additional cooling benefits to the warming climate. The annual mean albedo for all biofuel crops in this study ranged between 0.134 (reference forest), 0.223 (reference maize) to 0.245-0.268 for candidate bioenergy crops. Perennials such as miscanthus, had the highest mean ± SE αs during GS 2018 (0.251±0.003), while restored prairie (0.187±0.005), early successional (0.212±0.002) and switchgrass (0.217±0.004) have consistently higher growing season αs compared to annual croplands. GS α_s offered a good representation of what the annual albedo of a cropland will be as the pattern of α_s annually closely mirrored the pattern of GS α_s. The cooling effects were seen across most crops but were higher when converting from forest to another biofuel crop, compared to conversion from maize to another biofuel crop.

Albedo is one of several major warming factors that need to be taken into consideration when understanding what affects the energy balance and how it pertains to climate change (Abraha et al., 2021; Gelfand et al., 2013). Future research should examine the sensitivity of albedo to biogeophysical, biogeochemical and micrometeorological changes. Additionally, long-term observation-based, quantitative estimates of annual to decadal-scale changes of shortwave radiation may also be useful for capturing rare events that are not detected by shorter timescale methods (Schwarz et al., 2020). Lastly, these finding call for inclusion of albedo-induced contributions to climate in developing future bioenergy systems, as well as in the ecosystem models for holistic assessment of these systems.

APPENDIX

Table A3: Table showing full coverage of each crop species measurements taken at the Kellogg Biological Station over the entire study period from 2018 to 2020.

Crop	**Year**	**Days (N)**	**Coverage (%)**
Maize	2018	182	75%
	2019	315	86%
	2020	278	76%
Sorghum	2018	120	49%
	2019	220	60%
	2020	306	84%
Switchgrass	2018	194	80%
	2019	316	87%
	2020	296	81%
Miscanthus	2018	113	46%
	2019	303	83%
	2020	283	78%
Native	2018	198	81%
	2019	355	97%
	2020	330	90%
Early	2018	131	54%
	2019	335	92%
	2020	292	80%
Restored	2018	131	54%
	2019	262	72%
	2020	319	87%
Study	**2018**		**63%**
	2019		**82%**
	2020		**82%**

Table A4: Average radiative forcing (RF; W m^{-2}) due to conversion of annual row crops of maize compared to biofuel croplands as well as conversion of forested landscape compared to biofuel croplands. SE refers to ± 1 standard error.

Crop	**Conversion from Maize**						**Conversion from Forest**					
	Growing Season		Winter Season		Annual		Growing Season		Winter Season		Annual	
	Mean	SE	Mean	SE	Mean	SE	Mean	SE	Mean	SE	Mean	SE
Maize	-		-		-			-	-		-	
Sorghum	-3.72	0.58	-0.18	0.22	-3.08	0.49	-14.84	2.36	-10.76	2.23	-15.26	2.70
Switchgrass	-6.07	0.96	0.13	0.74	-2.13	0.71	-17.37	2.68	-11.66	2.48	-15.53	2.71
Miscanthus	-9.49	1.66	-0.22	0.28	-5.13	1.02	-20.99	3.45	-11.32	2.47	-18.48	3.36
Native Grasses	-1.68	0.38	-1.03	0.37	-4.26	0.91	-12.93	2.17	-16.42	3.43	-17.15	3.27
Early Successional	-4.41	0.70	-3.34	0.73	-6.77	1.16	-15.94	2.42	-15.08	3.16	-19.35	3.36
Restored Prairie	-1.87	0.50	-1.06	0.40	-1.59	0.39	-12.72	2.08	-13.12	2.69	-14.76	2.63
Forest	-		-		-		-		-		-	
Study Period	**-4.54**	**0.93**	**-0.95**	**0.88**	**-3.83**	**1.00**	**-15.80**	**2.53**	**-13.06**	**2.74**	**-16.75**	**3.01**

REFERENCES

REFERENCES

Abraha, M., Chen, J., Hamilton, S. K., Sciusco, P., Lei, C., Shirkey, G. ... & Robertson, G. P. (2021). Albedo-induced global warming impact of Conservation Reserve Program grasslands converted to annual and perennial bioenergy crops. *Environmental Research Letters*, *16*(8), 084059. https://doi.org/10.1088/1748-9326/ac1815

Abraha, M., Hamilton, S. K., Chen, J., Robertson, G. P. (2018). Ecosystem carbon exchange on conversion of Conservation Reserve Program grasslands to annual and perennial cropping systems. *Agricultural and Forest Meteorology*, *253*, 151-160. https://doi.org/10.1016/j.agrformet.2018.02.016

Ahmad, S. B., & Lockwood, J. G. (1979). Albedo. *Progress in Physical Geography*, *3*, 510–543. https://doi.org/10.1177/030913337900300403

Akbari, H., Menon, S., & Rosenfeld, A. (2009). Global cooling: increasing world-wide urban albedos to offset CO_2. *Climatic Change*, *94*(3), 275–286. https://doi.org/10.1007/s10584-008-9515-9

Bagley, J. E., Davis, S. C., Georgescu, M., Hussain, M. Z., Miller, J., Nesbitt, S. W. ... & Bernacchi, C. J. (2014). The biophysical link between climate, water, and vegetation in bioenergy agro-ecosystems. *Biomass and Bioenergy*, *71*, 187–201. https://doi.org/10.1016/j.biombioe.2014.10.007

Bastable, H. G., Shuttleworth, W. J., Dallarosa, R. L. G., Fisch, G., & Nobre, C. A. (1993). Observations of climate, albedo, and surface radiation over cleared and undisturbed Amazonian forest. *International Journal of Climatology*, *13*(7), 783–796. https://doi.org/10.1002/joc.3370130706

Betts, A. K., & Ball, J. H. (1997). Albedo over the boreal forest. *Journal of Geophysical Research: Atmospheres*, *102*(D24), 28901-28909. https://doi.org/10.1029/96JD03876

Betts, R. A. (2001). Biogeophysical impacts of land use on present-day climate: Near-surface temperature change and radiative forcing. *Atmospheric Science Letters*, *2*(1-4), 39–51. https://doi.org/10.1006/asle.2001.0037

Bonan, G. B. (1997). Effects of land use on the climate of the United States. *Climatic Change*, *37*(3), 449–486. https://doi.org/10.1023/A:1005305708775

Bonan, G. B. (2008). Forests and climate change: Forcings, feedbacks, and the climate benefits of forests. *Science*, *320*(5882), 1444–1449. https://doi.org/10.1126/science.1155121

Bright, R. M. Metrics for biogeophysical climate forcings from land use and land Cover changes and their inclusion in life cycle Assessment: A critical review. *Environmental Science Technology* 2015, *49*(6), 3191–3303. https://doi.org/10.1021/es505465t

Bright, R. M., Cherubini, F., & Strømman, A. H. (2012). Climate impacts of bioenergy: Inclusion of carbon cycle and albedo dynamics in life cycle impact assessment. *Environmental Impact Assessment Review, 37*. 2-11. https://doi.org/10.1016/j.eiar.2012.01.002

Brown, D. G., Pijanowski, B. C., & Duh, J. D. (2000). Modeling the relationships between land use and land cover on private lands in the Upper Midwest, USA. *Journal of Environmental Management*, *59*(4), 2427–263. https://doi.org/10.1006/jema.2000.0369

Burakowski, E., Tawfik, A., Ouimette, A., Lepine, L., Novick, K., Ollinger, S. ... & Bonan, G. (2018). The role of surface roughness, albedo, and Bowen ratio on ecosystem energy balance in the Eastern United States. *Agricultural and Forest Meteorology*, *249*, 367–376. https://doi.org/10.1016/j.agrformet.2017.11.030

Cai, H., Wang, J., Feng, Y., Wang, M., Qin, Z., & Dunn, J. B. (2016). Consideration of land use change-induced surface albedo effects in life-cycle analysis of biofuels. *Energy Environmental Science, 9*(9), 2855–2867. https://doi.org 10.1039/C6EE01728B

Caiazzo, F., Malina, R., Staples, M. D., Wolfe, P. J., Yim, S. H. L., & Barrett, S. R. H. (2014). Quantifying the climate impacts of albedo changes due to biofuel production: A comparison with biogeochemical effects. *Environmental Research Letters*, *9*(2). https://doi.org/10.1088/1748-9326/9/2/024015

Campbell, G. S., & Norman, J. (2012). Radiation Fluxes in Natural Environments. In *An Introduction to Environmental Biophysics*; Eds. 2; Springer-Verlag: New York, USA, pp. 167–184.

Carrer, D., Pique, G., Ferlicoq, M., Ceamanos, X., & Ceschia, E. (2018). What is the potential of cropland albedo management in the fight against global warming? A case study based on the use of cover crops. *Environmental Research Letters*, *13*(4). https://doi.org/10.1088/1748-9326/aab650

Chen, J., Lei, C., Sciusco, P. (2021). Biophysical Models and Applications in Ecosystem Analysis. In *Modeling Ecosystem Global Warming Potentials*; Eds. 1; Michigan State University Press: East Lansing, USA, pp. 119–149. https://muse.jhu.edu/book/82816.

Chen, J., Paw U, K. T., Ustin, S. L., Suchanek, T. H., Bond, B. J., Brosofske, K. D., & Falk, M. (2004). Net ecosystem exchanges of carbon, water, and energy in young and old-growth Douglas-fir forests. *Ecosystems, 7*(5), 534–544. https://doi.org/10.1007/s10021-004-0143-6.

Chen, J., Sciusco, P., Ouyang, Z., Zhang, R., Henebry, G. M., John, R., & Roy, D. (2019). Linear downscaling from MODIS to Landsat: Connecting landscape composition with ecosystem functions. *Landscape Ecology*, *34*(12), 2917-2934. https://doi.org/10.1007/s10980019-00928-2

Cherubini, F., Bright, R. M., & Strømman, A. H. (2012). Site-specific global warming potentials of biogenic CO_2 for bioenergy: contributions from carbon fluxes and albedo dynamics. *Environmental Research Letters, 7*. https://doi.org/10.1088/1748-9326/7/4/045902

Cleveland, R. B., Cleveland, W. S., McRae, J. E., & Terpenning, I. (1990). STL: A seasonal-trend decomposition procedure based on Loess. *Journal of Official Statistics*, 6(1), 3-73. https://www.proquest.com/scholarly-journals/stl-seasonal-trend-decomposition-procedure-based/docview/1266805989/se-2.

Cleveland, W. S. (1979). Robust locally weighted regression and smoothing scatterplots. *Journal of the American Statistical Association, 74*(368), 829-836. https://doi.org/10.1080/01621459.1979.10481038

Cleveland, W. S., & Devlin, S. J. (1988). Locally weighted regression: an approach to regression analysis by local fitting. *Journal of the American Statistical Association*, 83(403), 596-610. https://doi.org/10.1080/01621459.1988.10478639

Davin, E. L., Seneviratne, S. I., Ciais, P., Olioso, A., & Wang, T. (2014). Preferential cooling of hot extremes from cropland albedo management. *Proceedings of the National Academy of Sciences*, *111*(27), 9757-9761. https://doi.org/10.1073/pnas.1317323111

Davis, S. C., Anderson-Teixeira, K. J., & DeLucia, E. H. (2009). Life-cycle analysis and the ecology of biofuels. *Trends in Plant Science*, *14*(3), 140–146. https://doi.org/10.1016/j.tplants.2008.12.006

Duveiller, G., Filipponi, F., Ceglar, A., Bojanowski, J., Alkama, R., & Cescatti, A. (2021). Revealing the widespread potential of forests to increase low level cloud cover. *Nature Communications 12*(1), 1–15. https://doi.org/10.1038/s41467-021-24551-5

Fan, J., & Gijbels, I. (2018). *Local Polynomial Modelling and its Applications. Monographs on Statistics and Applied Probability 66*. First Edition, Routledge, New York, NY, USA. https://doi.org/10.1201/9780203748725

Fang, H. L., Liang, S. L., Kim, H. Y., Townshend, J. R., Schaaf, C. L., Strahler, A. H., & Dickinson, R. E. (2007). Developing a spatially continuous 1 km surface albedo data set over North America from Terra MODIS products. *Journal of Geophysical Research*, *112*(D20). https://doi.org/10.1029/2006JD008377

Feng, Q., Chaubey, I., Engel, B., Cibin, R., Sudheer, K. P., & Volenec, J. (2017). Marginal land suitability for switchgrass, miscanthus and hybrid poplar in the Upper Mississippi River Basin (UMRB). *Environmental Modelling Software*, *93*, 356–365. https://doi.org/10.1016/j.envsoft.2017.03.027

Field, J. L., Richard, T. L., Smithwick, E. A., Cai, H., Laser, M. S., LeBauer, D. S., ... & Lynd, L. R. (2020). Robust paths to net greenhouse gas mitigation and negative emissions via advanced biofuels. *Proceedings of the National Academy of Sciences*, *117,* 21968–21977. https://doi.org/10.1073/pnas.1920877117

Flato, G., Marotzke, J., Abiodun, B., Braconnot, P., Chou, S.C., Collins, W., Cox, P., Driouech, F., Emori, S., Eyring, V., Forest, C., Gleckler, P., Guilyardi, E., Jakob, C., Kattsov, V., Reason, C... & Rummukainen, M. (2013). Evaluation of Climate Models. In *Climate Change 2013: The Physical Science Basis. Contribution of Working Group I to the Fifth Assessment Report of the Intergovernmental Panel on Climate Change*; pp. 741-866, Cambridge University Press, Cambridge, United Kingdom and New York, NY, USA.

Forster, P., Ramaswamy, V., Artaxo, P., Berntsen, T., Betts, R., Fahey, D. W. ... & Van Dorland, R. (2007). Changes in atmospheric constituents and in radiative forcing. In *Climate change 2007. The Physical Science Basis*. Broadway, Cambridge University Press, Cambridge, United Kingdom and Boulder, CO, USA. http://www.ipcc.ch/pdf/assessment-report/ar4/wg1/ar4-wg1-chapter2.pdf

Fritschen, L. J. (1967). Net and solar radiation relations over irrigated field crops. *Agricultural Meteorology*, 1967, *4*(1), 55–62. https://doi.org/10.1016/0002-1571(67)90042-8

Fu, B., Li, B., Gasser, T., Tao, S., Ciais, P., Piao, S. ... & Xu, J. (2021). The contributions of individual countries and regions to the global radiative forcing. *Proceedings of the National Academy of Sciences*, *118*(15). https://doi.org/10.1073/pnas.2018211118

Gelfand, I., & Robertson, G. P. (2015). Mitigation of greenhouse gases in agricultural ecosystems. In: *The Ecology of Agricultural Landscapes: Long-term Research on the Path to Sustainability*, 310-339. Oxford University Press, New York, NY, USA.

Gelfand, I., Hamilton, S. K., Kravchenko, A. N., Jackson, R. D., Thelen, K. D., & Robertson, G. P. (2020). Empirical evidence for the potential climate benefits of decarbonizing light vehicle transport in the US with bioenergy from purpose-grown biomass with and without BECCS. *Environmental Science & Technology*, *54*(5), 2961-2974. https://doi.org/10.1021/acs.est.9b07019

Gelfand, I., Sahajpal, R., Zhang, X., Izaurralde, R. C., Gross, K. L., & Robertson, G. P. (2013). Sustainable bioenergy production from marginal lands in the US Midwest. *Nature*, *493*(7433), 514-517. https://doi.org/10.1038/nature11811

Georgescu, M., Lobell, D. B., & Field, C. B. (2011). Direct climate effects of perennial bioenergy crops in the United States. *Proceedings of the National Academy of Sciences, 108*(11), 4307–4312. https://doi.org/10.1073/pnas.1008779108

Georgescu, M., Lobell, D. B., & Field, C. B. (2009). Potential impact of US biofuels on regional climate. *Geophysical Research Letters*, *36*(21). https://doi.org/10.1029/2009GL040477

Grant, I. F., Prata, A. J., & Cechet, R. P. (2000). The impact of the diurnal variation of albedo on the remote sensing of the daily mean albedo of grassland. *Journal of Applied Meteorology*, *39*(2), 231–244. https://doi.org/10.1175/1520-0450(2000)039<0231:TIOTDV>2.0.CO;2

Hartmann, D. L. (1994). *Global Physical Climatology*. Second Edition, Elsevier, Waltham, MA, USA.

Heaton, E. A., Dohleman, F. G., & Long, S. P. (2008). Meeting US biofuel goals with less land: The potential of miscanthus. *Global Change Biology*, *14*(9), 2000–2014. https://doi.org/10.1111/j.1365-2486.2008.01662.x

Henderson-Sellers, A. (1980). Albedo changes—surface surveillance from satellites. *Climatic Change*, *2*(3), 275–281. https://doi.org/10.1007/BF00137991

Henderson-Sellers, A., & Hughes, N. A. (1982). Albedo and its importance in climate theory. *Progress in Physical Geography*, *6*(1), 1–44. https://doi.org/10.1177%2F030913338200600101

Henderson-Sellers, A., & Wilson, M. (1983). Surface albedo data for climatic modeling. *Reviews of Geophysics*, *21*(8), 1743–1778. https://doi.org/10.1029/RG021i008p01743

IPCC. (2013). Climate change 2014: Synthesis report. Contribution of working groups I, II and III. In *Fifth Assessment Report of the Intergovernmental Panel on Climate Change*. Pachauri, R.K., Meyer, L.A., Geneva, Switzerland 2008, pp. 151.

Jonsell, U., Hock, R., & Holmgren, B. (2003). Spatial and temporal variations in albedo on Storglaciären, Sweden. *Journal of Glaciology*, *49*(164), 59–68. https://doi.org/10.3189/172756503781830980

Jørgensen, S. V., Cherubini, F., & Michelsen, O. (2014). Biogenic CO_2 fluxes, changes in surface albedo and biodiversity impacts from establishment of a miscanthus plantation. *Journal of Environmental Management*, *146*, 346–354. https://doi.org/10.1016/j.jenvman.2014.06.033

Krishnan, P., Meyers, T. P., Scott, R. L., Kennedy, L., & Heuer, M. (2012). Energy exchange and evapotranspiration over two temperate semi-arid grasslands in North America. *Agricultural and Forest Meteorology*, *153*, 31–44. https://doi.org/10.1016/j.agrformet.2011.09.017

Kuhn, P. M., & Suomi, V. E. (1958). Airborne observations of albedo with a beam reflector. *Journal of Meteorology*, *15*(2), 172–174. https://doi.org/10.1029/JZ065i011p03669

Lei, C., Abraha, M., Chen, J., & Su, Y. J. (2021). Long-term variability of root production in bioenergy crops from ingrowth core measurements. *Journal of Plant Ecology*, *14*(5), 757-770. https://doi.org/10.1093/jpe/rtab018

Lenton, T. M., & Vaughan, N. E. (2009). The radiative forcing potential of different climate geoengineering options. *Atmospheric Chemistry and Physics, 9*(15), 5539-5561. https://doi.org/10.5194/acp-9-5539-2009

Loarie, S. R., Lobell, D. B., Asner, G. P., Mu, Q., & Field, C. B. (2011). Direct impacts on local climate of sugar-cane expansion in Brazil. *Nature Climate Change*, *1*(2), 105-109. https://doi.org/10.1038/nclimate1067

Lugato, E., Cescatti, A., Jones, A., Ceccherini, G., & Duveiller, G. (2020). Maximising climate mitigation potential by carbon and radiative agricultural land management with cover crops. *Environmental Research Letters*, *15*(9), 094075. https://doi.org/10.1088/1748-9326/aba137

Luyssaert, S., Jammet, M., Stoy, P. C., Estel, S., Pongratz, J., Ceschia, E. ... & Gielen, B. (2014). Land management and land-cover change have impacts of similar magnitude on surface temperature. *Nature Climate Change*, *4*(5), 389–393. https://doi.org/10.1038/nclimate2196

Miller, J. N., VanLoocke, A., Gomez-Casanovas, N., & Bernacchi, C. J. (2016). Candidate perennial bioenergy grasses have a higher albedo than annual row crops. *Global Change Biology: Bioenergy*, *8*(4), 818–825. https://doi.org/10.1111/gcbb.12291

Mishra, U., Torn, M. S., & Fingerman, K. (2013). Miscanthus biomass productivity within US croplands and its potential impact on soil organic carbon. *Global Change Biology: Bioenergy*, *5*(4), 391–399. https://doi.org/10.1111/j.1757-1707.2012.01201.x

Monteith, J. L. (1959). The reflection of short-wave radiation by vegetation. *Quarterly Journal of the Royal Meteorological Society*, *85*(366), 386–392. https://doi.org/10.1002/qj.49708536607

Moore, C. E., von Haden, A. C., Burnham, M. B., Kantola, I. B., Gibson, C. D., Blakely, B. J., ... & Bernacchi, C. J. (2021). Ecosystem-scale biogeochemical fluxes from three bioenergy crop candidates: How energy sorghum compares to maize and miscanthus. *Global Change Biology: Bioenergy*, *13*(3), 445–458. https://doi.org/10.1111/gcbb.12788

Muñoz, J. D., & Kravchenko, A. (2011). Soil carbon mapping using on-the-go near infrared spectroscopy, topography and aerial photographs. *Geoderma*, *166*(1), 102–110. https://doi.org/10.1016/j.geoderma.2011.07.017

Mykleby, P. M., Snyder, P. K., & Twine, T. E. (2017). Quantifying the trade-off between carbon sequestration and albedo in midlatitude and high-latitude North American forests. *Geophysical Research Letters*, *44*(5), 2493–2501. https://doi.org/10.1002/2016GL071459

NCDC. (2013). Climate Data Online (CDO), *National Climatic Data Center (NCDC). NCDC National Oceanic and Atmospheric Administration*, https://www.ncdc.noaa.gov/cdo-web/search

NOAA. (2005). ESRL Global Monitoring Laboratory - Global Radiation and Aerosols. Earth System Research Laboratories Global Monitoring Laboratory. https://gml.noaa.gov/grad/solcalc/

Noormets, A. (2016). Trade-off between forest productivity and carbon sequestration in soil. In: *Proceedings of the 18th biennial southern silvicultural research conference*, e-Gen. Tech. Rep. SRS-212. Asheville, NC: US Department of Agriculture, Forest Service, Southern Research Station. *212*, 351-354. https://www.fs.usda.gov/treesearch/pubs/50700

Odum, E.P. (1984). Properties of agroecosystems. pp 5-11 in R. Lowrance, B.R. Stinner, and G.J. House, editors. *Agricultural Ecosystems: Unifying Concepts*. John Wiley, New York, USA.

Ojekanmi, A., & Johnson, J. M. (2021). Quantifying improvements in water-stable aggregation caused by corn stover retention. *Soil Science Society of America Journal*, *85*(3), 776-788. https://doi.org/10.1002/saj2.20198

Ollinger, S. V., Richardson, A. D., Martin, M. E., Hollinger, D. Y., Frolking, S. E., Reich, P. B., ... Smith, M. L. (2008). Canopy nitrogen, carbon assimilation, and albedo in temperate and boreal forests: Functional relations and potential climate feedbacks. *Proceedings of the National Academy of Sciences*, *105*(49), 19336-19341. https://doi.org/10.1073/pnas.0810021105

Pachauri, R. K., Allen, M. R., Barros, V. R., Broome, J., Cramer, W., Christ, R. ... & van Ypserle, J. P. (2014). Climate change 2014: synthesis report. Contribution of Working Groups I, II and III. In *The Fifth Assessment Report of the Intergovernmental Panel on Climate Change*, 151.

Perkins, S. (2019). Core Concept: Albedo is a simple concept that plays complicated roles in climate and astronomy. *Proceedings of the National Academy of Sciences*, *117*(3), 1816-1816. https://doi.org/10.1073/pnas.1918770116

Pielke Sr, R. A., Pitman, A., Niyogi, D., Mahmood, R., McAlpine, C., Hossain, F. ... & Reichstein, M. (2011). Land use/land cover changes and climate: modeling analysis and observational evidence. *Wiley Interdisciplinary Reviews: Climate Change*, *2*(6), 828–850. https://doi.org/10.1002/wcc.144

Poe, J., Reed, D. E., Abraha, M., Chen, J., Dahlin, K. M., Desai, A. R. (2020). Geospatial coherence of surface-atmosphere fluxes in the upper Great Lakes region. *Agricultural and Forest Meteorology*, *295*, 108188. https://doi.org/10.1016/j.agrformet.2020.108188

R Development Team. (2013). *R Foundation for Statistical Computing*, Vienna, Austria, *3*.

Raupach, M. R. (1994). Simplified expressions for vegetation roughness length and zero-plane displacement as functions of canopy height and area index. *Boundary-Layer Meteorology*, *71*(1), 211–216. https://doi.org/10.1007/BF00709229

Robertson, G. P., Hamilton, S. K., Barham, B. L., Dale, B. E., Izaurralde, R. C., Jackson, R. D., Landis, D. A., Swinton, S. M., Thelen, K. D., & Tiedje, J. M. (2017). Cellulosic biofuel contributions to a sustainable energy future: Choices and outcomes. *Science*, *356*(6345). https://doi.org/10.1126/science.aal2324

Robinson, D. A., & Kukla, G. (1984). Albedo of a dissipating snow cover. *Journal of Applied Meteorology and Climatology*, *23*(12), 1626-1634. https://doi.org/10.1175/1520-0450(1984)023<1626:AOADSC>2.0.CO;2

Russel, H.N. (1916). On the albedo of the planets and their satellites. *Proceedings of the National Academy of Sciences*, *2*(2), 74-77. https://doi.org/10.1073/pnas.2.2.7

Sanford, G. R., Oates, L. G., Jasrotia, P., Thelen, K. D., Robertson, G. P., & Jackson, R. D. (2016). Comparative productivity of alternative cellulosic bioenergy cropping systems in the North Central USA. *Agriculture, Ecosystems & Environment*, *216*, 344-355.https://doi.org/10.1016/j.agee.2015.10.018

Schwarz, M., Folini, D., Yang, S., Allan, R. P., & Wild, M. (2020). Changes in atmospheric shortwave absorption as important driver of dimming and brightening. *Nature Geoscience*, *13*(2), 110–115. https://doi.org/10.1038/s41561-019-0528-y

Sciusco, P., Chen, J., Abraha, M., Lei, C., Robertson, G. P., Lafortezza, R. ... & John, R. (2020). Spatiotemporal variations of albedo in managed agricultural landscapes: inferences to global warming impacts (GWI). *Landscape Ecology*, *35*(6), 1385–1402. https://doi.org/10.1007/s10980-020-01022-8

Sciusco, P., Chen, J., Giannico, V., Abraha, M., Lei, C., Shirkey, G. ... & Robertson, G. P. (2022). Albedo-Induced global warming impact at multiple temporal scales within an upper Midwest USA watershed. *Land*, *11*(2), 283. https://doi.org/10.3390/land11020283

Sprunger, C. D., Oates, L. G., Jackson, R. D., & Robertson, G. P. (2017). Plant community composition influences fine root production and biomass allocation in perennial bioenergy cropping systems of the upper Midwest, USA. *Biomass and Bioenergy*, *105*, 248-258. https://doi.org/10.1016/j.biombioe.2017.07.007

Thoen, G. F. (1990). *Soil Survey of Barry County, Michigan*. (USDA Soil Conservation Service, Michigan Agricultural Experiment Station, and Michigan Technological University, Washington DC), pp. 187, 286.

Ustin, S. L., Middleton, E. M. (2021). Current and near-term advances in Earth observation for ecological applications. *Ecological Processes*, *10*(1), 1–57. https://doi.org/10.1186/s13717-020-00255-4

Wang, K., Liu, J., Zhou, X., Sparrow, M., Ma, M., Sun, Z., & Jiang, W. (2004). Validation of the MODIS global land surface albedo product using ground measurements in a semidesert region on the Tibetan Plateau. *Journal of Geophysical Research: Atmospheres*, *109*(D5). https://doi.org/10.1029/2003JD004229

Wang, S., Sanford, G. R., Robertson, G. P., Jackson, R. D., & Thelen, K. D. (2020). Perennial bioenergy crop yield and quality response to nitrogen fertilization. *Bioenergy Research*, *13*(1), 157-166. https://doi.org/10.1007/s12155-019-10072-z

Weidong, L., Baret, F., Gu, X.-F., Tong, Q.-X., Zheng, L.-F., & Zhang, B. (2002). Relating soil surface moisture to reflectance. *Remote Sensing of the Environment*, *81*(2-3), 238-246. https://doi.org/10.1016/S0034-4257(01)00347-9

Zeri, M., Anderson-Teixeira, K., Hickman, G., Masters, M., DeLucia, E., & Bernacchi, C. J. (2011). Carbon exchange by establishing biofuel crops in Central Illinois. *Agriculture, Ecosystems & Environment*, *144*(1), 319–329. https://doi.org/10.1016/j.agee.2011.09.006

Zhang, X. T., Liang, S. L., Wang, K. C., Li, L., & Gui, S. (2010). Analysis of global land surface shortwave broadband albedo from multiple data sources. *IEEE Journal of Selected Topics in Applied Earth Observations and Remote Sensing*, *3*(3), 296–305. https://doi.org/10.1109/jstars.2010.2049342

Zumkehr, A., & Campbell, J. E. (2013). Historical US cropland areas and the potential for bioenergy production on abandoned croplands. *Environmental Science Technology*, *47*(8), 3840–3847. https://doi.org/10.1021/es3033132

CHAPTER 3. LAND COVER AND CLIMATE CHANGE ALTERS SURFACE ALBEDO DURING THREE CULTIVATION SEASONS

Abstract

The impact on albedo of climate and agronomic practices such as diverse plantings, fertilization, and stover removal have not been well investigated in bioenergy systems. This study quantified through instantaneous measurements, the albedo (α_s) in managed biofuel croplands in southwestern Michigan at the Kellogg Biological Station over three growing seasons. The cropping systems were (i) continuous corn stover (*Zea mays L.*), energy sorghum (*Photoperiod insensitive hybrid TAM 17900 variety*) (iii) switchgrass (*Panicum virgatum L.*), (iv) giant miscanthus (*Miscanthus* × *giganteus*), (v) native grass mix, (vi) early successional community, and (vii) restored prairie. Evidence of changes in surface reflectivity for all replicates ranged between 0.180 and 0.212. Significant variance between surface albedo (α_s) and yearly change (ω^2 = 11.01%), biofuel crop (ω^2 = 6.05%), and seasonality (ω^2 = 9.10%) were observed. Average chlorophyll content was highest for maize (45.1±4.8), and lower in perennials switchgrass, sorghum, restored prairie and native grasses averaged (34.4±3.1). Overall, only about 28% of fertilized treatments were higher than their non-fertilized counterpart, showing that treatments did not explain much of the variation observed in albedo (ω^2: only 0.20%). Investigating the effects of fertilizer, unique biofuel croplands and dynamic landscapes on albedo will be an important strategy for fully understanding the climate benefits of biofuel production.

Introduction

Numerous crops have been proposed as bioenergy alternative for the emerging cellulosic ethanol industry, but information is lacking about the importance of bioenergy production and its effects on surface reflectivity and climate. As land is continuously converted into crops primed for biofuel productivity, concern has recently grown over changes in land use and land cover (LULC) and how it affects surface reflectivity (e.g., albedo) and thus climate benefits (i.e., warming/cooling). Given the benefits of expanding biofuels include soil carbon accumulation, reduced greenhouse gas emissions (GHGs) combat fossil fuel consumption, research on additional next-generation fuels has been ongoing. However, issues including land requirements, environmental sustainability, biodiversity, and crop management are major concerns which need to be addressed in order to maintain environmental benefits from biofuel crop production (Robertson et al., 2011, 2017).

Albedo (α_s) is the ratio of outgoing shortwave radiation ($SW_{\uparrow}$) from a surface (e.g., grassland, forest, urban) to incident shortwave radiation ($SW_{\downarrow}$), ranging from 0 (complete absorption) to 1 (complete reflection) (Henderson-Sellers & Hughes, 1982; Russel, 1916). Warming occurs when there is less reflection of radiation back to space, whereas cooling occurs when there is more reflectance (Lenton & Vaughn, 2009; Ollinger et al., 2008). Surface albedo dynamics are closely related to landscape dynamics and can vary widely depending on the characteristics of the surface (e.g., texture, lead area index, soil water content). Land use and land management further influence these characteristics. Collectively, these directly affect local to regional climate by altering surface energy balance through changes in albedo reflectance. For a cultivated landscape, land use, specifically through crop selection, can influence albedo through crop phenology. Characteristics of crops that can influence albedo include: the height of the crop, percentage of ground cover exposed or shielded during the growing season (GS), and specific features, such as the angle of leaves and leaf area index (Ahmad and Lockwood, 1979; Hartmann, 1994; Henderson-Sellers & Hughes, 1982; Moore, 2020). Vegetative surface reflectance and chlorophyll content both heavily depends on climate and soil moisture, which are strongly related to the precipitation and its distribution over time, as well as plant phenology and texture including leaf area surface and indices (Luyssaert et al., 2014), plant height (Betts, 2001) as most importantly, agricultural practices (Robertson et al., 2017). As such, impacts of climate change and variations on ecosystem processes subsequently affect surface albedo characteristics.

Biological crop yield is the total dry matter, including both the economically useful portions of the crops and the remainder (Yoshida, 1972). Crops with greater dry matter will tend to have more mass and surface area. This is consistent with the idea that the amount of chlorophyll is related to plants' growth rate (Brougham, 1960). Chlorophyll content has also been observed to be strongly related to leaf nitrogen content, also known as foliar nitrogen (N) (Houles et al., 2007; Van den Berg & Perkins, 2004; Yuan et al., 2016). First, there is the positive relationship between chlorophyll content and biological crop yield (Ghimire et al., 2015; Ramesh et al., 2002). This is important as some perennial crops are known to produce similar or greater biomass than maize depending on climate, soil, and land management. Moreover, the relationship between chlorophyll content and crop yield is moderated by fertilization (Islam et al., 2014), illustrating the intersection between agronomic practice and plant anatomy on surface reflectivity. One study revealed significant relationships between albedo and canopy nitrogen, where plants with higher concentrations of nitrogen absorbed less radiation than plants with less nitrogen (Ollinger et al., 2008). This can be due to increased temperatures, foliar N–photosynthesis relationships, or from over-fertilizing, where crops are given more nitrogen than needed. This can influence surface reflectance, canopy/internal leaf structure, which in turn causes more light to scatter and an increase in reflectance.

Despite the capacity of agronomic practices (e.g., diverse plantings, tillage, fertilization, pest protection and stover removal) to impact plant phenology, the specific relationships between agronomic practices and albedo have not been thoroughly investigated (Robertson et al., 2017). Fertilizer—particularly the use of nitrogen—has become a primary input in biofuel crop production and management. Some prior work has shown that crop residue and bare soil have varying surface reflectance (Chen & McKyes, 1993), but does not specifically address agronomic practices, such as the relationship between stover removal, fertilization and albedo. Investigations of land use change has also indicated potential variance in surface reflectance in correspondence to the species of crops planted (Cai et al., 2016). Cresswell et al. (1993) has posited that the impact of soil tillage on albedo is negligible based on their results with minimum, intermediate, and excess tillage. Consequently, the present study focused on fertilization, residue, and crop type as potential influencers of albedo.

Traditionally, studies have quantified albedo through remote sensing and large, expansive eddy covariance towers, but more in-depth analysis at the local scale has not been fully investigated. For example, Wang (2004) analyzed MODIS land surface albedo and noted its effectiveness in scientific studies. Building on this framework, MODIS albedo products can be used to study the changes in surface albedo at landscape scale, for a range of cover types, including cropland, biofuel crops of maize, forests, and grasslands. (Cai et al., 2016; Sciusco et al., 2020; Wang & Davidson, 2007). These results suggest that biogeophysical (i.e., temperature, plant phenology, land dynamics, climate) effects of albedo from LULC changes are critically important, with implications that could outweigh the biogeochemical (i.e., GHG emissions of CO_2, N_2O, CH_4, water availability, field operation emissions) effects usually modeled in traditional life cycle assessments (LCAs). Another main disadvantage of remote sensing products is their inability to continuously monitor changes throughout the same day, instead only providing a snapshot at a certain time as the satellite passes over. This study provides an overview of changes on albedo and its determinants based on real ground measurements of different biofuel crops, which offer higher spatial and temporal resolution over existing agroecosystems in determining accurate albedo.

This study explored the following hypotheses:

1. Perennial crops have a higher albedo compared to annual row crops.
2. The albedo of different crops are significantly different due to plant seasonality during the growing season (i.e., plant vegetative stages of early GS, peak GS and senescence).
3. Agronomic practices of fertilization/ non-fertilization and stover removal/ retaining stover treatments will affect surface reflectivity.
4. Chlorophyll content and its relationship with plants' anatomical and physiological characteristics are related to surface reflectivity, and are dependent on climate, plant growth stage, and plant type and phenology.

The study site was the Kellogg Biological Station, an agricultural station within southwest Michigan, located within semirural landscape and home to a cropping system typical of the U.S. Great Lakes and upper Midwest regions. The overarching goal of the study was to quantify the spatiotemporal changes of albedo (α_s) across managed bioenergy crop systems (maize, sorghum, switchgrass, miscanthus, native grasses, early successional and restored prairie) by using instantaneous measurements at the surface. To explore the hypotheses, the study aimed to (a) estimate the magnitudes and temporal (i.e., intra-annual and inter-annual scales) changes of albedo in bioenergy crops during three growing seasons (2018, 2019, 2020), (b) investigate the effects of agronomic practices through the treatments of fertilization and stover removal on different biofuel crop albedo, and (c) determine how changes in climate and chlorophyll content affect albedo of each type of biofuel crop. This work will provide a greater understanding of the effects of unique cropping, agronomic practices and climate on surface reflectivity.

Methods

Study site

The study site is situated at the Great Lakes Bioenergy Research Center (GLBRC) Biofuel Cropping System Experiment (BCSE, https://lter.kbs.msu.edu/). The climate is observed to have an average annual air temperature of 9.9° C, with 1005 mm of average annual precipitation (NCDC, 2013; Robertson and Hamilton, 2015). The physiography of my study site is representative of southwest Michigan, with a mature glacial outwash plain and moraine complex consisting of the Kalamazoo series (fine-loamy, mixed, mesic Typic Hapludalfs) and Oshtemo series (coarse-loamy, mixed, mesic Typic Hapludalfs) soils (Crum et al., 1995; Muñoz & Kravchenko, 2011; Thoen, 1990). Established in 2008, the BCSE study site includes 5 replicated blocks of 10 cropping systems which were replicated in 28 m × 40 m plots. Each plot is then further divided into a main plot (22 m x 40 m) and a subplot (5 m x 40 m), which provided a means for comparing alternative agronomic practices such as stover removal vs. remaining (maize) and fertilized (F) or unfertilized (NF) treatments for all additional candidate bioenergy crops (Figure. 3.1). The cropping systems measured included annual row crops of continuous no-till maize (G1, *Zea mays L.*) and energy sorghum (G2, *photoperiod insensitive hybrid TAM 17900*), monoculture perennials of switchgrass (G5, *Panicum virgatum L.*) and miscanthus (G6, *Miscanthus x giganteus*) and polyculture perennials of native grasses (G7, a mix of 4 species), early successional vegetation (G9), and restored prairie (G10) (See Supplementary Table A5 for detailed summary of crop used). Maize was planted in early May and harvested around mid-October each year, while sorghum was planted later in June and harvested in November. Perennials were planted in 2008 and are fertilized annually on their respective macro-plot (Table 3.1).

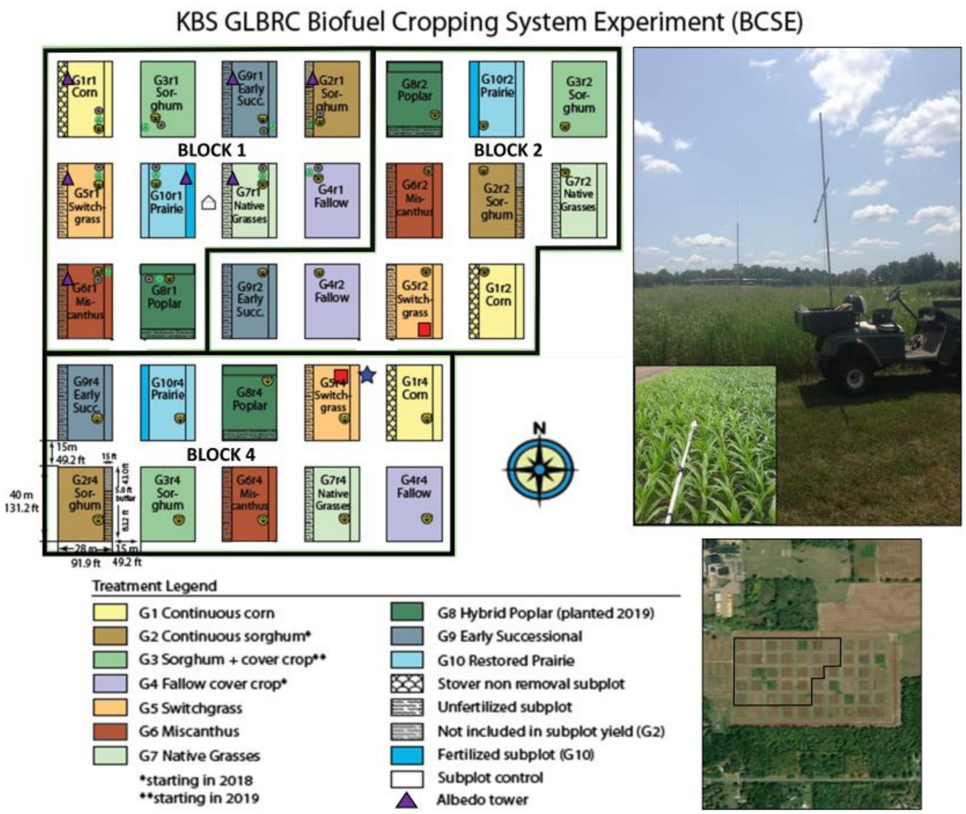

Figure 3.1: Principal study site GLBRC Biofuel Cropping System Experiment (BCSE) at the Kellogg Biological Station. Replicates 1, 2 and 4 in study are outlined in black. Image depicts method of instantaneous measurements with insert showing sensor above the vegetation canopy. Map has been modified from https://lter.kbs.msu.edu.

Table 3.1: Management dates for all sites at the BCSE site, Kellogg Biological Station, MI, which include planting and harvesting. Initial planting of perennials were included.

Crop	**Year**											
	2008			**2018**			**2019**			**2020**		
	Plant	**Fert**	**Harv**	**Plant**	**Fert**	**Harv**	**Plant**	**Fert**	**Harv**	**Plant**	**Fert**	**Harv**
Maize	05/07	05/07	11/04	05/01	06/07	10/04	05/19	06/05	10/29	05/13	05/04	10/29
Sorghum	05/07	05/07	11/04	06/02	06/07	11/07	06/07	06/05	11/20	05/27	05/27	11/17
Switchgrass	06/19		09/11	-	05/23	10/24	-	05/16	11/08	-	05/21	10/17
Miscanthus	05/23		07/28	-	05/23	11/07	-	05/16	11/05	-	05/21	11/14
Native Grasses	06/17		09/11	-	05/23	10/24	-	05/16	10/24	-	05/21	10/17
Early Successional	05/05			-	05/23	10/24	-	05/16	10/23	-	05/21	10/17
Restored Prairie	06/17		09/11	-	05/23	10/24	-	05/16	10/23	-	05/21	10/17

Acronyms: Fert = Fertilized; Plant = Planted; Harv = Harvested.

Data collection and instrumentation

Data was collected at BCSE during the growing season from May 1st to October 30th for three years 2018-2020. Measurements were taken at the restricted treatments of block one (N = 478), block two (N = 471) and block four (N = 445) and were taken weekly during peak growing season (May to August) and biweekly up to plant senescence (August to October) (See Supplementary Table A6 for detailed summary of measurements per crop). To perform instantaneous measurements at my study site, a portable four-component net radiometer (CNR4, Kipp & Zonen, Netherlands) was mounted on a mobile unit. The height of the mobile measurements in each plot changed according to the current plant height in order to maintain optimal sensor field of view to the vegetation. The instruments were always higher than $1.41h_c$, where h_c is the average height of the crop (Raupach, 1994; Zeri et al., 2011). Shortwave incoming and outgoing radiation was recorded at one-second intervals and converted to per-minute averages that were logged at 10-Hz using a Campbell 1000X datalogger (Campbell Scientific Inc., Logan, UT, USA) in order to determine albedo (Eq. 1). Measurements included both main plots and subplots in within each site and were taken approximately between 10:00 and 14:00 hours UTC-5 to coincide with MODIS satellite imaging trajectories, as well as to ensure that data measurements were consistent around solar noon to reduce bias.

Data was also collected to evaluate the contribution and relationship that chlorophyll content had on albedo, land cover and management practices biweekly. At each site, a Soil Plant Analysis Development (SPAD; a.u.) was used to measure chlorophyll content within crops within all blocks and at both treatment sites. During measurement, a healthy crop representing the majority of the treatment plot was selected. To calculate average chlorophyll, three measurements were taken per leaf and the leaf was kept under shade of the body to avoid color variance caused by sun's angle and sunlight intensity.

Precipitation and air temperature from a nearby micrometeorological tower (42°24'36.8"N 85°22'22.3"W) were retrieved over the period of 2018–2020 (https://lter.kbs.msu.edu/datatables). Precipitation was measured using a NOAH IV gauge (ETI Instruments, Severance, CO, USA), while air temperature was measured by a model 107 temperature probe (Campbell Scientific Inc., Logan, UT, USA), housed in a vented shield, at 3 meters. The cumulative precipitation and average air temperature during the study period were calculated for the study site to determine the effects of climate on plant growth and subsequently on changes in albedo.

Statistical analysis

Data were analyzed in the statistical software R (R Development Team, 2013) and Esri ArcGIS v.10.2.2 (ESRI, 2011). Albedo (hereafter referred to as α_s) was calculated as follows (Eq. 1):

$$\alpha_s = \frac{SW_\uparrow}{SW_\downarrow} \tag{1}$$

Where $SW_\uparrow$ is the outgoing shortwave radiation, and $SW_\uparrow$ is the incoming shortwave radiation. Instantaneous observations of albedo, chlorophyll content, air temperature and precipitation were recorded and plotted annually to observe change over time. As albedo measurements were carried out over multiple blocks and treatments for different biofuel crops, albedo was also averaged to investigate changes in surface reflectivity over time.

An analysis of variance (ANOVA) was used to examine the change in albedo within the three-year study period and across three seasons, where the following model was used for albedo:

$$\alpha_s = crop \cdot year \cdot treatment \cdot season \tag{2}$$

where α_s (dependent variable) is the surface instantaneous albedo, 'crop' is the biofuel crop, 'year' is the year of study (i.e., 2018-2020), 'treatment' refers to agronomic practices (i.e., fertilization versus no fertilization or stover removed versus no stover removed from the maize sites), and 'season' refers to the three major delineations of the growing season (i.e., early, peak, and senescence), respectively. All interaction terms between each independent variables were investigated to determine the estimate of how much the dependent variance accounted for by the independent variable in my study. Lastly, the distribution of all residuals was examined

Mean albedo among years and sites were compared using Tukey's HSD test with treatment effects considered significant at $p < 0.05$. A linear regression was completed between albedo and chlorophyll content, using the treatment micro-plots as effects. All solid lines were fitted using a local loess regression model. Finally, ArcGIS was used to plot visual effects of albedo for three times during the year: (a) early growing season (May), (b) peak growing season (June-August) and (c) plant senescence (September) for each biofuel crop for all three blocks.

Results

Precipitation and air temperature

Observations from 2018 to 2020 for the study site indicated temperature was highest in 2020 (10 °C) with peak temperature occurring in the months of mid-July and lowest in 2019 (9.21 °C) with largest dips occurring in January (Figure 3.2). Precipitation events were more frequent in the spring months (Feb-April), with highest total rainfall in 2019 (1104 mm) and lowest in 2020 (1009 mm).

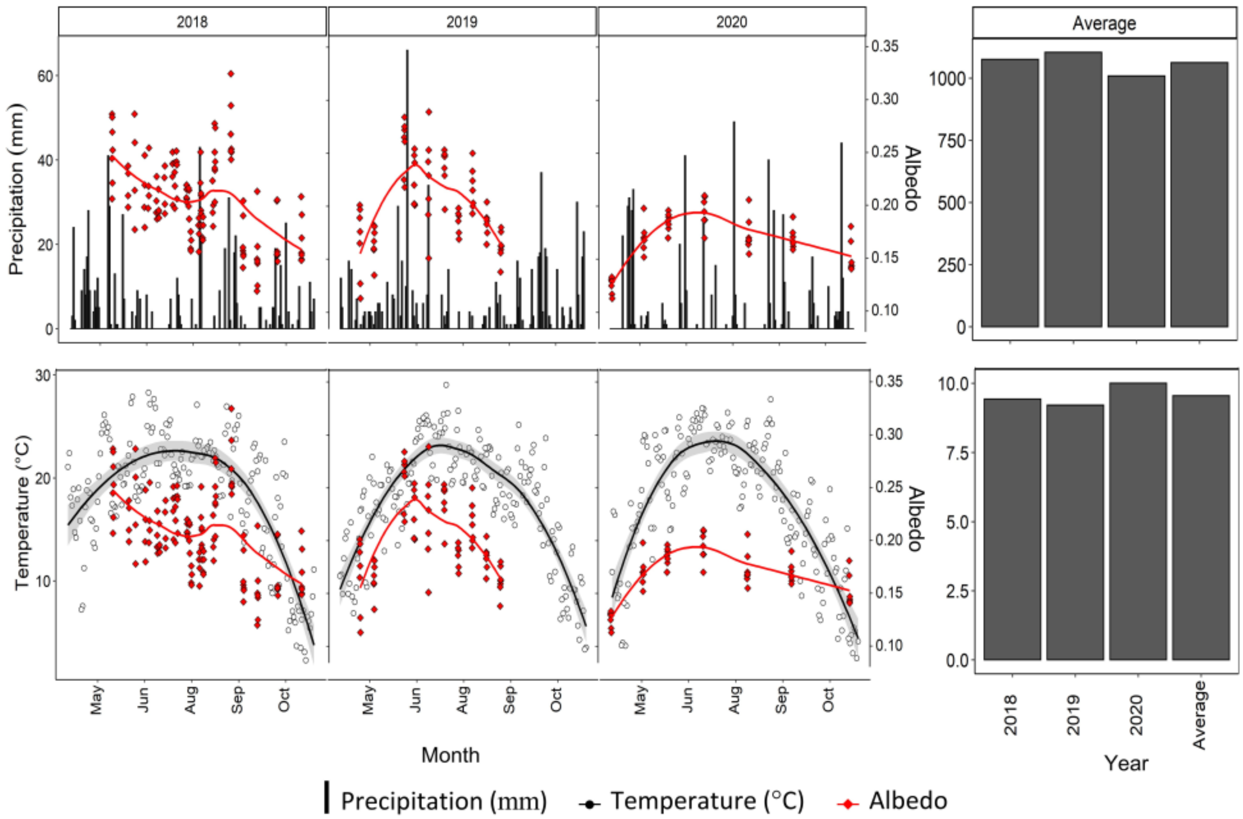

Figure 3.2: Daily air temperature (top) and precipitation (bottom) for the Kellogg Biological Station for the period 2018-2020. Average BCSE albedo measurements are overlaid in red (diamonds), with respective cumulative averages (bar graphs) depicting averages for the study period.

Albedo across different crops

Average albedo ranged from 0.180 to 0.211. Average albedo (mean ± SD) during 2018 was much more variable (α_s: 0.207±0.05), while 2019 albedo was 0.204±0.05. In 2020, average albedo was much more consistent but lower (α_s: 0.167±0.03) (Figure 3.3). During the early growing season (May into beginning of June) albedo was higher, but then decreased in June-August when canopies were closed. Perennials had higher albedo on average (α_s: 0.199±0.04) compared to annual crops of maize (α_s: 0.184±0.03), while miscanthus had the highest observed albedo throughout the study period (α_s: 0.212±0.07). Early successional and maize had the lowest albedo (α_s: 0.180±0.04; α_s: 0.184±0.03 respectively; Figure 4). Among the perennials, restored prairie and switchgrass had similar albedo on average (α_s: 0.197±0.04), while annual row crop sorghum had higher albedo than some perennials on average (α_s: 0.203±0.04). Tukey HSD indicated significance between all albedo and biofuel crops ($p < 0.05$). The analysis of variance (Table 3.2) indicated that the study variables (Eq. 2) were significant ($p < 0.05$), with the three years showing the highest contribution (ω^2 = 11.01%) to the variation of α_s, followed by biofuel crop (ω^2 = 6.05%), and accounted for most of the variance within my study.

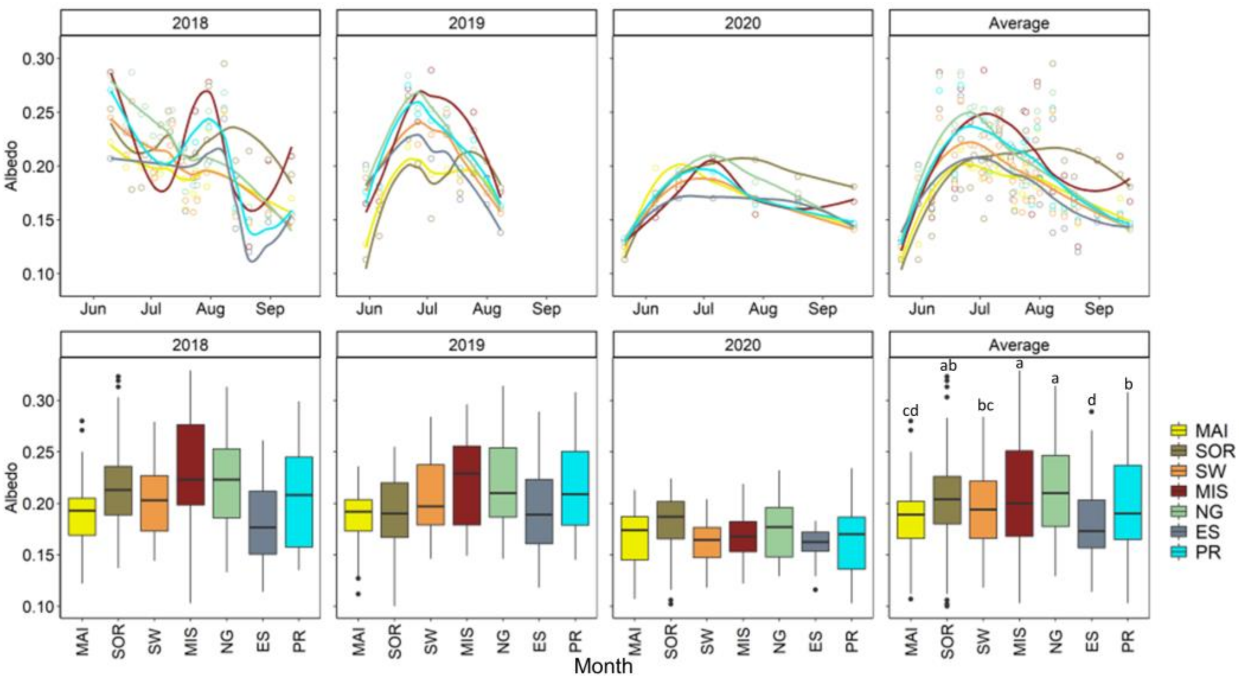

Figure 3.3: Comparison of average albedo measurements taken for three consecutive growing seasons from 2018 to 2020 for each biofuel crop at the Kellogg Biological Station. Lines are smoothed using Loess smoothing, error bars indicate ±1.5 IQR.

Effects of seasonality

Analyzing the block replicates for the entire GS, early successional showed the lowest albedo within each block replicate, while miscanthus, native grasses and sorghum performed well regardless of block replicate (Figure 3.4). However, differences were observed between different crops when divided into the early GS, peak GS, and senescence. During early growing season

(May), annual row crops of maize and sorghum had low albedo at all blocks (α_s: 0.121±0.01; α_s: 0.113±0.01) respectively (Figure S1). Perennials such as switchgrass (0.157±0.03), restored prairie (α_s: 0.152±0.02) and early successional (α_s: 0.165±0.04) all had higher albedo due to their early growing period starting in spring with higher temperatures. Miscanthus albedo (α_s: 0.143±0.02) at all block replicates were also still low due to plant phenology.

Table 3.2: Analysis of variance (ANOVA) with dependent variable: α_s, where ω^2 indicated how much variance in the dependent variable is accounted for by the independent variables (crop, year, treatment, season and their interactions). p values indicate level of significance: ***: $p < 0.001$, **: $p < 0.01$, *: $p < 0.05$. Variable 'crop' is the biofuel crop, 'year' is the year of study (i.e., 2018-2020), 'treatment' refers to agronomic practices (i.e., fertilization versus no fertilization or stover removed versus no stover removed from the maize sites), and 'season' refers to the three major delineations of the growing season (i.e., early, peak, and senescence), respectively.

Variable	**DF**	**SS**	**MS**	**F**	**p**	$\boldsymbol{\omega^2}$	**R^2**
Year	1	0.280	0.280	209.494	***	11.01	
Season	2	0.233	0.116	87.093	***	9.10	
Crop	6	0.161	0.027	0.027	***	6.05	
Crop * Year	6	0.037	0.006	4.566	***	1.13	
Crop * Season	12	0.045	0.004	2.814	***	1.12	
Year * Season	2	0.019	0.010	7.270	***	0.66	
Crop * Treatment	5	0.015	0.003	2.234	**	0.33	
Treatment	3	0.009	0.003	2.249	*	0.20	
Crop * Year * Season	12	0.016	0.001	0.979		0	
Year * Treatment	2	0.001	0	0.200		0	
Treatment * Season	4	0.000	0	0.074		0	
Crop * Year * Treatment	5	0.002	0	0.286		0	
Crop * Treatment * Season	10	0.001	0	0.082		0	
Year * Treatment * Season	4	0	0	0.050		0	
Crop * Year * Treatment * Season	10	0	0	0.030		0	
Residuals	1279	1.7	0.01				**0.30**

During the peak growing season (June-August) (Figure A6), native grasses (α_s: 0.217±0.01) and miscanthus (α_s: 0.221±0.03) displayed their highest albedo, while switchgrass and restored prairie were both slightly lower (α_s: 0.201±0.02; α_s: 0.206±0.02 respectively). Maize increased its albedo during this time, but was still the lowest of all bioenergy crops (α_s: 0.187±0.01), while sorghum at all block replicates had increased their albedo by approximately 0.03 (α_s: 0.207±0.01). Interestingly, early successional plots struggled during peak growing season and had the lowest albedo of all perennials at 0.185±0.02.

During plant senescence in September to October, perennials including switchgrass (α_s: 0.148±0.01), early successional (α_s: 0.147±0.01), native grasses (α_s: 0.146±0.00) and restored prairie (α_s: 0.151±0.01) all started to brown (Figure A7). Maize was observed to have a low albedo of α_s: 0.153±0.02. Miscanthus and sorghum still had relatively high albedo (α_s: 0.188 ± 0.02) due to its large, broad leaves and enclosed canopies during the months of September. The analysis of variance indicated that seasonality was also significant ($p < 0.05$) at $\omega^2 = 9.10\%$, with the interactions of 'crop*season' and 'year*season' showing a weak but significant variance of $\omega^2 = 1.78\%$.

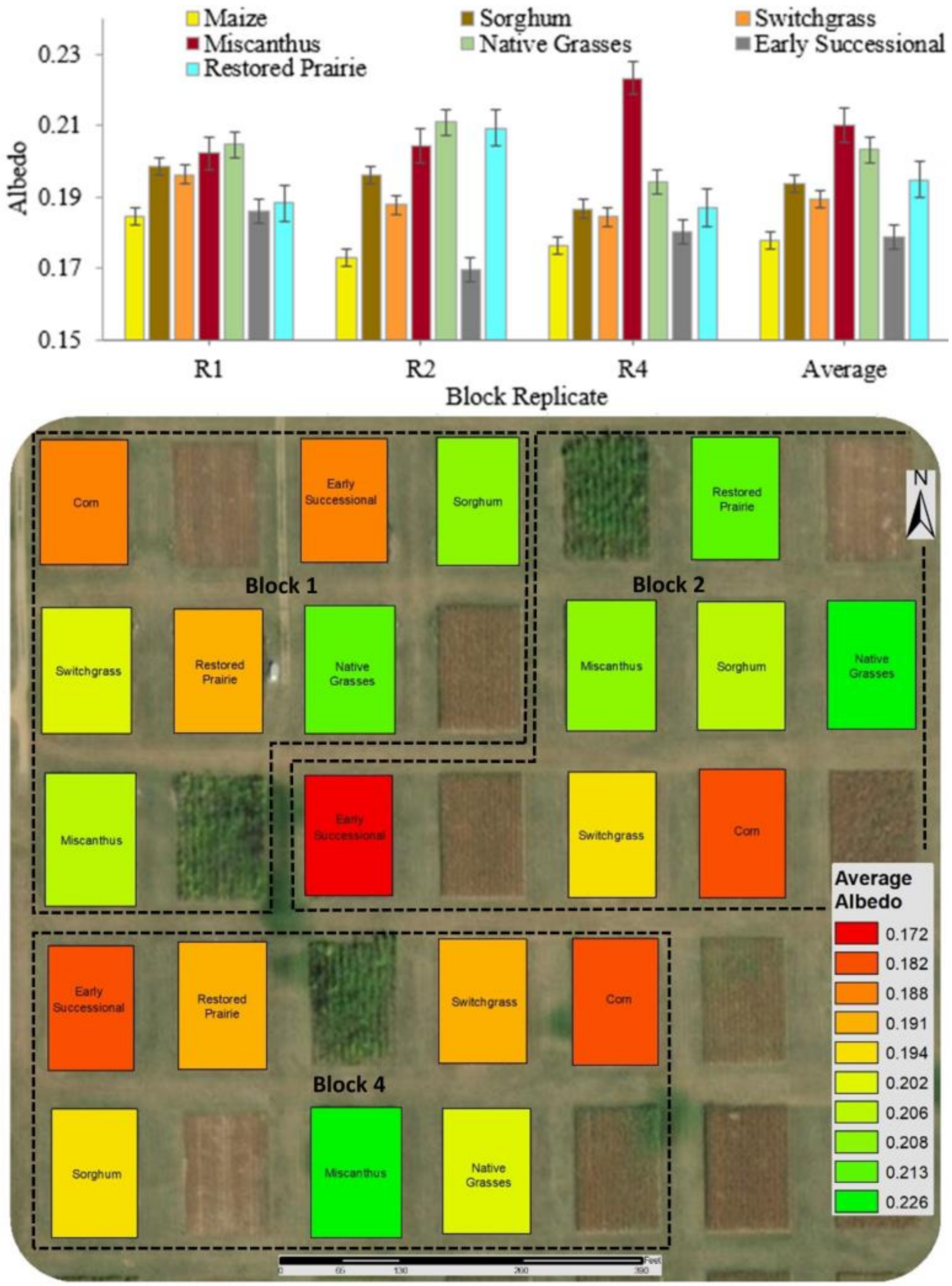

Figure 3.4: Average albedo for all block replicates (R1, R2 and R4) over three consecutive growing seasons from 2018 to 2020 at the Kellogg Biological Station. Map visualizes mean albedo over the entire study period. Error bars indicate 1 ± SD.

Effects of agronomic practices

Overall, only about 28% of fertilized treatments were higher than their non-fertilized counterpart (Figure 3.5). In 2018, only fertilized biofuel crop switchgrass (F α_s: 0.211±0.04; NF

α_s: 0.194±0.04) and native grasses (F α_s: 0.224±0.05; NF α_s: 0.214±0.04) had a higher albedo in all replicate blocks than their unfertilized counterparts. In 2019, miscanthus, native grasses and switchgrass fertilized crops in all replicate blocks all had higher albedo than their unfertilized counterparts (average F α_s: 0.223±0.06; average NF α_s: 0.209±0.05). In 2020 however, most non-fertilized treatments albedo exceeded their counterparts, with dips in fertilized albedo in August coinciding with low observed precipitation. Unexpectedly, treatments of stover removal in maize for all years were similar to the plots where stover was not harvested (Figure 3.6) (α_s: 0.178±0.03). When delving into the differences between each replicate, block one where stover was harvested had a higher albedo (2018: 0.208±0.03; 2019: 0.190±0.03; 2020: 0.169±0.03), while albedo in the plots where stover was not removed was higher in replicate block two (2018: 0.193±0.03; 2019: 177±0.06; 2020:0.166±0.03). Interestingly, differences in treatments, as well as the interaction between 'crop*treatment' did not explain much of the variation in albedo measurements observed (ω^2 = 0.43%).

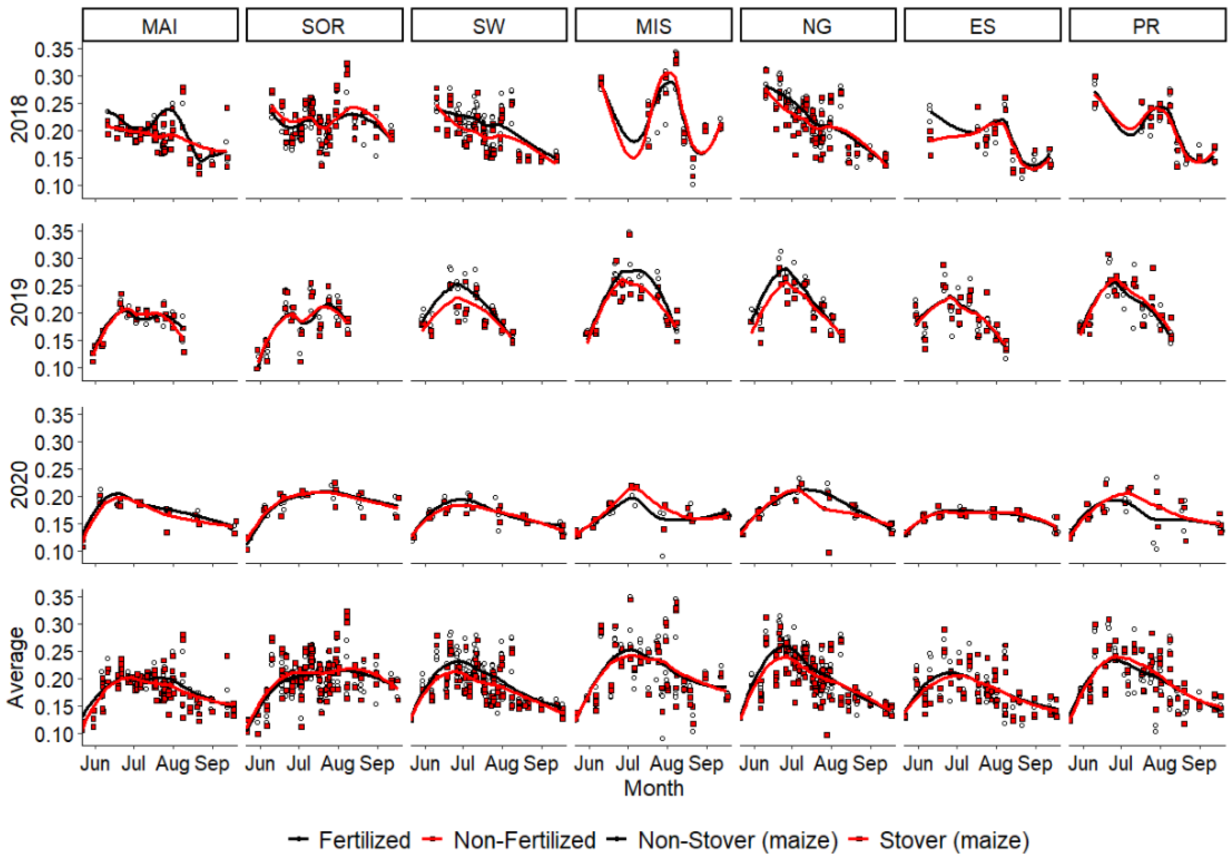

Figure 3.5: Comparison between fertilized/no-stover (black circles; trendline) and unfertilized/stover (red squares; trendline) treatments for (a) maize, (b) early successional, (c) miscanthus, (d) native grasses, (e) restored prairie (f) sorghum, and (g) switchgrass over three consecutive growing seasons from 2018 to 2020 at the Kellogg Biological Station. Stover and no-stover only refer to maize. Lines are smoothed using Loess smoothing.

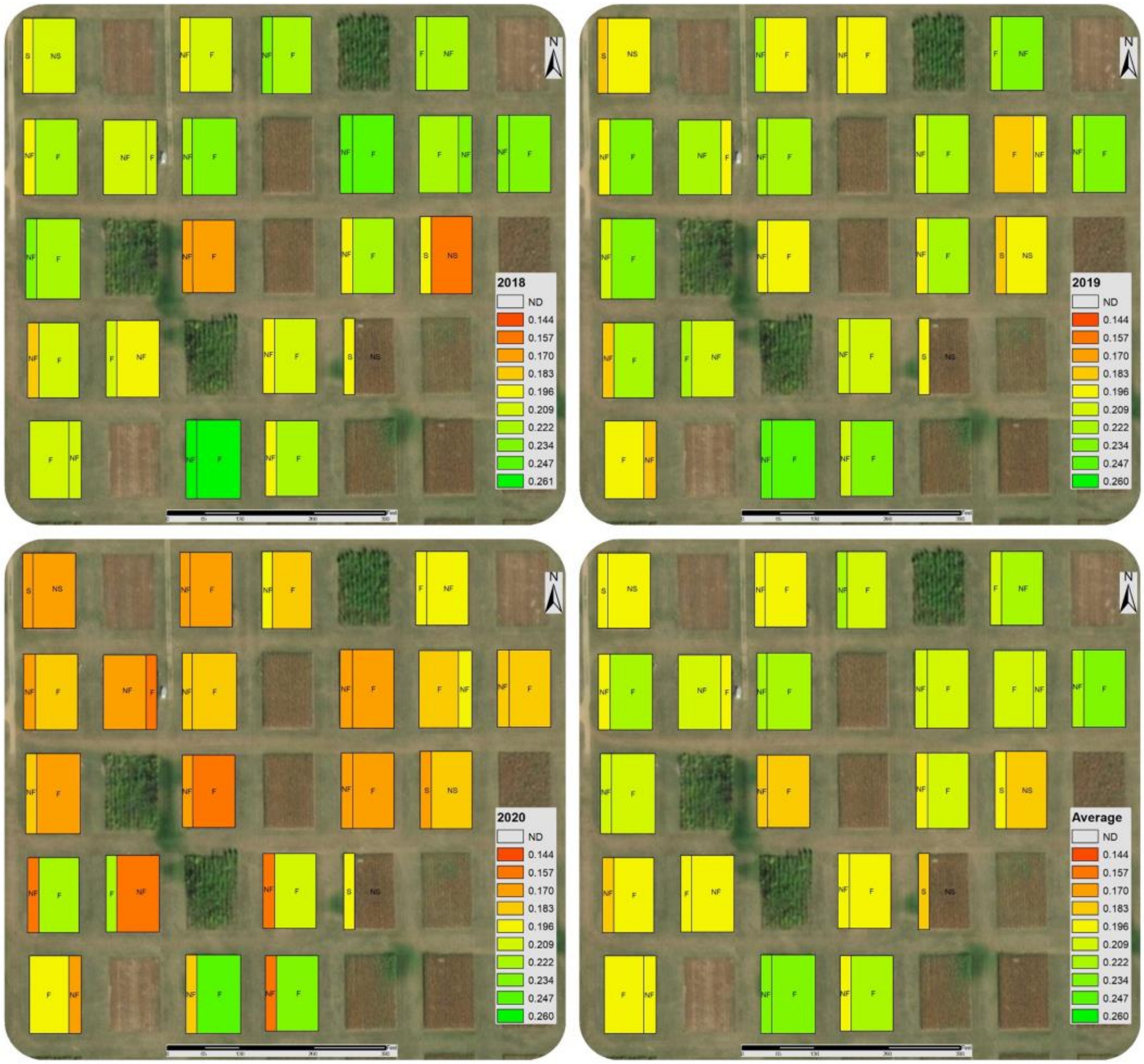

Figure 3.6: Visual representation of average albedo for each type of treatment (fertilized versus unfertilized and stover retention versus stover removal (maize only)) in all replicates (1, 2 and 4) over three consecutive growing seasons from 2018 to 2020 and averaged at the Kellogg Biological Station. ND = No Data.

Patterns of chlorophyll content on albedo observations

Average chlorophyll content was highest for maize (45.1±4.8), followed by miscanthus (39.8 ±5.1) and early successional (35.1±2.5; $p < 0.05$). However, when considering the three years average (34.4±3.1) between switchgrass, sorghum, restored prairie and native grasses, there were no significant differences in chlorophyll content (Figure 3.7). Chlorophyll content was highly variable at the beginning of the growing season, ranging from 24.6 to 59.5, but then became more consistent around peak growing season (36.2). Among the fertilized perennials, Miscanthus had the highest observed SPAD values (40), while most non-fertilized perennials remained similar in chlorophyll content to each other (36.1). In analyzing albedo with chlorophyll content, perennials were graphed with increasing chlorophyll content, albedo decreased, while with annual row crops, as chlorophyll content increased, albedo also increased (Figure 3.8). However, 12 of the 14 interactions did not display significant connections ($p \geq 0.05$).

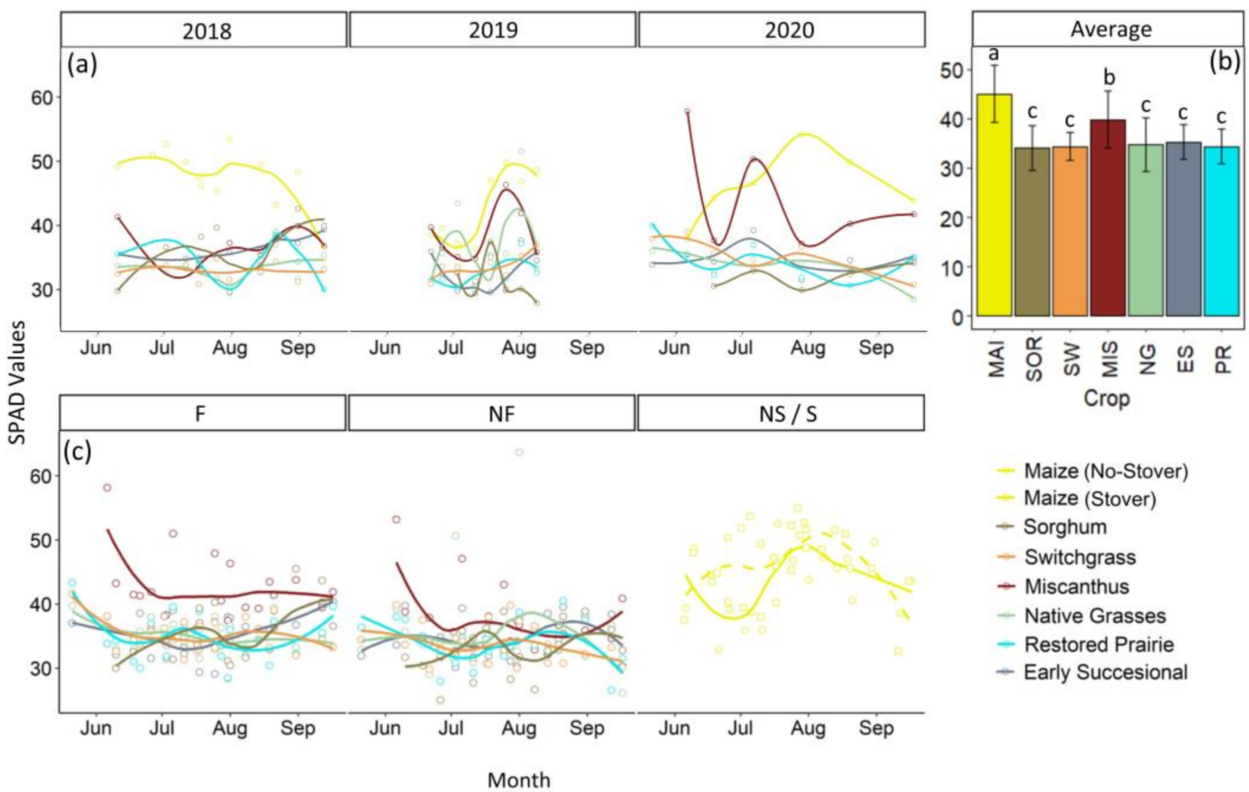

Figure 3.7: Temporal changes in canopy leaf SPAD values per biofuel site (a), and averages over the entire study period (b) at the Kellogg Biological Station. Solid lines were fitted using a local loess regression model. Monthly differences between fertilized (F) versus unfertilized (NF) and stover (S, maize only) versus stover removal (NS, maize only) treatments (c). Lines are smoothed using Loess smoothing.

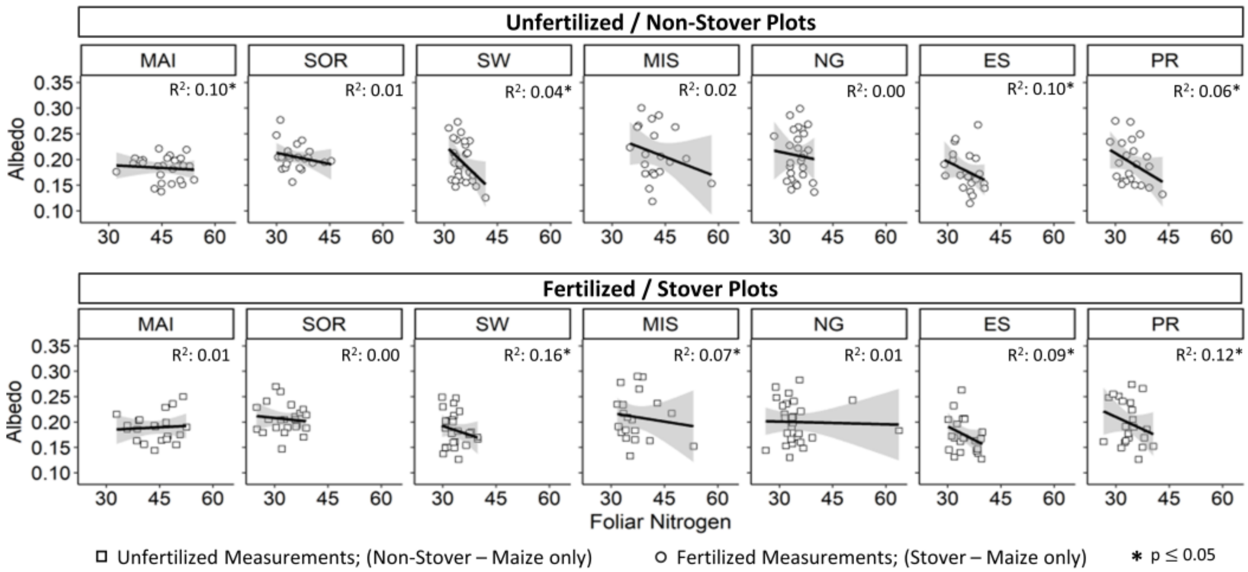

Figure 3.8: Linear regression comparison of chlorophyll content (SPAD; a.u.) and albedo based on fertilized (F) versus unfertilized (NF) and stover (S, maize only) versus stover removal (NS, maize only) treatments over the entire study period at the Kellogg Biological Station.

Discussion

Effects of climate on albedo

These findings suggest that climate can affect albedo indirectly through precipitation and temperature. As precipitation decreased within the study site, temperature increased. Since albedo tends to decrease with increased temperature, these findings indicate that albedo can be affected by climate, which is consistent to what was theorized by Andersen et al. (2013).

Albedo differs between crops

The analysis of how albedo varies between the early growing season, peak greenness of biofuel crops, and senescence for three consecutive growing seasons support the hypothesis that annual row crops have lower albedo than perennial croplands. Average albedo for the study site ranged between 0.144 to approximately 0.260 for all biofuel crops (Table A7; Figure 4.3). Perennials had higher albedo (average α_s: 0.199±0.04; $p < 0.05$) compared to annual crops of maize (α_s: 0.185±0.04; $p < 0.05$). The albedo difference among different biofuel crop sites were probably due to plant phenology including leaf characteristics (i.e., leaf texture, angle, width), crop morphology (i.e., number of leaves, leaf area index, plant development over a season) as well as management practices (i.e., timing of planting and plant row density). Miller et al. (2017) also reported similar results with perennials portraying higher albedo compared to annual row maize.

Differences in growing season albedo were also probable due to early green-up in the spring for perennials, and large leaf growth for all bioenergy crops in the summer. The closed homogeneous canopies during the peak growing season offered little change in surface reflectivity, while during senescence most crops are brown, withered and subsequently harvested (Luyssaert et al., 2014; Odum, 1984; Robertson et al., 2017). As maize was planted in late May and sorghum in early June, the landscape was still mostly bare during the early growing season, which likely caused lower albedo values. Perennial grasses usually start their canopies during spring right after snowmelt (March-April), while annual row crops such as maize and sorghum are not planted until much later in the season (May-June). This is noted by the higher albedo of perennials during the early growing season (Figure A5). From my direct observations, perennials such as switchgrass (0.157), restored prairie (α_s: 0.152) and early successional (α_s: 0.165) which all had higher albedos due to their early growing period starting in late spring and early summer with accompanying higher temperatures and greater rainfall (Figure 4.2). The observed albedo ranges (0.180 to 0.212) were lower than those noted in Campbell & Norman (2012), where albedo in unmanaged grass ecosystems were reported to be around 0.24 to 0.26. As these sites were in a managed agricultural field, albedo can be expected to be slightly different than that of natural grasslands.

Agronomic practices on surface reflectivity

An interesting scope in this study is the seeding of annual row crops of maize and sorghum. Both biofuel crops were planted at similar temporal periods, have similar plant structure, and both seem to respond similarly to N deficiency. However, sorghum was planted in much denser rows (15 in) compared to its maize counterpart (30 in). This simple change in planning allowed a higher amount of solar radiation to be reflected by the sorghum canopy layer, instead of infiltrating through the leaves and warming the land surface. This was especially crucial at peak growing season (June-July) where temperatures are at their highest, and soil water retention, canopy closure and surface reflection is crucial. Sorghum depicted a higher albedo, reflecting more radiation over the course of the season, and cooling the surface (Figure 4.4). These findings are consistent with prior research on crop cover relationships with albedo. Eichelmann's (2016) found that the average albedo of maize was lower than switchgrass over a three-year experimental period. Similarly, Moore et al. (2020) found sorghum and miscanthus had higher albedo than maize. Good agronomic management by farmers is essential grow and care for plants and soils in certain environments. As factors such as climate, moisture, weeds, pests, seeding, and erosion can all pose significant challenges during a crop year, producing crops sustainably can increase the ability of a landscape to maintain stable quality of food and fuel production in the long term without increasing the demand and requirements of agricultural chemical inputs to control the system.

Fertilization vs non-fertilization

Other than the absence of green vegetation outside of the growing season annually (i.e., harvest and winter periods), albedo was influenced by ecosystem processes and management on each bioenergy crop. This study revealed that differing landscapes (i.e., different crops), treatment types (i.e., fertilized versus unfertilized and stover versus no-stover), and growing seasons (i.e., seasonality) all contributed to the overall variation of observed albedo (Figure 4.5, 4.6).

In 2018, only fertilized biofuel crops of switchgrass had higher albedo than their unfertilized counterparts (F α_s: 0.211±0.02; NF α_s: 0.194±0.02), while in 2020, both types of treatments for all biofuel crops were similar in albedo. Tilman et al. (2006) also produced similar results in switchgrass, where the infertile soil bioenergy yield was almost the same as its treatment site with generous applications of fertilizer. Other studies completed within southwest Michigan also showed that switchgrass yields became less responsive each year to nitrogen fertilizer (Roley et al., 2018; Ruan et al., 2016), and those perennial crops were capable of producing as much or more biomass than corn stover alone with fewer costly inputs (Sandford et al., 2017). There is a great advantage of not having to supplement nitrogen through fertilization, as some crops such as soybean fix their own nitrogen into the soil, while other crops such as sugar beet, switchgrass and miscanthus need very little to no fertilizer in order to thrive (Erisman et al., 2010; Vogel et al., 2002). In supporting innovation to produce and use bioenergy crops in more sustainable ways, these results could bring about positive impacts of reducing the amount of fertilizer input needed for sustainable agricultural management.

Stover vs non-stover removal

Due to its abundance, maize stover is one of the most investigated cellulosic feedstocks for bioethanol production *(*Kumar & Singh, 2019). In the United States, a small percentage of maize stover is unharvested, left in the field to integrate into soil with tillage to maintain soil productivity and water-holding capacity (DeJong-Hughes & Vetsch, 2007). This is common Michigan, where the state is among the top ten that produce most of the nation’s maize and is designated as a part of the United States Corn Belt (Robertson & Hamilton, 2015). Although both stover removal and non-stover removal plots in my study portrayed the same overall albedo (0.178 ± 0.03), higher albedo was observed in replicate block one when stover was removed from the plot (0.189±0.03), while albedo in the plots where stover was not removed was lower (0.180 ± 0.03).

Fertilizer application for maize is one of the largest expenses for farmers growing cereal crops, but much of those nutrients are lost to the environment. Studies have showed that lower nutrient availability occurred from plots where residue was removed, in comparison to the plots where residue was left or incorporated, especially if nutrients were not replaced accordingly (Galindo et al., 2022). Not harvesting stover can be beneficial for the landscape long-term, as incorporating corn stover can improve soil organic carbon content, nutrient cycling, maintain soil structure, decrease soil erosion, and lead to improved microbial diversity. Removing stover from a landscape could increase the carbon footprints/GHG emissions and mitigate the effects of land conversion (Ruan et al., 2020), as well as negatively impact soil nutrient availability and soil health, which implies additional fertilizer applications for main nutrients such as nitrogen (N), phosphorus (P), and potassium (K) will be needed in the long term to replace the nutrients that are removed with the stover (Khanna & Paulson, 2016). Overall, stover removal depends on soil characteristics, climate, and agronomic management practices including planting and tillage.

Crop replication

The landscape between the replicates was similar, with most crops on each replicate situated on mostly flat surface and similar soil. When analyzing differences in albedo between replicates, miscanthus had the highest albedo within all block replicates, while maize had the lowest (Figure 4.4). Albedo was also similar between blocks over the entire study period. No measurements were taken from Maize in replicate 4 throughout the entire study, as the landscape was too steep to provide an adequate surface to measure solar radiation and albedo, however, chlorophyll content was retrieved using the SPAD sensor. Regardless of replicate, perennial-dominated landscapes showed a higher intra-annual variability of albedo between the early, peak growing seasons, and senescence, compared to annual row maize. This was most likely due to the effects of agronomic practices such as fertilization (which affect chlorophyll content), land management (which affect crop planting density and stover removal), as well as climate (i.e., air temperature and precipitation).

In the United States, there has been an ongoing discussion on maximizing the productivity of biofuel crops (Robertson et al., 2008). Species such as miscanthus performed well in my study, having high potentials of cooling the landscape. Following concern over fossil fuel dependence beginning in the 1970s, miscanthus and several other species have been studied as promising bioenergy crops. However, as an exotic species in some geographic regions, the adoption of miscanthus as a monoculture bioenergy crop comes with accompanying risks (Robertson & Doran, 2013). Some studies have revealed that transitioning to large expanses of maize can potentially warm the atmosphere due to its low albedo properties (Abraha et al., 2021; Cai et al., 2016). Other longitudinal studies provide disadvantages associated with the initial cost production of miscanthus, along with potential diseases, invasive tendencies, or tolerances to extreme weather (i.e., flooding, heat, drought, extreme cold). However, miscanthus requires no insecticides, can increase soil carbon, and provide many ecosystem services (i.e., high yields, organic matter, habitat and wildlife diversity) (Heaton et al., 2008). As an alternative, native grasslands such as switchgrass, restored prairie and native grasses, also provide promising results of cooling the landscape by reflecting more radiation back into the atmosphere, while maintaining current biodiversity and polycultures in an ecosystem.

Chlorophyll content

Seven of twelve perennial treatments showed a weak but significant correlation that with increasing chlorophyll content, albedo decreased, while one of four annual row crop treatments showed an increase in albedo with increased chlorophyll content (Figure 4.8). Plant greenness is essential for the functioning of biofuel ecosystems as the chlorophyll content of leaves is used to predict the physiological condition of the leaves, which can be influenced by various natural and anthropogenic factors (Yuan et al., 2016). The use of SPAD helps quantifies delicate changes or subtle trends in plant health long before they're visible to the human eye. Chlorophyll content for switchgrass, sorghum, restored prairie and native grasses averaged around 34.4 ± 3.1 for the study period (Figure 4.7). Annual row crops of maize showed higher chlorophyll content, similar to studies found by Thind et al. (2011), where one of their subplots received the same type of N and treatment (no-stover) as the BCSE site and saw similar chlorophyll content levels around ~ 40-50, depending on the growth stages of maize. Successful measurements of chlorophyll content can be affected by many factors, including climate, plant growth stage, plant phenology such as leaf thickness and leaf position (Hu et al., 2014; Yuan et al., 2016). Previous studies by Yuan et al. (2016) noted that chlorophyll content varied in the leaves of rice at different growth stages and under different fertilization rates. Thus, being able to assess chlorophyll content needs of biofuel crops is useful at determining different growth stages of biofuel crops, needs (or lack thereof) of nitrogen, and their subsequent effects on surface albedo.

Assumptions and uncertainty

There were a few limitations in this study. Firstly, it is well known that SPAD values can vary depending on m chlorophyll content measurements of location of on leaves of the plant (Lin et al., 2010). To mitigate this limitation, the measurement this study used a standardized measurement procedure to document observations of chlorophyll in an area that represented the majority of the study site, ensure multiple samples on the leaf, as well as sampling away from the leaf rib, in order to gain an accurate sample.

Secondly, it is worth mentioning the scale-dependent uncertainties when measuring albedo at one specific location and applying it to a larger scale. Many studies usually perform a top-down approach from remote sensing avenues such as Landsat and MODIS in order to gain surface reflectivity on a large surface which is beneficial in regions which are mostly homogenous (Chrysoulakis et al., 2018; Dahlin et al., 2020). However, disadvantages of this process include associating pixels that are not biofuel croplands and vice versa. This study instead performs a bottom-top approach of measuring surface reflectivity at certain regions and comparing it to a larger scale, using measurements on the land surface (e.g., eddy covariance tower, micrometeorology tower, UAV technology). This investigation in scaling up to a regional scale is the subject of ongoing research. Finally, there is the potential for differences in albedo due to winter snow and thaw, both at the landscape scale, as well as between crops.

One final limitation is the delineation of the study period using the growing season (May–October) in calculating albedo, rather than on an annual timescale. Previous studies (Bonan 2008; Bright et al., 2015; Campbell & Norman, 1998; Kaye & Quemada 2017; Liang et al., 2013; Sciusco et al., 2022) have addressed the importance of snow cover in understanding the variability of albedo among different croplands due to changes in snow cover, freeze/thaw cycles, intense snowfall events, and landscape dynamics (i.e., cover crops, harvest, stover on landscape). Thus, the study was restricted to just the growing season to better understand the human disturbance on the landscape through agronomic practices activities, crop phenology and summer climate. Despite these uncertainties, the observation of strong albedo linkages in bioenergy crops add a fundamental dimension to understanding the role of landscape dynamics and agronomic practices on climate.

Conclusion

The effects of albedo with increasing transitions to biofuel croplands is uncertain as the productivity of the landscape shifts and its subsequent range of cooling mitigation. This study indicated that albedo was influenced by both species' composition and agronomic practices. The choice of biofuel crop will become fundamentally important when considering its economic benefits due to variance in albedo. Findings also further support the importance of plant phenology as a consideration of a crop as potential biofuel and its overall impact on global warming. Future studies will delve deeper into the changes of winter and non-growing seasons and their effects on crop productivity and surface reflectivity. In addition, future work is needed to investigate the impact of other agronomic practices that are beyond the scope of the current study.

APPENDIX

Table A5: Summary of bioenergy crops used within the study, as well as their abbreviation, treatment (T): (F= Fertilized; NF= Non-Fertilized; S= Stover not harvested; NS= Stover removed), and species composition.

Crop	**Abr**	**ID**	**T**	**Row spacing (in)**	**Species**	**Assessment**
Maize	MAI	G1	NS/S	30	*Zea mays L*	Monoculture annual row crop member of the grass family Poaceae
Sorghum	SOR	G2	NF/F	15	*Photoperiod insensitive hybrid TAM 17900 variety*	Monoculture annual row crop variety for continuous improvement of yield and adaptation
Switchgrass	SW	G5	NF/F	7.5	*Panicum virgatum L.*	Monoculture perennial Cave-n-Rock perennial variety, consisting of "warm season" (C4) native grass
Miscanthus	MIS	G6	NF/F	30	*Miscanthus x giganteus*	Monoculture perennial sterile hybrid crossed between two grasses (*Miscanthus sinensis* and *Miscanthus sacchariflorus*
Native Grasses	NG	G7	NF/F	NA	A mix of species	Polyculture perennial consisting of Little Bluestem (Schizachyrium scoparium), Big Bluestem (Andropogon gerardii), Indiangrass (Sorghastrum nutans) and Cordgrass (Spartina pectinata)
Early Successional	ES	G9	NF/F	NA	A mix of species	Polyculture perennial comprised of grasses and forbs which grow naturally following land removed from agriculture use
Restored Prairie	PR	G10	NF/F	NA	A mix of species	Polyculture perennial North American tallgrass prairie composed of a diverse mix of "cool season" (C3) and "warm season" (C4) plant species

Table A6: Instantaneous measurements taken for each crop species at the BCSE taken for years 2018, 2019 and 2020 at the Kellogg Biological Station.

Crop	**# of Observations**	**Replicate**
	68	1
Maize	61	2
	41	4
Total	**170**	
	84	1
Sorghum	83	2
	81	4
Total	**248**	
	84	1
Switchgrass	85	2
	83	4
Total	252	
	52	1
Miscanthus	52	2
	52	4
Total	**156**	
	86	1
Native Grasses	86	2
	84	4
Total	**256**	
Early Successional	52	1
	52	2
	52	4
Total	**156**	
Restored Prairie	52	1
	52	2
	52	4
Total	**156**	
Block 1	478	
Block 2	471	
Block 4	445	
Total Site Measurements	**1394**	

Table A7: Albedo values averaged for each replicate and treatment temporally for the Kellogg Biological Station BCSE site for the period 2018-2020. T= Treatment; SD = 1±Standard deviation.

Crop	**T**	**Replicate**	**2018**		**2019**		**2020**		**Average**	
			Albedo	SD	Albedo	SD	Albedo	SD	Albedo	SD
Maize	NS	G1R1	0.208	0.03	0.190	0.03	0.169	0.03	0.191	0.03
Maize	S	G1R1	0.195	0.03	0.182	0.04	0.163	0.03	0.187	0.03
Maize	NS	G1R2	0.144	0.00	0.185	0.06	0.172	0.03	0.171	0.03
Maize	S	G1R2	0.193	0.03	0.177	0.06	0.166	0.03	0.185	0.04
Maize	NS	G1R4	No Data							
Maize	S	G1R4	0.184	0.03	0.187	0.02	0.159	0.03	0.180	0.03
Sorghum	NF	G2R1	0.228	0.03	0.188	0.04	0.185	0.04	0.211	0.04
Sorghum	F	G2R1	0.216	0.03	0.194	0.04	0.181	0.03	0.205	0.04
Sorghum	NF	G2R2	0.223	0.04	0.192	0.04	0.184	0.03	0.209	0.04
Sorghum	F	G2R2	0.220	0.04	0.177	0.04	0.181	0.03	0.203	0.04
Sorghum	NF	G2R4	0.205	0.05	0.181	0.07	0.169	0.06	0.193	0.06
Sorghum	F	G2R4	0.201	0.05	0.192	0.07	0.172	0.07	0.194	0.06
Switchgrass	NF	G5R1	0.196	0.04	0.195	0.03	0.168	0.02	0.191	0.03
Switchgrass	F	G5R1	0.222	0.06	0.223	0.04	0.173	0.03	0.214	0.04
Switchgrass	NF	G5R2	0.193	0.03	0.196	0.03	0.160	0.02	0.188	0.03
Switchgrass	F	G5R2	0.209	0.03	0.209	0.03	0.159	0.02	0.201	0.03
Switchgrass	NF	G5R4	0.193	0.04	0.199	0.04	0.150	0.02	0.187	0.03
Switchgrass	F	G5R4	0.202	0.03	0.205	0.04	0.158	0.02	0.195	0.03
Miscanthus	NF	G6R1	0.232	0.06	0.207	0.07	0.170	0.03	0.206	0.05
Miscanthus	F	G6R1	0.210	0.05	0.229	0.08	0.165	0.02	0.204	0.05
Miscanthus	NF	G6R2	0.242	0.05	0.206	0.07	0.164	0.03	0.207	0.05
Miscanthus	F	G6R2	0.238	0.06	0.219	0.08	0.158	0.03	0.209	0.06
Miscanthus	NF	G6R4	0.252	0.12	0.242	0.11	0.172	0.02	0.223	0.08
Miscanthus	F	G6R4	0.260	0.12	0.246	0.11	0.168	0.06	0.228	0.10
Native Grasses	NF	G7R1	0.221	0.04	0.217	0.04	0.178	0.03	0.213	0.03
Native Grasses	F	G7R1	0.222	0.04	0.218	0.04	0.171	0.02	0.213	0.04
Native Grasses	NF	G7R2	0.225	0.04	0.215	0.03	0.182	0.03	0.216	0.04
Native Grasses	F	G7R2	0.231	0.04	0.230	0.04	0.182	0.03	0.223	0.04
Native Grasses	NF	G7R4	0.195	0.05	0.199	0.07	0.152	0.03	0.188	0.05
Native Grasses	F	G7R4	0.218	0.06	0.227	0.08	0.173	0.03	0.212	0.06
Early Successional	NF	G9R1	0.193	0.07	0.210	0.04	0.166	0.02	0.192	0.04
Early Successional	F	G9R1	0.199	0.07	0.185	0.03	0.163	0.02	0.183	0.04
Early Successional	NF	G9R2	0.164	0.04	0.188	0.03	0.160	0.02	0.172	0.03
Early Successional	F	G9R2	0.168	0.04	0.186	0.04	0.153	0.01	0.171	0.03
Early Successional	NF	G9R4	0.178	0.07	0.181	0.04	0.151	0.01	0.172	0.04
Early Successional	F	G9R4	0.199	0.07	0.211	0.04	0.160	0.02	0.193	0.05
Restored Prairie	NF	G10R1	0.203	0.04	0.210	0.03	0.169	0.03	0.197	0.03
Restored Prairie	F	G10R1	0.196	0.03	0.195	0.03	0.156	0.02	0.185	0.03
Restored Prairie	NF	G10R2	0.216	0.05	0.232	0.05	0.189	0.03	0.215	0.04
Restored Prairie	F	G10R2	0.211	0.06	0.221	0.04	0.187	0.03	0.209	0.04
Restored Prairie	NF	G10R4	0.192	0.07	0.207	0.04	0.147	0.02	0.186	0.05
Restored Prairie	F	G10R4	0.207	0.08	0.219	0.05	0.148	0.03	0.196	0.05
Average		**Entire**	**0.207**	**0.05**	**0.204**	**0.05**	**0.167**	**0.03**	**0.198**	**0.04**

Figure A5: Visual representation of average albedo for early growing season in all replicates (1, 2 and 4) over three consecutive growing seasons from 2018 to 2020 at the Kellogg Biological Station. Legend shows albedo variance from low surface reflectivity (red) to high surface reflectivity (green).

Figure A6: Visual representation of average albedo for peak growing season in all replicates (1, 2 and 4) over three consecutive growing seasons from 2018 to 2020 at the Kellogg Biological Station. Legend shows albedo variance from low surface reflectivity (red) to high surface reflectivity (green).

Figure A7: Visual representation of average albedo for senescence in all replicates (1, 2 and 4) over three consecutive growing seasons from 2018 to 2020 at the Kellogg Biological Station. Legend shows albedo variance from low surface reflectivity (red) to high surface reflectivity (green).

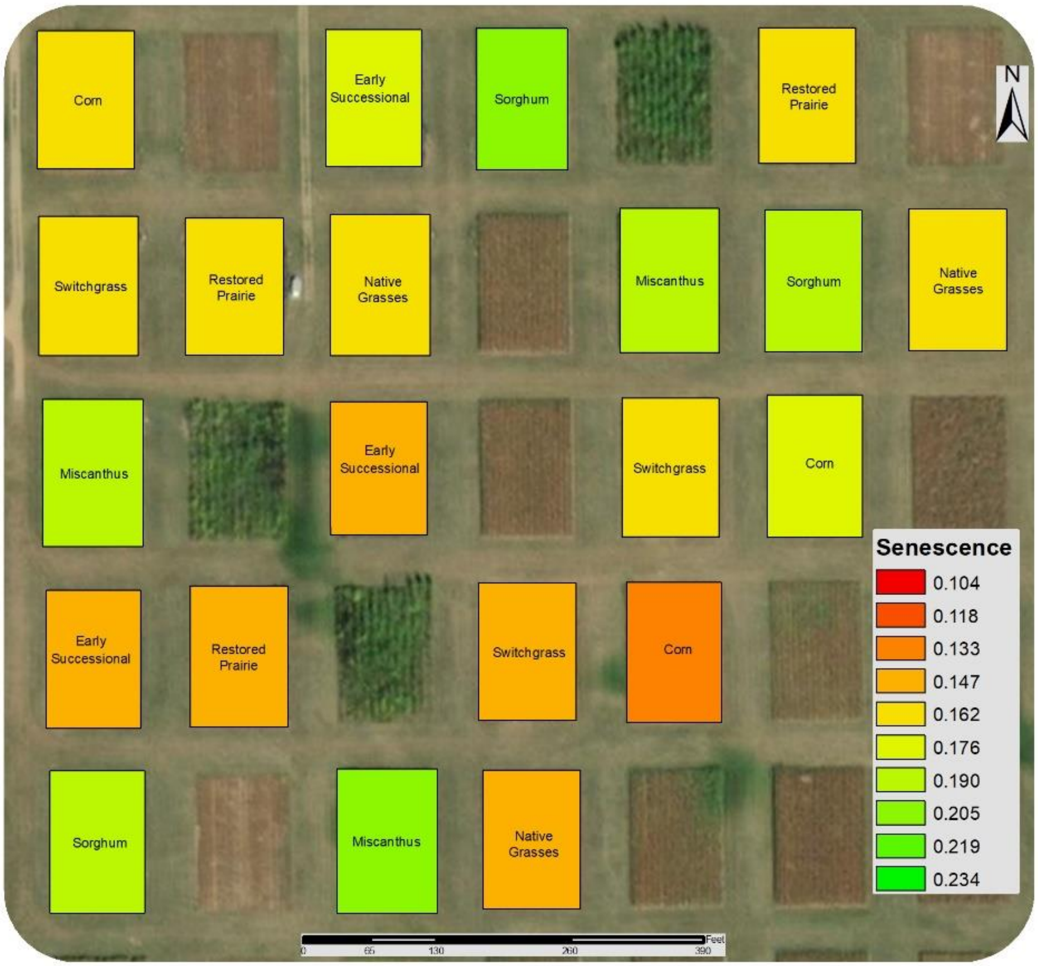

REFERENCES

REFERENCES

Abraha, M., Chen, J., Hamilton, S. K., Sciusco, P., Lei, C., Shirkey, G., Yuan, J., & Robertson, G. P. (2021). Albedo-induced global warming impact of Conservation Reserve Program grasslands converted to annual and perennial bioenergy crops. *Environmental Research Letters*, *16*(8), 084059. https://doi.org/10.1088/1748-9326/ac1815

Ahmad, S. B., & Lockwood, J. G. (1979). Albedo. *Progress in Physical Geography*, *3*(4), 510-543. https://doi.org/10.1177/030913337900300403

Andresen, J., Hilberg, S., Kunkel, K., & Center, M. R. C. (2012). Historical climate and climate trends in the Midwestern USA. *US National Climate Assessment Midwest Technical Input Report*, 1-18. http://glisa.msu.edu/docs/NCA/MTIT_Historical.pdf.

Betts, R. A. (2001). Biogeophysical impacts of land use on present-day climate: Near-surface temperature change and radiative forcing. *Atmospheric Science Letters*, *2*(1-4), 39-51. https://doi.org/10.1006/asle.2001.0037

Bonan G. B. (2008). Forests and climate change: Forcings, feedbacks, and the climate benefits of forests. *Science*, *320*(5882), 1444–1449. https://doi.org/10.1126/science.1155121

Bright, R. M., & Kvalevåg, M. M. (2013). Technical Note: Evaluating a simple parameterization of radiative shortwave forcing from surface albedo change. *Atmospheric Chemistry and Physics*, *13*(22), 11169–11174. https://doi.org/10.5194/acp-13-11169-2013

Brougham, R. K. (1960). The relationship between the critical leaf area, total chlorophyll content, and maximum growth-rate of some pasture and crop plants. *Annals of Botany*, *24*(4), 463-474. https://doi.org/10.1093/oxfordjournals.aob.a083719

Cai, H., Wang, J., Feng, Y., Wang, M., Qin, Z., & Dunn, J. B. (2016). Consideration of land use change-induced surface albedo effects in life-cycle analysis of biofuels. *Energy & Environmental Science*, *9*(9), 2855-2867. https://doi.org/10.1093/C6EE01728B

Caiazzo, F., Malina, R., Staples, M. D., Wolfe, P. J., Yim, S. H. L., & Barrett, S. R. H. (2014). Quantifying the climate impacts of albedo changes due to biofuel production: A comparison with biogeochemical effects. *Environmental Research Letters*, *9*(2), 024015. https://doi.org/10.1088/1748-9326/9/2/024015

Campbell, G. S., & Norman, J. (2012). Radiation Fluxes in Natural Environments. In *An Introduction to Environmental Biophysics*; Eds. 2; Springer-Verlag: New York, USA, pp. 167–184.

Chen, Y., & McKyes, E. (1993). Reflectance of light from the soil surface in relation to tillage practices, crop residues and the growth of corn. *Soil and Tillage Research*, *26*(2), 99-114. https://doi.org/10.1016/0167-1987(93)90037-P

Cresswell, H. P., Painter, D. J., & Cameron, K. C. (1993). Tillage and water content effects on surface soil hydraulic properties and shortwave albedo. *Soil Science Society of America Journal*, *57*(3), 816-824. https://doi.org/10.2136/sssaj1993.03615995005700030031x

Chrysoulakis, N., Mitraka, Z., & Gorelick, N. (2019). Exploiting satellite observations for global surface albedo trends monitoring. *Theoretical and Applied Climatology*, *137*(1), 1171-1179. https://doi.org/10.1007/s00704-018-2663-6

Crum, J.R., & Collins, H.P. (1995). *KBS Soils*. W.K. Kellogg Biological Station Long-Term Ecological Research Project, Michigan State University, Hickory Corners, MI. http://doi.org/10.5281/zenodo.2581504

Dahlin, K. M., Akanga, D., Lombardozzi, D. L., Reed, D. E., Shirkey, G., Lei, C., Abraha, M., & Chen, J. (2020). Challenging a global land surface model in a local socio-environmental system. *Land*, *9*(10), 398. https://doi.org/10.3390/land9100398

DeJong-Hughes, Jodi; Vetsch, Jeffrey. (2007). *On-farm Comparison of Conservation Tillage Systems for Corn Following Soybeans.* University of Minnesota Extension. Retrieved from the University of Minnesota Digital Conservancy, https://hdl.handle.net/11299/48314.

Eichelmann, E., Wagner-Riddle, C., Warland, J., Deen, B., & Voroney, P. (2016). Comparison of carbon budget, evapotranspiration, and albedo effect between the biofuel crops switchgrass and corn. *Agriculture, Ecosystems & Environment*, 231, 271-282. https://doi.org/10.1016/j.agee.2016.07.007

Erisman, J. W., van Grinsven, H., Leip, A., Mosier, A., & Bleeker, A. (2010). Nitrogen and biofuels; An overview of the current state of knowledge. *Nutrient Cycling in Agroecosystems*, *86*(2), 211-223. https://doi.org/10.1007/s10705-009-9285-4

ESRI, R. (2011). ArcGIS Desktop: Release 10. *Environmental Systems Research Institute, Redlands, CA.*

Galindo, F. S., Strock, J. S., & Pagliari, P. H. (2022). Impacts of corn stover management and fertilizer application on soil nutrient availability and enzymatic activity. *Scientific Reports*, *12*(1), 1-16. https://www.nature.com/articles/s41598-022-06042-9

Ghimire, B., Timsina, D., & Nepal, J. (2015). Analysis of chlorophyll content and its correlation with yield attributing traits on early varieties of maize (Zea mays L.). *Journal of Maize Research and Development*, *1*(1), 134-145. https://doi.org/10.3126/jmrd.v1i1.14251

Henderson-Sellers, A., & Hughes, N. A. (1982). Albedo and its importance in climate theory. *Progress in Physical Geography*, *6*(1), 1-44. https://doi.org/10.1177%2F030913338200600101

Houles, V., Guerif, M., & Mary, B. (2007). Elaboration of a nitrogen nutrition indicator for winter wheat based on leaf area index and chlorophyll content for making nitrogen recommendations. *European Journal of Agronomy*, *27*(1), 1-11. https://doi.org/10.1016/j.eja.2006.10.001

Islam, M. R., Haque, K. S., Akter, N., & Karim, M. A. (2014). Leaf chlorophyll dynamics in wheat based on SPAD meter reading and its relationship with grain yield. *Journal of Scientia Agriculture*, *8*(1), 13-18.

Khanna, M. & Paulson, N. (2016). *To Harvest Stover or Not: Is it Worth it?* (6):32, Department of Agricultural and Consumer Economics, University of Illinois at Urbana-Champaign, February 18, 2016. https://farmdocdaily.illinois.edu/2016/02/to-harvest-stover-or-not-is-it-worth-it.html

Kumar, D., & Singh, V. (2019). Bioethanol production from corn. In *Corn: Chemistry and Technology*, Third Edition (pp. 615-631). Elsevier Inc. in cooperation with AACC International. Cambridge, MA, United States https://doi.org/10.1016/B978-0-12-811971-6.00022-X

Lark, T. J., Meghan Salmon, J., & Gibbs, H. K. (2015). Cropland expansion outpaces agricultural and biofuel policies in the United States. *Environmental Research Letters*, *10*(4), 044003. https://doi.org/10.1088/1748-9326/10/4/044003

Lenton, T. M., & Vaughan, N. E. (2009). The radiative forcing potential of different climate geoengineering options. *Atmospheric Chemistry and Physics*, *9*(15), 5539-5561. https://doi.org/10.5194/acp-9-5539-2009, 2009.

Li, Y., Song, H., Zhou, L., Xu, Z., & Zhou, G. (2019). Vertical distributions of chlorophyll and nitrogen and their associations with photosynthesis under drought and rewatering regimes in a maize field. *Agricultural and Forest Meteorology*, 272, 40-54. https://doi.org/10.1016/j.agrformet.2019.03.026

Liang, S., Zhao, X., Liu, S., Yuan, W., Cheng, X., Xiao, Z. ... & Townshend, J. (2013). A long-term Global Land Surface Satellite (GLASS) data-set for environmental studies. *International Journal of Digital Earth*, 6(sup1), 5-33. https://doi.org/10.1080/17538947.2013.805262

Lin, F. F., Deng, J. S., Shi, Y. Y., Chen, L. S., & Wang, K. (2010). Investigation of SPAD meter-based indices for estimating rice nitrogen status. *Computers and Electronics in Agriculture*, *71*, S60-S65. https://doi.org/10.1016/j.compag.2009.09.006

Luyssaert, S., Jammet, M., Stoy, P. C., Estel, S., Pongratz, J., Ceschia, E. ... & Gielen, B. (2014). Land management and land-cover change have impacts of similar magnitude on surface temperature. *Nature Climate Change*, *4*(5), 389-393. https://doi.org/10.1038/nclimate2196

Miller, J. N., VanLoocke, A., Gomez-Casanovas, N., & Bernacchi, C. J. (2016). Candidate perennial bioenergy grasses have a higher albedo than annual row crops. *Global Change Biology: Bioenergy*, *8*(4), 818-825. https://doi.org/10.1111/gcbb.12291

Moore, C. E., von Haden, A. C., Burnham, M. B., Kantola, I. B., Gibson, C. D., Blakely, B. J., Dracup, E.C., Masters, M.D., Yang, W., DeLucia, E.H., & Bernacchi, C. J. (2021). Ecosystem-scale biogeochemical fluxes from three bioenergy crop candidates: How energy sorghum compares to maize and miscanthus. *Global Change Biology: Bioenergy*, *13*(3), 445-458. https://doi.org/10.1111/gcbb.12788

Muñoz, J. D., & Kravchenko, A. (2011). Soil carbon mapping using on-the-go near infrared spectroscopy, topography and aerial photographs. *Geoderma*, *166*(1), 102-110. https://doi.org/10.1016/j.geoderma.2011.07.017

NCDC. (2013). Summary of Monthly Normal 1981–2010 (MI, USA: Gull Lake Biology Station) (www.ncdc.noaa.gov/cdo-web/search)

Odum, E.P. (1984). Properties of agroecosystems. pp 5-11 in R. Lowrance, B.R. Stinner, and G.J. House, editors. In *Agricultural Ecosystems: Unifying Concepts*. John Wiley, New York, USA.

Ollinger, S. V., Richardson, A. D., Martin, M. E., Hollinger, D. Y., Frolking, S. E., Reich, P. B., Plourde, L. C., Katul, G. G., Munger, J.W., Oren, R., Smith, M. L., Paw U., K. T., Bolstad, B. D., Day, M. C., Matrin, T. A., Monson, R. K., & Schmid, H. P. (2008). Canopy nitrogen, carbon assimilation, and albedo in temperate and boreal forests: Functional relations and potential climate feedbacks. *Proceedings of the National Academy of Sciences*, https://doi.org/10.1073/pnas.0810021105

R Development Team (2013). R foundation for statistical computing. Vienna, Austria, *3*(0).

Ramesh, K., Chandrasekaran, B., Balasubramanian, T. N., Bangarusamy, U., Sivasamy, R., & Sankaran, N. (2002). Chlorophyll dynamics in rice (Oryza sativa) before and after flowering based on SPAD (chlorophyll) meter monitoring and its relation with grain yield. *Journal of Agronomy and Crop Science*, *188*(2), 102-105. https://doi.org/10.1046/j.1439-037X.2002.00532.x

Raupach, M. R. (1994). Simplified expressions for vegetation roughness length and zero-plane displacement as functions of canopy height and area index. *Boundary-layer meteorology*, *71*(1), 211-216.

Robertson, B. A., & Doran, P. J. (2013). Biofuels and biodiversity: The implications of energy sprawl. *Encyclopedia of Biodiversity*, 528-539.https://doi.org/10.1016/B978-0-12-384719-5.00341-5

Robertson, G. P., Dale, V. H., Doering, O. C., Hamburg, S. P., Melillo, J. M., Wander, M. M., ... & Wilhelm, W. W. (2008). *Agriculture.* Sustainable biofuels redux. *Science* (New York, NY), 322(5898), 49-50. https://doi.org/10.1126/science.1161525

Robertson, G. P., & Hamilton, S. K. (2015*).* Long-term ecological research at the Kellogg Biological Station LTER site. *The Ecology of Agricultural Landscapes: Long-Term Research on the Path to Sustainability*, 1-32. Oxford University Press, New York, NY, USA.

Robertson, G. P., Hamilton, S. K., Barham, B. L., Dale, B. E., Izaurralde, R. C., Jackson, R. D., Landis, D. A., Swinton, S. M., Thelen, K. D., & Tiedje, J. M. (2017). Cellulosic biofuel contributions to a sustainable energy future: Choices and outcomes. *Science*, *356*(6345). https://doi.org/10.1126/science.aal2324

Roley, S. S., Duncan, D. S., Liang, D., Garoutte, A., Jackson, R. D., Tiedje, J. M., & Robertson, G. P. (2018). Associative nitrogen fixation (ANF) in switchgrass (Panicum virgatum) across a nitrogen input gradient. *The Public Library of Science One*, *13*(6). https://doi.org/10.1371/journal.pone.0197320

Ruan, L., Bhardwaj, A. K., Hamilton, S. K., & Robertson, G. P. (2016). Nitrogen fertilization challenges the climate benefit of cellulosic biofuels. *Environmental Research Letters*, *11*(6), 064007. https://doi.org/10.1088/1748-9326/11/6/064007

Ruan, L., & Robertson, G. P. (2020). No-till establishment improves the climate benefit of bioenergy crops on marginal grasslands. *Soil Science Society of America Journal*, *84*(4), 1280-1295. https://doi.org/10.1002/saj2.20082

Russel, H.N. (1916). On the albedo of the planets and their satellites. *Proceedings of the National Academy of Sciences, 2*(2), 74-77. https://doi.org/10.1073/pnas.2.2.7

Sanford, G. R., Oates, L. G., Roley, S. S., Duncan, D. S., Jackson, R. D., Robertson, G. P., & Thelen, K. D. (2017). Biomass production a stronger driver of cellulosic ethanol yield than biomass quality. *Agronomy Journal*, *109*(5), 1911-1922. https://doi.org/10.2134/agronj2016.08.0454

Sciusco, P., Chen, J., Abraha, M., Lei, C., Robertson, G. P., Lafortezza, R., Shirkey, G., Ouyang, Z., & John, R. (2020). Spatiotemporal variations of albedo in managed agricultural landscapes: inferences to global warming impacts (GWI). *Landscape Ecology*, *35*(6), 1385-1402. https://doi.org/10.1007/s10980-020-01022-8

Thind, H. S., Kumar, A., & Vashistha, M. (2011). Calibrating the leaf colour chart for need based fertilizer nitrogen management in different maize (Zea mays L.) genotypes. *Field Crops Research*, *120*(2), 276-282. https://doi.org/10.1016/j.fcr.2010.10.014

Thoen, G. F. (1990). *Soil Survey of Barry County, Michigan*. (USDA Soil Conservation Service, Michigan Agricultural Experiment Station, and Michigan Technological University, Washington DC), pp. 187, 286.

Tilman, D., Hill, J., & Lehman, C. (2006). Carbon-negative biofuels from low-input high-diversity grassland biomass. *Science*, *314*(5805), 1598-1600. https://doi.org/10.1126/science.1133306

Van den Berg, A. K., & Perkins, T. D. (2004). Evaluation of a portable chlorophyll meter to estimate chlorophyll and nitrogen contents in sugar maple (Acer saccharum Marsh.) leaves. *Forest Ecology and Management*, *200*(1-3), 113-117. https://doi.org/10.1016/j.foreco.2004.06.005

Vogel, K. P., Brejda, J. J., Walters, D. T., & Buxton, D. R. (2002). Switchgrass biomass production in the Midwest USA: harvest and nitrogen management. *Agronomy Journal*, *94*(3), 413-420. https://doi.org/10.2134/agronj2002.0413

Wang, S., & Davidson, A. (2007). Impact of climate variations on surface albedo of a temperate grassland. *Agricultural and Forest Meteorology*, *142*(2–4), 133–142. https://doi.org/10.1016/j.agrformet.2006.03.027

Yang, H., Yang, J., Lv, Y., & He, J. (2014). SPAD values and nitrogen nutrition index for the evaluation of rice nitrogen status. *Plant Production Science*, *17*(1), 81-92. https://doi.org/10.1626/pps.17.81

Yoshida, S. (1972). Physiological aspects of grain yield. *Annual Review of Plant Physiology*, *23*(1), 437-464.

Yuan, Z., Cao, Q., Zhang, K., Ata-Ul-Karim, S. T., Tian, Y., Zhu, Y., Cao, W & Liu, X. (2016). Optimal leaf positions for SPAD meter measurement in rice. *Frontiers in Plant Science, 7,* 719. https://doi.org/10.3389/fpls.2016.00719

Zeri, M., Anderson-Teixeira, K., Hickman, G., Masters, M., DeLucia, E., & Bernacchi, C. J. (2011). Carbon exchange by establishing biofuel crops in Central Illinois. *Agriculture, Ecosystems & Environment*, *144*(1), 319-329. https://doi.org/10.1016/j.agee.2011.09.006

CHAPTER 4. CELLULOSIC GLOBAL WARMING IMPACTS OF MODELING THE CONVERSION OF FOREST INTO BIOENERGY CROPLANDS

Abstract

Understanding the associated global warming impacts (GWI) due to changes in surface reflectivity is vital in order to assess the magnitude of bioenergy crops in mitigating climate change. *In-situ* micrometeorological towers were installed to measure the magnitudes and temporal changes of albedo (α), radiative forcing ($RF_{\Delta\alpha}$), and global warming impacts from albedo changes (GWI_{α}) for seven cellulosic crops in Southwest Michigan. The crops were annual row crops of maize and energy sorghum, monoculture perennials switchgrass, miscanthus, and polyculture perennials of native grasses, early successional grassland and restored prairie continuously from May 2018 to December 2020. A nearby forest was used as the reference for calculating Δ_{α}.

For all bioenergy crops, modeling the land conversion from the reference forest revealed cooling effects, with annual GWI_{α} varying by crop type, season and year. Growing season GWI_{α} values closely resembled annual GWI_{α}, with values at both time scales significant between crop species ($p < 0.05$). Greater cooling effects were observed during the growing season in early successional, miscanthus, sorghum and switchgrass sites with annual average GWI_{α} more pronounced in 2020 compared to preceding years. Seasonal and monthly changes in GWI_{α} were observed during June-September, with the greatest cooling observed in August and the lowest in November-December. Specifically, temporal periods annually accounted for the highest significant interaction (ω^2 = 29.7%) towards the variation in albedo, followed by the interactions between biofuel crop and seasonality (ω^2 = 17.0%) and biofuel crop (ω^2 = 10.7%). The methods and data presented in this study could support greater comprehensive assessments of agricultural ecosystems where bioenergy crops can potentially mitigate against global warming.

Introduction

Albedo is defined as the ratio of outgoing radiation from the Earth's surface to incident radiation from the sun. (Henderson-Sellers, 1980; Henderson-Sellers & Hughes, 1982; Russel, 1916). As a dimensionless component, the more reflective a surface, the higher its albedo, and the greater the relative potential for radiative cooling of the climate. The dynamics of albedo are primarily determined by climatic conditions (e.g., cloud cover, temperature) and land surface properties (e.g., cover type, vegetation coverage, canopy roughness, snow cover, etc.) (Henderson-Sellers & Hughes, 1982; Ollinger et al., 2008; Campbell & Norman 2012; Bright et al., 2015). Soil moisture and agronomic practices (e.g., tilling, stover retention practices) can also affect the amount of albedo reflected from different grasses and croplands (Campbell & Norman, 2012; Davin et al., 2014). Surface albedo is also linked to surface temperature changes (Lenton & Vaughn, 2009), which can affect sensible heat fluxes such as conduction and convection through the exchange of heat energy between a surface and the surrounding air. In high latitude regions, albedo is more affected by the sun's zenith angle, while in the mid-latitudes albedo is more related to land use and land cover changes, including factors of surface roughness and climate (Burakowski et al., 2018). As such, albedo is thought to be a critical modeling parameter when performing life cycle analyses and climate modeling (Fu et al., 2021). However, little is known about the dynamics of albedo in grasslands (Cai et al., 2016) and the effects of climate across different time scales (Bright et al., 2012).

Albedo can also vary based on the landscape dynamic. Urban ecosystems, for example, are dominated by surfaces such as asphalt (0.05 – 0.10) and concrete (0.25 – 0.30) (Sanjuán et al., 2021), which absorb great amounts of radiation (Blumthaler & Ambach, 1988), while fresh snow and ice reflect much of the sunlight directed onto their surfaces due to their white surface and smooth texture, resulting in albedo of around 0.70 – 0.89 (Blumthaler & Ambach, 1988; Henderson-Sellers et al., 1983). Other ecosystems fall in the middle, such as 0.08 – 0.15 for forests, 0.18 – 0.24 for grasslands, 0.20 – 0.30 for croplands, ~0.40 for deserts, and 0.06 – 0.44 for waterbodies (Henderson-Sellers et al., 1983; Schaeffer et al., 2006). Forest albedo can range from 0.07-0.12 in evergreen coniferous forests, to 0.13-0.18 in deciduous broadleaf. Modeling conversions of forest to another landscape: e.g., forest to soy/palm (Caiazzo et al., 2016), forest to agricultural cropland (Sciusco et al., 2020, 2021), results in all cases, in a negative RF, equivalent to cooling landscape effects. The present study focuses on agricultural and forested land use on surface albedo, as bioenergy expansion can provide a significant opportunity in minimizing greenhouse gas (GHG) emissions and reducing the dependence on fossil fuels.

Understanding the factors that drive bioenergy is important, with variables including yields (Lei et al., 2021; Heaton et al., 2008), GHG mitigation (Abraha et al., 2019), water use efficiency (Abraha et al., 2016), recycling of nutrients (Robertson et al., 2008, 2011), sustainability, best agronomic practices (Luyssaert et al., 2014; Robertson et al., 2017) and policy being critical. Within the United States, maximizing the productivity of biofuel crops has been at the forefront of scientific research and policy debate (Robertson et al., 2008). Miscanthus is one of the most promising bioenergy crops due to its high productivity, water and nutrient use efficiency, pest resistance, and perennial nature, while switchgrass gives relatively high biomass yield, and can be grown on marginal lands with low establishment costs (Robertson et al., 2011). Other perennials (i.e., restored prairie, native grasses) and annual row crops (i.e., energy sorghum and sweet sorghum) are also being examined for their suitability for bioenergy. There are many advantages to planting these crops, including ease of propagation, establishment, lower fertilization needs, high biomass yields, and providing ecosystem services (Don et al., 2012; Tilman et al., 2006; Lei et al., 2021; Zeri et al., 2011). However, none of the above crops have been grown at large scales in the Midwest nor across the United States.

Albedo change can directly change the Earth's radiative balance at the top-of-atmosphere (TOA) and exert a radiative forcing (RF) on the global climate system. Agriculture and forestry are acknowledged for their climate change mitigation potential (Smith et al., 2014). Sieber et al. (2019) observed RF cooling from conversions of fallow to biofuel willow (-6.3 W m^{-2}) as well as clearcutting a forest (-11.7 W m^{-2}). Miller et al. (2016) also observed up to -8 Wm^{-2} cooling RFs when maize was converted to miscanthus or switchgrass. Sciusco et al. (2020) utilized remote sensing through MODIS measurements modeling the conversion of reference forests over southwest Michigan and observed RFs up to -6 W m^{-2}, and global warming impact (GWI) mitigation of -1.3 Mg CO_2e ha^{-1} yr^{-1} due to large expanses of agricultural cropping landscapes proving a higher albedo reflectance. These results show that the GWI benefit from albedo-induced radiative forcing due to potentially transitioning from maize to soybean, miscanthus and switchgrass bioenergy crops can be as high as six times larger compared to the benefits from offsetting fossil fuel usage within the USA (Georgescu et al., 2011).

The calculation of global warming impact (GWI) provides a simple means to quantify and compare the contribution of landscape albedo on bioenergy crops. GWI is a cumulative metric that investigates the integrated effect of GHG emissions over a specific temporal period in terms of radiative forcing (Bright et al., 2011, 2012; Chen et al., 2021; Forster et al., 2007; Shine et al., 1990). Comparisons of carbon sequestration and GWI for climate mitigation of GHGs from ecosystems are assessed in terms of radiative forcing (RF), so that albedo forcing impacts can be compared to CO_2-equivalent (CO_2e) emissions for an ecosystem (Betts, 2001; Bright et al., 2011).

Comprehensive reviews (Abraha et al., 2021; Carrer et al., 2018; Lobel & Field, 2007) around the globe point to clear evidence that trends of agricultural planting and yield declines can signal climate warming, and that adaptation strategies comprising of sustainable agronomic management can offset negative impacts. As the science for integrating the effects of albedo-induced RF and GWI is still nascent, my study intends to fill this data gap in order to capture the most accurate observations of climate forcings that occur at different temporal scales and among agricultural lands.

The following direct measurements were taken at the land surface to test these hypotheses: the spatiotemporal changes of Δ_{α}, RF and GWI in annual row crops of maize and energy sorghum, monoculture crops of switchgrass and miscanthus, and polyculture perennials of native grasses, early successional grasses and restored prairie bioenergy systems. It was hypothesized that:

1. Perennial crops would have a higher albedo compared to annual row crops, and all crops will be higher than forest.
2. Secondly, the RF and GWI of different crops would be significantly different due to plant seasonality.
3. Third the conversion of a historically forested landscape to another bioenergy crop would result in increased albedo and cooling of the local climate.

The objectives were to (a) investigate how albedo fluctuates seasonally and temporally, (b) estimate spatiotemporal variations of RF and GWI at daily, monthly and seasonal time scales, and finally, (c) estimate the cooling/warming effects of albedo-induced GWI includes climate impacts from changes in surface albedo due to land use change. The goal of this study was to quantify the importance of albedo-induced RFs in bioenergy croplands and relate it to climate impact of GHG gases over a 3-year period, in order to identify effective alternative land uses for biofuel energy.

Methods

Study site

The W.K. Kellogg Biological Station (KBS) is an agricultural station within southwest Michigan, located within a diverse, rural-to-semirural landscape and cropping system typical of the U.S. Great Lakes and upper Midwest regions. The Great Lakes Bioenergy Research Center (GLBRC) Biofuel Cropping System Experiment (BCSE, http://glbrc.org/) was established in 2008 (42° 24′ N 85° 24′ W, 288 m asl) at KBS. The climate is humid continental temperate with a 30-year (1981–2010) average annual air temperature of 9.9°C and average annual precipitation of 1027 mm (NCDC, 2013). The physiography of the study site is the Kalamazoo series (comprised of fine-loamy, mixed, mesic Typic Hapludalfs) and Oshtemo series (coarse-loamy, mixed, mesic Typic Hapludalfs) (Crum et al., 1995; Muñoz & Kravchenko, 2011). Cover crops were added to the no-till continuous corn treatment in 2012. The treatment was replicated in 28 m × 40 m replicate plots which are further divided into a main plot (22 m x 40 m) and a subplot (5 m x 40 m). The cropping systems measured included annual row crops of continuous no-till maize (G1, *Zea mays L.*) and energy sorghum (G2, *Photoperiod insensitive hybrid TAM 17900 variety*), monoculture perennials of switchgrass (G5, *Panicum virgatum L.*) and miscanthus (G6, *Miscanthus x giganteus*) and polyculture perennials of native grasses (G7, a mix of 4 species), early successional vegetation (G9), and restored prairie (G10) (See Supplementary Table A8 for detailed summary of cropping systems).

The reference forest was situated at the W. K. Kellogg Experimental Forest (KEF, 42° 21' N, 85° 21'W). Established in 1932, this 87-year-old, 716-acre managed hybrid-spruce forest was once abandoned agricultural land, but now is a center for research on tree breeding and genetics.

The site provide researchers a historical reference of what the dominant Michigan land cover type was before European settlement (Brown, 2000).

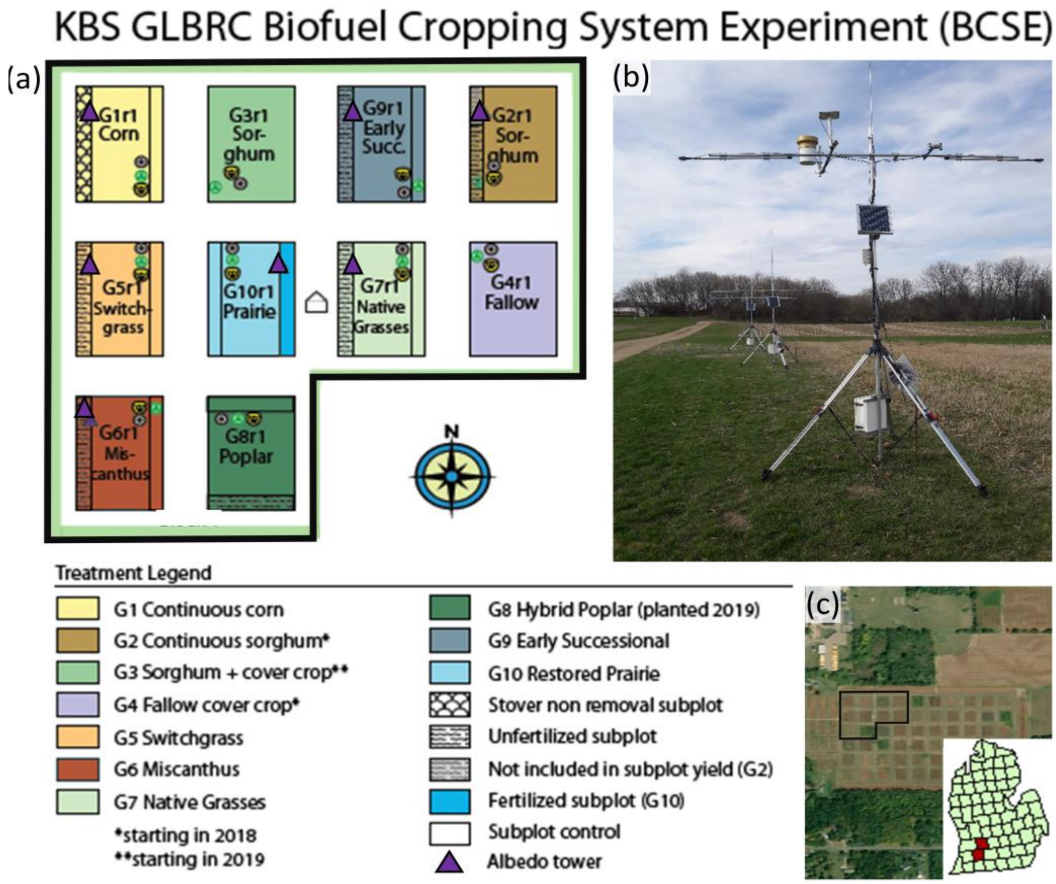

Figure 4.1: Principal study site Great Lakes Bioenergy Research Center Biofuel Cropping System Experiment at the W.K. Kellogg Biological Station. Albedo towers are indicated by purple triangles, located in block 1.

Data collection and instrumentation

Field stations provide high-resolution measurements of albedo in specific fields, often providing measurements for multiple years. Micrometeorological towers for continuous measurements at BCSE were installed in block one in May 2018 to December 2020 (Figure 4.1). Each tower was equipped with one four-component net radiometer (SN-500, Apogee Instruments, Utah, USA), two net radiometers (Q.7.1L, REBS, USA) to measure agronomic treatments (i.e., fertilization, stover practices) on the main/subplots, and one soil moisture probe (CS616, Campbell Scientific Inc., Logan, UT, USA). One tower was also equipped with a precipitation gauge (TE525L, CSI, Logan, UT, USA), and a sensor to measure relative humidity and temperature (HMP 60L, CSI, Logan, UT, USA) as ancillary data for the entire site. Data were collected at 30-minute intervals during the winter, and at 5-minute intervals during the summer months. The heights of the towers were changed to maintain optimal sensor field of view to the vegetation and minimize the situations when the area measured by the instrumentation extended beyond the plot's edge. The instruments were horizontally leveled above the surface and were always higher than $1.41h_c$, where h_c is the average height of the crop, to avoid measuring the layer just above the vegetation that is strongly affected by individual canopy elements (Raupach, 1994; Zeri et al., 2011).

At the Kellogg Experimental Forest, the eddy covariance tower was situated 34 meters (110 feet) above the ground surface and is equipped with a four-component net radiometer (CNR4, Kipp & Zonen, Netherlands), a precipitation gauge (TE525L, Campbell Scientific Inc., Logan, UT, USA), two temperature and relative humidity sensors (HMP45, Campbell Scientific Inc., Logan, UT, USA) to measure the upper and lower levels of the forest, and an IRGASON (Campbell Scientific Inc., Logan, UT, USA). All data were logged at 10-Hz using a datalogger (Campbell Scientific Inc., Logan, UT, USA) and stored at 30-minute intervals.

Incident and reflected solar radiation

Albedo (α_s) was calculated from incoming and outgoing shortwave radiation (Eq.1):

$$\alpha_s = \frac{SW_\uparrow}{SW_\downarrow} \tag{1}$$

where $SW_\uparrow$ is the 5-minute average outgoing shortwave radiation, and $SW_\downarrow$ is the 5-minute average incoming shortwave radiation. Observations of α_s where $SW_\uparrow > SW_\downarrow$ can sometimes occur from multiple reflections, especially during the winter season, giving high reflectivity that causes α_s to be greater than 1. To avoid this, outgoing irradiance was not allowed to exceed incoming irradiance in the same interval. All raw data were corrected for values that were outside an acceptable range, e.g., $0 < \alpha_s < 1$; $0 < SW_{\downarrow} < 1500$ W m^{-2}. Then the dataset was screened, and any data potentially subject to errors (e.g., instrument tilt; snow cover on upfacing dome, tower removal from plots) were eliminated. In the case of maize and restored prairie where two four-component net radiometers existed on the albedo tower, gap-filling from the functioning sensor was completed where data gaps existed. Otherwise, discarded observations were treated as gaps for both incoming and outgoing irradiance at the same interval. This method removed approximately 3% of incident solar radiation values. Larger gaps of several hours to up to 30 consecutive days existed due to instrument failure. Some sites were known to remove nighttime noises by setting solar radiation to greater than zero (Sieber et al., 2019). Statistical analysis was limited to sunlit hours of day, calculated using Campbell and Norman (2012) for calculating sun angles and day-length for each day (Eq.2):

$$t_{r/s} = t_o \pm \frac{ACOS(-TAN(\phi)*TAN(\delta))*(180/PI())}{15} \tag{2}$$

where $t_{r/s}$ is the time of sunrise/sunset, t_o is solar noon, determined from longitude and the equation of time (difference between mean solar time and true solar time), ϕ is latitude, and δ is the solar declination at each calendar day. As the earth turns at a rate of 360 degrees per 24 hours, a factor of 15 is used to convert hours to degrees.

The changes in local surface albedo (Δ_α) was determined by converting the reference forest to different biofuel crops:

$$\Delta_\alpha = \alpha_{crop} - \alpha_{ref} \tag{3}$$

where α_{crop} is albedo from a bioenergy crop, and α_{ref} is albedo of the reference forest. As multiple reflection take place from reflected shortwave radiation toward TOA, additional atmospheric absorption can occur, which may reduce the impact of Δ_{α} upon the TOA flux changes. This accounted for through the calculation of the atmospheric transmittance (T_a). T_a is usually derived from clear-sky conditions, using a constant of 0.854 (Bright & Kvalevåg, 2013; Lenton & Vaughan, 2009), which is representative of regions with very little cloud cover, such as deserts (Muñoz et al., 2010), or can be determined daily using the solar zenith angle and latitude (Boussaada et al., 2018; Campbell & Norman, 2012; NOAA, 2005). Calculation of T_a reduces the amount of error and bias recorded in calculations of RF. Daily albedo model parameters were retrieved for the growing season (GS), as well as the non-growing season (NGS). The GS was defined as April through mid-October following previous studies similar biofuel species (Abraha et al., 2020; Sciusco et al., 2020; Zeri et al., 2011), where plant emergence for perennials occur in late March / early April, seeding for annual row crops are completed late May, and harvesting is completed in late October. The NGS consisted of all days of the year which were not included in the GS (Figure 4.2).

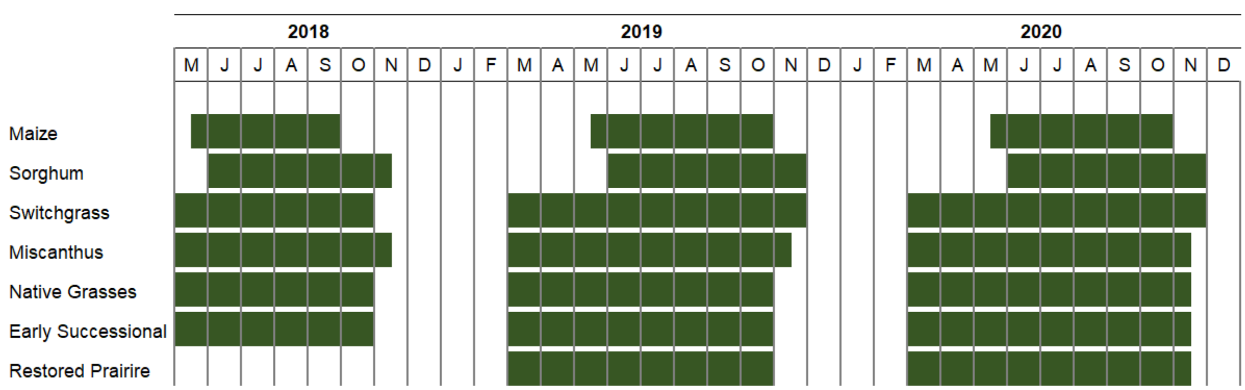

Figure 4.2: Growing season under normal weather conditions in Southwest Michigan production region (green bars). For annual crops, the growing season started with sowing and ended with harvesting. For perennials, the growing season started with non-freezing temperatures in spring and ended with harvesting.

Radiative forcing

Surface albedo changes from radiative forcings (RF_α) were determined by investigating the change in the energy available to the climate system caused by a change between a cover type and a reference vegetation. Forest was used as it was the dominant land cover type as it represents a reference landscape prior to European settlement historically (Williams, 1992). Hence, RF_α was calculated as:

$$RF_\alpha(y) = -\frac{1}{N}\sum_{d=1}^{N} SW_\downarrow T_a \, \Delta_\alpha \qquad (4)$$

where RF_α is the change in net radiative flux from the surface driven by surface albedo (W m^{-2}) at the top of the atmosphere, *y* is the year, $Sw_\downarrow$ is local incoming solar radiation incident to the surface (W m^{-2}), T_a is the upwelling transmittance derived from estimating thermal radiant fluxes within the environment (Campbell & Norman, 2012), N is the number of days, and Δ_α is the local change in albedo between two specific surfaces (Eq.3). The value of RF_α is a representation of the daily local power in W m^{-2} that would be reflected back to the atmosphere (Carrer et al., 2018). This basis is a key factor for other climate metrics such as Global Warming Impact (GWI), which is used in life cycle analyses. GWI allows a comparison of different GHGs by converting them into a pulse emission of carbon dioxide ($CO_{2eq.}$) that exerts the same cumulative RF over a given time horizon (TH). Positive RFs from a decrease in the surface albedo can correspond to carbon emissions, while negative RFs correspond to carbon sequestrations, which can determine whether a crop ecosystem is actively mitigating against global warming (Caiazzo, 2014).

Calculation of GWI

To form direct comparisons between changes in surface albedo and its effects on a landscape, RF can be converted into carbon equivalences and assessed as a GWI (Figure 4.3). GWI was introduced as a relative measure of how much heat a GHG traps in the atmosphere compared with the same amount of heat trapped by CO_2. Hence, the baseline GWI factor of CO_2 is 1. GWI calculation is simple once albedo change has been converted to RF using a radiative transfer model (Eq. 4) (Betts, 2001; Caiazzo et al., 2014; Carrer et al., 2018; Cherubini et al., 2012; Munoz et al., 2010).

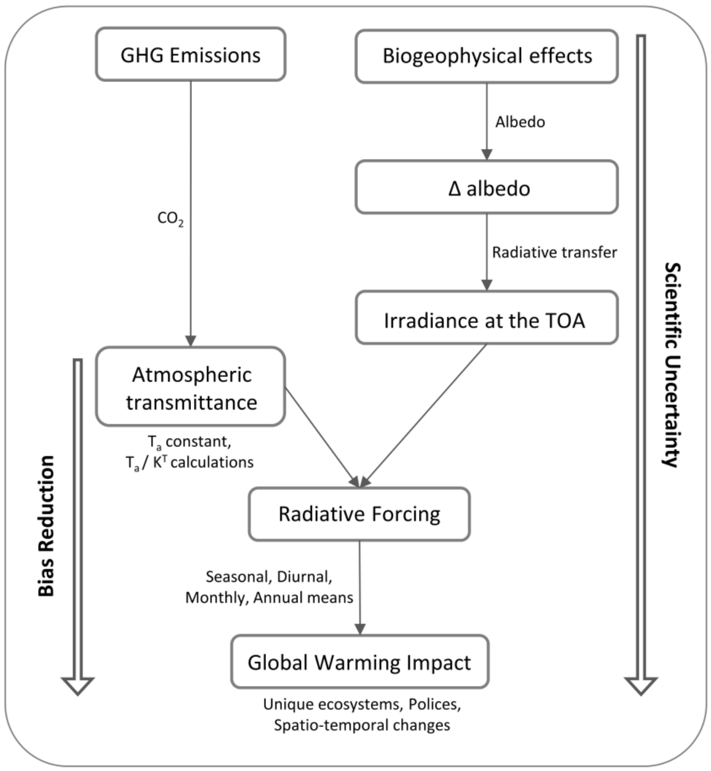

Figure 4.3: Conceptual framework for using albedo and GHGs to determine global warming impact for the study site. TOA refers to the top of the atmosphere.

The use of rf_{CO_2} in GWI analyzes the fraction of CO_2 remaining in the atmosphere after a single pulse emission from interactions between the atmosphere, oceans, and terrestrial biosphere (Joos et al., 2013). It is determined by calculating the time-integrated atmospheric response function of CO_2 with its radiative forcing and converting it into equivalent CO_2 using the following equation:

$$rf_{CO_2} = \frac{(ln\,2) * pCO_{2ref} * M_{CO_2} * m_{air}}{S_{Earth} * \Delta F_{2X} * M_{air}} \quad (5)$$

where pCO_{2ref} is a reference of partial CO_2 pressure in the atmosphere (389 ppmv or 0.383 g kg^{-1}), S_{Earth} is the area of the Earth's surface (5.1×10^{14} m^2), M_{CO_2} is the molecular weight of CO_2 (44.01 g mol^{-1}), m_{air} is the mass of the atmosphere (5.148×10^{18} kg), ΔF_{2X} is the radiative forcing resulting from a doubling of current CO_2 concentration in the atmosphere (+3.7 W m^{-2}), and M_{air} is the molecular weight of dry air (28.95 g mol^{-1}). The inverse of this equation then provides us with a constant of 0.908 (W kg^{-1} CO_2), which can then be compared to other sources of CO_2 emissions, such as CO_2 fluxes in agriculture (Cherubini et al., 2011). Airborne Fraction (*AF)* is the ratio of the annual increase in atmospheric CO_2 to the total CO_2 emissions, and has been debated by many researchers, ranging from 0.53 (Joos et al., 2013), to 0.55 (Akbari, 2009) and 0.52 (Bright et al., 2015). However, most agree on the 20% uncertainty in predicting the amount of CO_2 remaining in the atmosphere due to changing weather and anthropogenic diurnal patterns. The combination of all previously stated variables allow the conversion into GWI (kg CO_2e yr^{-1}), following previous work by Betts (2001), Munoz et al. (2010), Bright et al. (2012), Bright (2015), and Carrer et al. (2018). The GWI can be calculated as:

$$GWI_\alpha = \frac{\sum_{n=1}^{TH} RF_\alpha \; S}{AF \;\; rf_{CO_2}} * \frac{1}{TH} \tag{6}$$

where, RF_α is the radiative forcing from changes in albedo TOA in equation 4 (W m^{-2}), S is the local area subjected to albedo change (m^2), AF is percentage of human-emitted CO_2 that remains in the atmosphere after a period of time from anthropogenic sources, rf_{CO_2} is the derived radiative forcing from 1 kg of CO_2, and TH is the time horizon for 100 years (TH = 100). Negative values of GWI_α indicate CO_2e mitigation impact due to differences between mean cropland and forest albedos. GWI_α was then converted to Mg CO_2e ha^{-1} yr^{-1}.

Statistical analysis

Data were analyzed in the statistical software R (R Development Team, 2013). All corrected 30-minute data were aggregated to daily, monthly and yearly means. Linear mixed model fits were used to analyze all temporal changes of albedo between all sites, perennials vs annual row crops, and cropland as a whole. Changes in GWI_{α} were also analyzed using linear mixed models for the seasonal (growing season, non-growing season), and inter-annual time scales. Site averages were compared using Tukey's HSD test with p-values significant at $p < 0.05$. Daily means for all seven sites were plotted from 2018 to 2020. Annual GWI_{α} was calculated as 1/100 of the total CO_2e to allow direct comparisons with annual GWIs from other vegetated landscapes. The temporal changes of GWI for the three most common time horizons (GWI_{20}, GWI_{100} and GWI_{500} years) were also explored to better characterize GHG emissions. TH was used to represent the time horizon for which a gas affects the atmosphere. This can range from 20 years, to 100 and even longer up to 500 years as each TH is associated with a multiplier that is used to determine the potency of each greenhouse gas. Many, but not all, regulatory agencies throughout the world use the 100-year benchmark. Small THs are intended to focus on near-term effects, while long THs are intended for cumulative impacts. These values are updated by the Intergovernmental Panel on Climate Change (IPCC) and are used regularly in climate regulations.

Results

Albedo and radiative forcing effects

Overall, the albedo of perennial grasses (0.257±0.01) was consistently higher than for annual row crops (0.235±0.01) $p < 0.05$ (Figure 4.4b). All biofuel crops sites combined as cropland (Figure 4.4c) had an annual average albedo (mean ± SE) of 0.252±0.01, with a lower albedo of

0.209±0.01 during the growing season (April-October), a higher albedo of 0.368±0.02 during the winter months (October-March), and up to 0.65±0.10 on days where snowfall occurred ($p < 0.05$). Early successional had the highest average α_s during the study period (0.268±0.175) followed in order by, miscanthus (0.266±0.01), restored prairie (0.264±0.01), native grasses (0.254±0.01), sorghum (0.248±0.01), switchgrass (0.245±0.01), and then maize having the lowest α_s (0.238±0.01) (Figure 4.4a). Annual albedo in native grasses (α_s: 0.225±0.01) and maize (α_s: 0.183±0.01) was lower in 2018 but rose throughout the study period to 0.255±0.01 and 0.248±0.01 respectively in 2020. Miscanthus had the lowest albedo in 2020 (α_s: 0.257±0.01), while 2018 had its highest crop albedo recorded (α_s: 0.283±0.01).

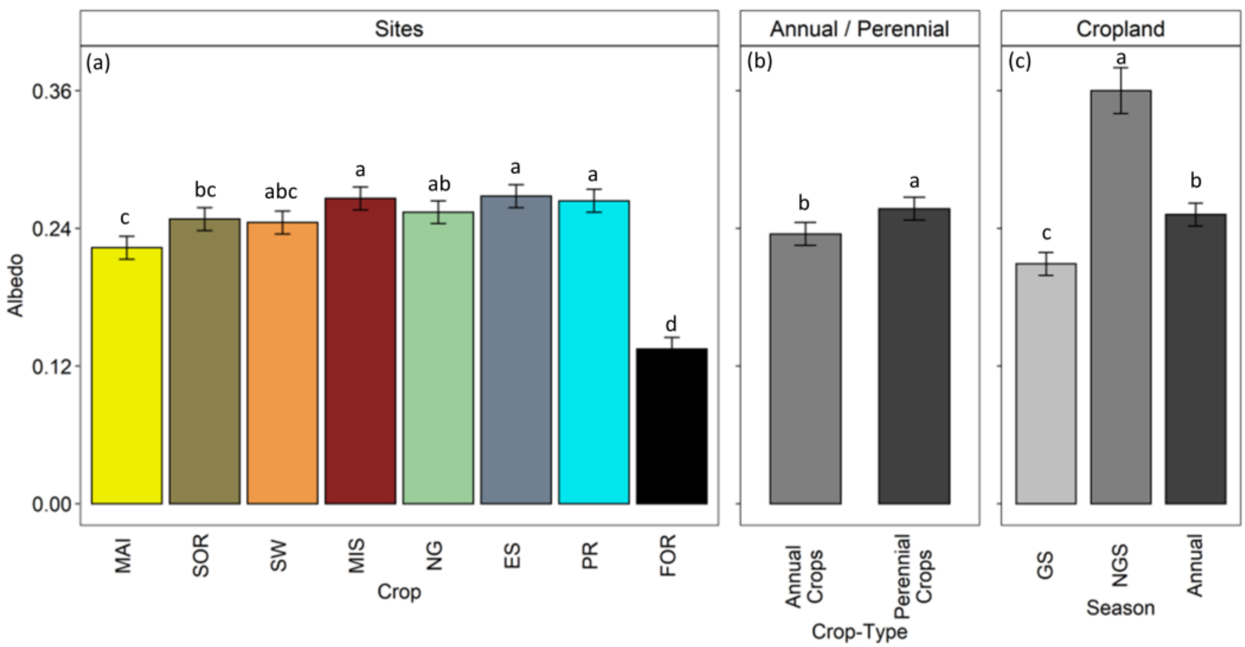

Figure 4.4: Graphs showing comparison of (a) average albedo of each site for the study period 2018-2020 alongside its forest reference, (b) annual row crops of maize and sorghum were averaged against albedo of all other perennial crops, and (c) analysis of cropland for the growing season, winter and annual means. Error bars represent ±1 S.E. Post hoc Tukey HSD treatments completed with different letters indicate significant differences in average albedo ($p < 0.05$).

During the growing season, miscanthus (α_s: 0.235±0.01) and switchgrass (α_s: 0.223±0.01) had the highest albedo, compared to annual row crops maize (α_s: 0.184±0.01) and sorghum (α_s: 0.206±0.01) which had the lowest albedo. All other perennials crops consistently averaged similar α_s of 0.205±0.01. However, during the non-growing season, albedo was noted to be much more variable during the winter season, suggesting alternating periods of high temperatures and mid-winter thaws during most snowmelt phases. The highest average monthly α_s for all sites occurred in February (0.61) while the lowest occurred in October (0.18) (Figure 4.5).

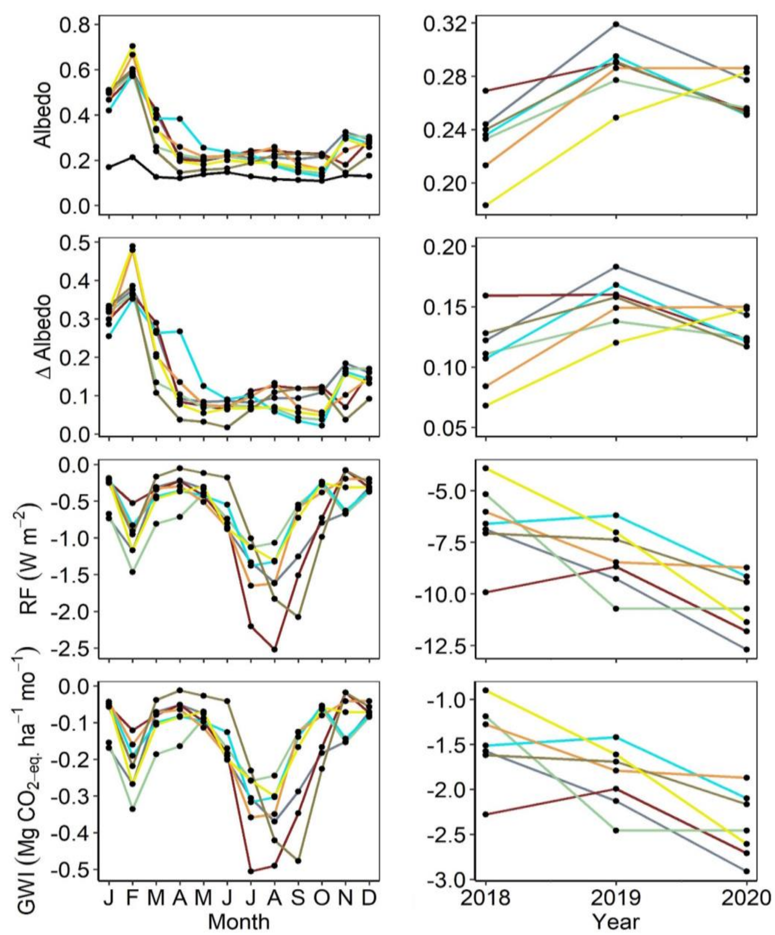

Figure 4.5: Graphs showing comparison between (a) average albedo α_s, (b) average albedo differences (Δ_α) at the surface compared to the reference forest site, (c) radiative forcings (RF_α) and (d) average albedo induced GWI (GWI_α) between forest (reference) and each biofuel crop for each month, as well as annually.

Maize and sorghum had significantly higher average α_s than all perennials in January and February (0.58), but significantly lower α_s in April and May (0.17), with similar albedo for all other months (0.19). Miscanthus had higher α_s than all other perennials during the growing season (0.24), while restored prairie, early successional and native grasses had similar surface albedo during the growing season months (α_s: 0.20) (Table 4.1). Due to changes in surface albedo, Δ_α varied across all biofuel croptypes, with average Δ_α ranging from 0.06-0.15 in 2018, 0.11-0.18 in 2019 and converging the most in 2020 (0.13-0.15). Reference site forest showed the smallest albedo change of all study sites, with reflectivity changing little throughout the year annually (0.135 ± 0.01), and from winter (0.155±0.01) to summer (0.122±0.01), much lower than both perennials and annual row crops.

Albedo-induced radiative forcing was highest during the summer months of June-September and lowest during harvest and spring periods (October-December and March-May) (Figure 4.5; Table 4.2). Miscanthus had the highest average RF_α during the months of July and August (RF_α: -7.09 W m^{-2}), while sorghum showed the lowest RF_α from March through June, when the land surface was bare of snow and vegetation (RF_α: -0.129 W m^{-2}). Miscanthus and early successional grasses showed the highest negative radiative forcings over the entire study period at -30.43 and -28.85 W m^{-2}, respectively. Consequently, albedo RF_α was more strongly negative in summer and more strongly positive in winter in every year.

Table 4.1: Surface albedo for 2018–2020 and monthly surface albedo from Jan-Dec for the Kellogg Biological Station.

				Albedo			
Year	Maize	Sorghum	Switchgrass	Miscanthus	Native Grasses	Early Successional	Restored Prairie
2018	0.179	0.248	0.215	0.283	0.225	0.233	0.225
2019	0.228	0.226	0.239	0.270	0.269	0.287	0.289
2020	0.248	0.262	0.281	0.257	0.255	0.267	0.260
Avg	0.223	0.248	0.245	0.266	0.254	0.268	0.264
Jan	0.50	0.51	0.47	0.47	0.50	0.50	0.42
Feb	0.70	0.60	0.67	0.57	0.58	0.59	0.58
Mar	0.34	0.24	0.33	0.42	0.26	0.40	0.39
Apr	0.20	0.15	0.26	0.20	0.22	0.21	0.38
May	0.18	0.16	0.21	0.20	0.21	0.20	0.26
Jun	0.20	0.16	0.22	0.22	0.22	0.23	0.24
Jul	0.19	0.19	0.23	0.24	0.20	0.21	0.22
Aug	0.19	0.22	0.26	0.24	0.18	0.21	0.17
Sep	0.17	0.23	0.18	0.23	0.15	0.20	0.15
Oct	0.16	0.22	0.16	0.23	0.14	0.22	0.13
Nov	0.29	0.14	0.24	0.18	0.31	0.32	0.31
Dec	0.26	0.22	0.28	0.29	0.30	0.29	0.27
Avg	0.223	0.248	0.245	0.266	0.254	0.268	0.264

Table 4.2: Albedo-induced average RF (W m^{-2}) for 2018-2020 (3-year average: Cum), as well as monthly RF (W m^{-2} mo^{-1}) from Jan-Dec, with yearly (Yr.) for RF, in brackets. Cumulative RF, for the study site over the 3-year period is shown in bold.

	RF (W m^{-2})						
	Maize	Sorghum	Switchgrass	Miscanthus	Native Grasses	Early Successional	Restored Prairie
2018	-3.913	-7.060	-6.023	-9.929	-5.172	-6.875	-6.599
2019	-7.026	-7.370	-8.460	-8.684	-10.713	-9.276	-6.191
2020	-11.365	-9.438	-8.730	-11.812	-10.714	-12.695	-9.159
Avg$_{2018-2020}$	-7.43	-7.96	-7.74	-10.14	-8.87	-9.62	-7.32
Tot$_{2018-2020}$	**-22.30**	**-23.87**	**-23.21**	**-30.43**	**-26.60**	**-28.85**	**-21.95**

	RF (W m^{-2} mo^{-1})													
	Cum	Yr	Cum	Yr	Cum	Yr	Cum	Yr	Cum	Yr	Cum	Yr	Cum	Yr
Jan	-0.64	(-0.21)	-0.75	(-0.25)	-0.62	(-0.2)	-0.72	(-0.24)	-2.02	(-0.67)	-2.21	(-0.73)	-0.57	(-0.18)
Feb	-3.50	(-1.16)	-2.87	(-0.95)	-2.72	(-0.9)	-1.58	(-0.52)	-4.40	(-1.46)	-3.51	(-1.17)	-2.49	(-0.82)
Mar	-1.39	(-0.46)	-0.50	(-0.16)	-0.97	(-0.32)	-1.03	(-0.34)	-2.43	(-0.8)	-0.93	(-0.3)	-1.30	(-0.43)
Apr	-1.11	(-0.37)	-0.16	(-0.05)	-0.89	(-0.29)	-0.67	(-0.22)	-2.15	(-0.71)	-0.66	(-0.22)	-1.07	(-0.35)
May	-0.91	(-0.3)	-0.35	(-0.11)	-1.53	(-0.51)	-1.28	(-0.42)	-1.17	(-0.38)	-0.99	(-0.33)	-1.28	(-0.42)
Jun	-2.61	(-0.86)	-0.54	(-0.18)	-2.57	(-0.85)	-2.42	(-0.8)	-2.22	(-0.74)	-2.64	(-0.87)	-1.65	(-0.54)
Jul	-3.38	(-1.12)	-3.02	(-1)	-4.96	(-1.65)	-6.61	(-2.2)	-3.38	(-1.12)	-3.99	(-1.33)	-4.14	(-1.38)
Aug	-3.94	(-1.31)	-5.50	(-1.83)	-4.86	(-1.61)	-7.56	(-2.51)	-3.21	(-1.06)	-4.84	(-1.61)	-3.97	(-1.32)
Sep	-2.18	(-0.72)	-6.24	(-2.07)	-1.75	(-0.58)	-4.54	(-1.51)	-1.65	(-0.55)	-3.77	(-1.25)	-1.82	(-0.6)
Oct	-0.77	(-0.25)	-2.95	(-0.98)	-1.15	(-0.38)	-2.19	(-0.72)	-0.84	(-0.27)	-2.39	(-0.79)	-0.71	(-0.23)
Nov	-0.94	(-0.31)	-0.24	(-0.08)	-0.59	(-0.19)	-0.23	(-0.07)	-2.02	(-0.67)	-1.98	(-0.66)	-1.89	(-0.62)
Dec	-0.93	(-0.3)	-0.75	(-0.24)	-0.60	(-0.2)	-0.96	(-0.31)	-1.11	(-0.37)	-0.92	(-0.3)	-1.06	(-0.35)
Avg$_{Jan-Dec}$	-1.86	(-0.61)	-1.99	(-0.66)	-1.93	(-0.64)	-2.48	(-0.82)	-2.22	(-0.73)	-2.40	(-0.8)	-1.83	(-0.6)
Tot$_{Jan-Dec}$	**-22.30**		**-23.87**		**-23.21**		**-29.79**		**-26.60**		**-28.85**		**-21.95**	

Global warming impact over time horizons

In modeling the conversion of reference forest to a bioenergy crop provided us with a cooling effect on the local climate throughout the study period (Figure 4.6). Annual average GWI_{α} (Mg CO_2e ha^{-1} yr^{-1}) mitigation was observed to be more pronounced in 2020, compared to 2018 and 2019. Maize had the lowest impacts in 2018 at -0.89, but increased to -2.61 by 2020 (Table 4.3). Miscanthus and restored prairie initially had a higher GWI_{α} in 2019 compared to 2018, before having a cooling of -2.406. Highest albedo-induced GWI_{α} cooling effects were observed during the summer months (Mg CO_2e ha^{-1} mo^{-1}) of June-September, with the highest cooling observed in August at an average of -1.06, and lowest contributions observed in November-December. GWI_{α} values tended towards larger cooling effects during the growing season months (May-October) and closer to zero with warming effects in the winter months (January-February) (Figure 4.6). Maize, restored prairie, and native grasses resulted in the lowest average growing season (Mg CO_2e ha^{-1} gs^{-1}) albedo-induced GWI_{α} of -0.97, -0.96 and -0.88, respectively (Figure 4.5a). The growing season GWI_{α} values closely resembled annual GWI_{α} values, with values during both time scales being significant at $p < 0.05$ from a Tukey post-hoc test.

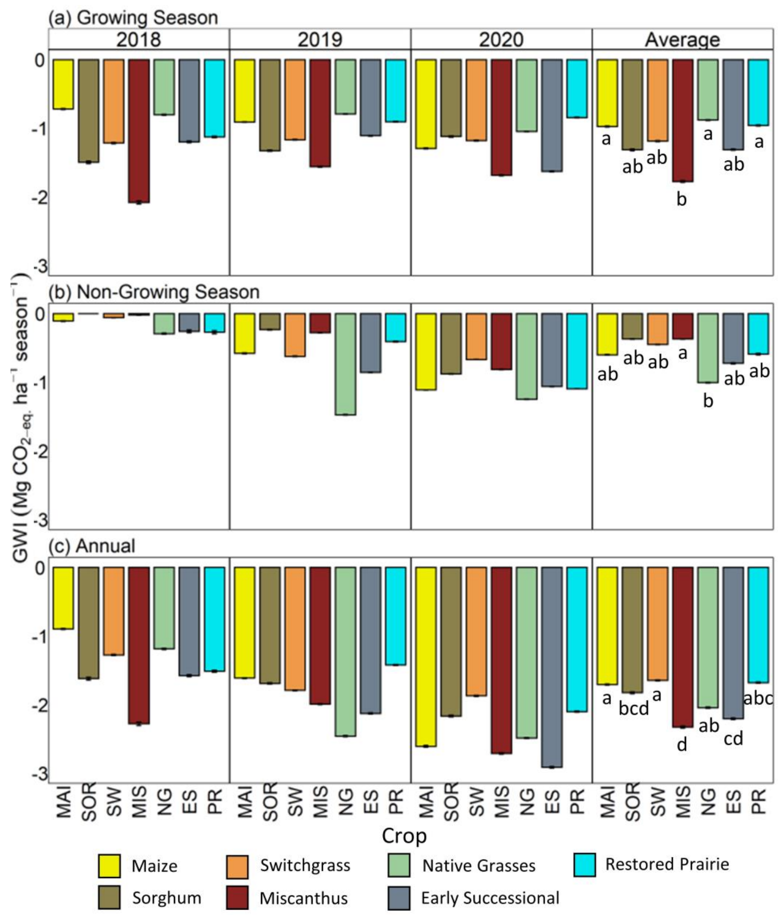

Figure 4.6: Average albedo induced global warming impact (GWI$_\alpha$) for conversions of reference forest to biofuel cropland during (a) the growing season (May-October), winter (November-May), and annually. GWI$_\alpha$ for all conversions were calculated over a 100-year time horizon. Error bars represent ±1 S.E. Post hoc Tukey HSD treatments completed with different letters indicate significant differences in average albedo ($p < 0.05$).

Table 4.3: Albedo-induced average GWI_{α} (Mg CO_2e ha^{-1} yr^{-1}) for 2018-2020 (3-year average: Cum), as well as monthly GWI_{α} (Mg CO_2e ha^{-1} yr^{-1}) from Jan-Dec, with yearly (Yr) for GWI_{α}, in brackets. Cumulative GWI_{α}, for the study site over the 3-year period is shown in bold.

	GWI (Mg CO_2e ha^{-1} yr^{-1})						
	Maize	Sorghum	Switchgrass	Miscanthus	Native Grasses	Early Successional	Restored Prairie
2018	-0.89	-1.62	-1.28	-2.28	-1.19	-1.58	-1.51
2019	-1.61	-1.69	-1.79	-1.99	-2.46	-2.13	-1.42
2020	-2.61	-2.17	-1.87	-2.71	-2.46	-2.91	-2.1
$Avg_{2018-2020}$	-1.71	-1.83	-1.65	-2.33	-2.04	-2.21	-1.68
$Tot_{2018-2020}$	**-5.12**	**-5.48**	**-4.94**	**-6.98**	**-6.13**	**-6.62**	**-5.04**

	GWI (Mg CO_2e ha^{-1} yr^{-1})													
	Cum	Yr	Cum	Yr	Cum	Yr	Cum	Yr	Cum	Yr	Cum	Yr	Cum	Yr
Jan	-0.15	(-0.04)	-0.17	(-0.05)	-0.13	(-0.04)	-0.17	(-0.05)	-0.46	(-0.15)	-0.51	(-0.16)	-0.13	(-0.04)
Feb	-0.8	(-0.26)	-0.66	(-0.21)	-0.48	(-0.16)	-0.36	(-0.12)	-1.01	(-0.33)	-0.81	(-0.26)	-0.57	(-0.19)
Mar	-0.32	(-0.1)	-0.11	(-0.03)	-0.22	(-0.07)	-0.24	(-0.07)	-0.56	(-0.18)	-0.21	(-0.07)	-0.3	(-0.09)
Apr	-0.26	(-0.08)	-0.04	(-0.01)	-0.19	(-0.06)	-0.15	(-0.05)	-0.49	(-0.16)	-0.15	(-0.05)	-0.25	(-0.08)
May	-0.21	(-0.06)	-0.08	(-0.02)	-0.34	(-0.11)	-0.29	(-0.09)	-0.27	(-0.08)	-0.23	(-0.07)	-0.29	(-0.09)
Jun	-0.6	(-0.19)	-0.12	(-0.04)	-0.57	(-0.19)	-0.55	(-0.18)	-0.51	(-0.16)	-0.61	(-0.2)	-0.38	(-0.12)
Jul	-0.78	(-0.25)	-0.69	(-0.23)	-1.08	(-0.35)	-1.52	(-0.50)	-0.78	(-0.25)	-0.92	(-0.3)	-0.95	(-0.31)
Aug	-0.9	(-0.30)	-1.26	(-0.42)	-1.05	(-0.35)	-1.47	(-0.49)	-0.74	(-0.24)	-1.11	(-0.37)	-0.91	(-0.30)
Sep	-0.5	(-0.16)	-1.43	(-0.47)	-0.38	(-0.12)	-1.04	(-0.34)	-0.38	(-0.12)	-0.86	(-0.28)	-0.42	(-0.13)
Oct	-0.18	(-0.05)	-0.68	(-0.22)	-0.24	(-0.08)	-0.5	(-0.16)	-0.19	(-0.06)	-0.55	(-0.18)	-0.16	(-0.05)
Nov	-0.22	(-0.07)	-0.06	(-0.01)	-0.13	(-0.04)	-0.05	(-0.01)	-0.46	(-0.15)	-0.45	(-0.15)	-0.43	(-0.14)
Dec	-0.21	(-0.07)	-0.17	(-0.05)	-0.13	(-0.04)	-0.22	(-0.07)	-0.26	(-0.08)	-0.21	(-0.07)	-0.24	(-0.08)
$Avg_{Jan-Dec}$	-0.43	(-0.14)	-0.46	(-0.15)	-0.41	(-0.14)	-0.55	(-0.18)	-0.51	(-0.17)	-0.55	(-0.18)	-0.42	(-0.14)
$Tot_{Jan-Dec}$	**-5.12**		**-5.48**		**-4.94**		**-6.98**		**-6.13**		**-6.62**		**-5.04**	

Biofuel crops miscanthus, switchgrass, and restored prairie had their highest cooling effects early in the growing season and tapered off closer to senescence, while native grasses and early successional were observed to have constant GWI_{α} values throughout the entire growing season. In the non-growing periods, albedo-induced GWI_{α} (Mg $CO_{2eq.}$ ha^{-1} wi^{-1}) was highest in early successional grasses and native grasses at -0.73 and −1.01 respectively (Figure. 4.4b). In analyzing the three most common time horizon periods (Figure 4.7), each bioenergy system caused a net cooling with all biofuel sites at GWI_{500} tending to be almost equal in negative contributions (-0.38 Mg $CO_{2eq.}$ ha^{-1} yr^{-1}). In all cases, differences in GWI_{α} were larger for GWI_{20} and tended to decrease with increasing TH. Average GWI_{α} (Mg $CO_{2eq.}$ ha^{-1} yr^{-1}) were -9.55, -1.92 and -0.38 for GWI_{20}, GWI_{100} and GWI_{500}, respectively.

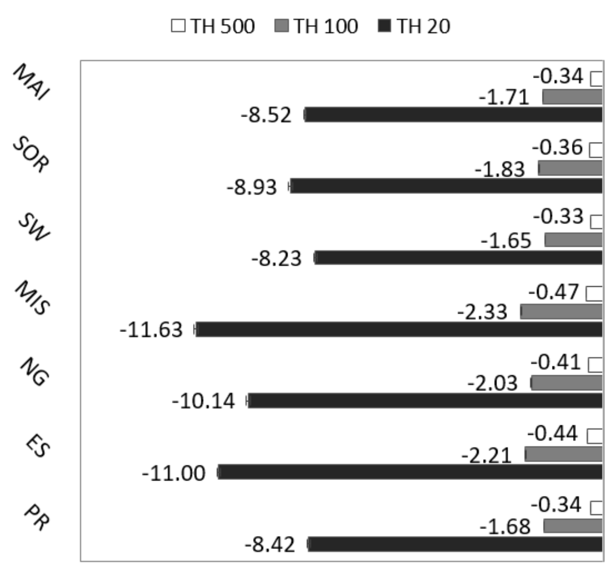

Figure 4.7: Direct contributions to GWI_{α} from conversion of forest to biofuel crops from surface albedo and three most common THs (20, 100 and 500 years) at the Kellogg Biological Station.

Table 4.4: Analysis of variance (ANOVA) with year as repeated measures, using dependent variable GWI_{α}, where ω^2 indicates how much variance in the dependent variable is accounted for by the independent variables (crop, year, season and their interactions, as well as climate variables RH: relative humidity, Air Temp: air temperature, VWC: soil moisture content). p values indicate level of significance: ***:p < 0.001, **:p < 0.01, .:p < 0.05.

Variable	**DF**	**SS**	**MS**	**F**	**p**	ω^2	R^2
Crop	6	4.181	0.697	5.108	**	0.107	
Season	2	2.56	1.28	9.384	**	0.073	
Year	2	9.61	4.805	35.221	***	0.297	
Crop: Season	12	6.99	0.583	4.27	**	0.170	
Crop: Year	12	3.402	0.283	2.078	.	0.056	
Season: Year	4	0.944	0.236	1.729		0.013	
Season: Year: Crop	21	2.865	0.136				
RH	1	0.211	0.211	1.544			
Air Temp	1	0.574	0.574	4.208	.	0.014	
VWC	1	0.005	0.005	0.037			
							0.73

The repeated measures analysis of variance indicated 73% variation in the dependent variable was accurately predicted by the independent variables (Table 4.4), where the variation of $GWI_{\Delta\alpha}$ was significant ($p < 0.001$) among all three years (ω^2 = 29.7%), by biofuel crop (ω^2 = 10.7%), and the interactions between biofuel crop and seasonality (ω^2 = 17.0%). Climate variables included in the ANOVA showed that only air temperature was significantly correlated with GWI_{α} values (ω^2 = 1.4%), with relative humidity and soil moisture content not having any impact on climate cooling at the study site.

Discussion

This study quantified the magnitude of climate impacts from converting a forested landscape to sustainable bioenergy crops using α_s, $RF_{\Delta\alpha}$ and GWI_{α} over a period of three years, in order to understand the impact on bioenergy cropping systems. Spatial and temporal variability in crop-specific albedo due to site conditions, land management, and climate were captured using continuous field observations. The method presented in this study shows how variances in albedo and radiative forcing spatiotemporally affects the cooling/warming of CO_2 GHG emissions.

Albedo

Within my study, perennial crops had a higher α_s compared to annual row crops. Albedo was highest for early successional (0.268±0.01) and lowest for maize (0.223±0.01) within the biofuel crops (Figure 4.4). These findings are within the range of 0.16–0.26 reported for grass and croplands (Campbell & Norman; 2012) and were similar in other studies (Kaye & Quemada, 2017; Miller et al., 2016), where other biofuel croplands showed comparable surface reflectivity. Perennial grasses usually green-up in April and have closed, homogeneous canopies by early June. In contrast, maize was planted sites around early/mid-May, causing the ground to be bare for much of the spring season (March-May). During this time, the ground surface in maize sites absorb more solar radiation resulting in lower albedo than perennial sites.

The potential to achieve a cooling effect from higher surface reflectivity has important implications for crop production. Perennials crops with longer growing seasons can give increased albedo in early spring into very late fall seasons. This is notable as monthly variations were also strong at sites between the GS and NGS. Seasonality from plant phenology in the summer, or snow deposition in the winter changed the surface properties temporally and caused albedo to vary significantly ($p < 0.05$). Sieber et al., (2019) also showed how similar perennial biofuel crops, such as fallow, willow and forest, have low albedo during summer months and higher variable α_s during winter months. α_s is highly dependent on factors including crop height, species composition, planting density, and canopy cover, and these variables change over the course of season, depending on agronomic management practices, local geology (Bright, 2015), and the environment (Henderson-Sellers & Wilson, 1983). Winter (0.360±0.02) and summer albedos

(0.209±0.01) (Figure 4.6) align well with studies completed for both winter and summer for grassland albedos in Germany, Australia, Canada, and Switzerland, which modeled various grassland types temporally (Iziomon & Mayer, 2002). During senescence (October-November), albedo was higher due to the landscape being bare from crops being harvested after the growing season in early October. In the months of December-March, albedo was noted to be much higher when temperature is low, and snow and ice are covering much of the landscape. These results align similarly with studies completed by Chen et al., (1993, 1995), where influences in local weather conditions of solar radiation, humidity and temperature were clear indicators between different types of forested landscapes, while additional evidence from Zeri et al., (2011) and Landsberg & Sands (2011) indicated how solar irradiance can vary based on landscape dynamics (i.e., bare ground, clearcut, harvest, vegetative states) and the seasonal period over biofuel cropland (i.e., summer, winter). This result is closely mirrored in studies performed by Wang & Davison (2007) and can be linked to ecosystem and landscape dynamics, where changes in an ecosystem (i.e., biomass production: fertilization, harvesting, residue removal) can cause highly responsive variations in albedo due to climatic conditions.

Albedo of the reference forest was an important variable in my study assessment. The reference forest had an average α_s of 0.13 ± 0.049. This value was just outside of the range of 0.15–0.20 reported for deciduous forest (Bonan, 2015), but within the lower range of 0.13-0.18 for deciduous forests in northern latitudes (Sieber et al., 2019). Though the forest ecosystem is comprised of deciduous trees, conifers are also dominant within the spread of canopy at my site, and this can inherently affect the amount of radiation which reaches the ground surface and subsequently, albedo. The reference forest also had lower albedo compared to all bioenergy crops studied. This was likely because not only as the forest site untouched by agronomic practices and human disturbances throughout the year, but also due to the complex canopy layers of the forest stand throughout the summer and winter periods, masking snow cover and resulting in lower albedo compared to the other field sites. In the reference forest, albedo did not rise significantly throughout the winter season (Figure 4.4a). This was likely due to forest canopy and high solar zenith angle, which do not allow solar radiation to directly reach and warm the surface. As such, even maximum coverage of snow on the ground of a forest would only increase the surface albedo by a small amount, similar to studies done by Davidson & Wang (2004). Sciusco et al. (2020) reported also similar values in forest but slightly lower values for cropland in his study at α_s: 0.17. This may be due to the difference in methods, where albedo was derived from satellite imagery, where pixels may be misclassified as cropland or omitted due to human error and satellite resolution. Due to lower averaged albedo, noted albedo-induced GWI values were also slightly smaller than my study. Thus, inherently analyzing crop-specific and seasonal variations in albedo can help in understanding the potential climate impact of land cover change as even small albedo changes can lead to considerable RF at the field scale and quantifiable climate impacts at GWI_{100} time horizons.

RF and GWI

The RF and GWI of different crops were noted to be significantly different due to plant seasonality. This is important as potential cooling from increased albedo needs to be balanced against GHG emissions, and direct and indirect consequences for crop production. Early successional, miscanthus, sorghum and switchgrass sites had, larger cooling effects during the growing seasons (early successional: 23%; miscanthus: 66%; sorghum: 53%; switchgrass: 44%) compared to the winter. This showed that perennials provided a higher amount of cooling compared to their annual counterparts, which can be vital during summertime temperatures, where more reflected radiation was reflected back into the atmosphere instead of warming the earth's surface. Maize, and restored prairie, on the other hand, had slightly higher cooling effects during the winter (maize: 11% higher; restored prairie: 14% higher), while native grasses had a 51% higher cooling effect during the winter season. As maize showed a high cooling effect in the winter over crops of miscanthus, switchgrass and energy sorghum, this could be due to landscape dynamics and farming practices such as stover retention, which helps breaks up dense snowpacks during the non-growing season. Growing season GWI_{α} values closely resembled annual GWI_{α} values, with annual being slightly lower. This is a critical finding, as growing season GWI_{α} provided an accurate representation of what the GWI_{α} of a cropland would be annually. These results are similar to Sciusco et al. (2020) and Miller et al. (2016) who modeled changes in RFs between biofuel crops such as miscanthus and switchgrass, compared to a conversion from another site, such as forest or maize. Each result saw similar cooling effects up to -27 Wm^{-2} in the growing season. As negative RFs correspond to carbon accrual and sequestrations, these crop ecosystems suggest large climate benefits where the landscapes are actively mitigating global warming (Caiazzo, 2014). Additional biophysical differences between cropping systems during green-up and senescence may lead to further impacts. Annual row crops are known to be more resource-intensive and usually reduce soil carbon stocks (Hillier et al., 2009), while perennial crops such as switchgrass and miscanthus are known for lower fertilization needs, having high biomass yields, and having the potential to sequester additional carbon in soil (Sieber et al., 2020). These results are also seen in similar studies, as well as other types of perennial crops (Don et al., 2012; Sieber et al., 2020; Zeri et al., 2011).

Forest albedo is one of the main factors which influence local climate by moving energy fluxes between the forest and the atmosphere. Modeling the conversion of reference forest landscapes to perennial and annual bioenergy crops caused a localized cooling on an annual scale, indicated by negative GWI_{α} values annual for 2018, 2019, 2020, as well as over the entire study period (Figure 4.4, 4.5). An overall cooling effect from modeling the conversion of forest over a three-year study period for seven different bioenergy crops yielded in total an average of 5.76 Mg CO_2e ha^{-1} yr^{-1} for each crop-species. Seasonal variations in vegetation influence albedo and forest reflectance properties through canopy structure, size and species of trees, and understory vegetation. As Sieber et al. (2022) discussed, the delineation of the land reference in the calculation of GWI is debatable. Many studies use grasslands or maize as their baseline, while this study focused on the climate cooling potentials of forest. Albedo change leads to RF that persists only as long as surface properties are modified, while the RF of GHGs decays gradually after emission and may persist for decades or centuries. The use of a deciduous forest as a comparison resulted in a lower reference albedo and provided higher albedo increase under crop conversion and higher cooling. A smaller delta albedo, achieved from smaller variances in $\alpha_{crop} - \alpha_{ref}$ brings smaller GWIs, as noted in Abraha et al. (2019), while higher changes observed from converting forest to another landscape can potentially provide higher cooling, depending on the biofuel crop. When the three most common time horizons were considered, differences were larger for GWI_{20} and tended to decrease with increasing TH. The albedo effect dominated over shorter time scales, but the relative importance of albedo induced RF and GWI_{α} was observed to decrease over longer periods of time. Previous studies have shown that different landscape dynamics can cause similar impacts due to albedo and GHGs using GWP_{100} as a metric (Abraha et al., 2020; Carrer et al., 2018; Georgescu et al., 2011; Sciusco et al., 2020). Thus, monitoring changes in albedo-induced GWI could provide important cooling mitigations compared to annual cropping systems, especially in regions with high solar irradiance.

Limitations and further research

There were some limitations to this work. Firstly, the location of the study site at high latitudes, snow cover (Davidson & Wang, 2004), upwelling transmittance (Bright & Kvalevåg, 2013; Lenton & Vaughn, 2009), solar zenith angle, sun-earth distance, and cloud cover have a large impact on the surface albedo of grassland and forests. Though some small gaps existed in my data due to snow or instrument failure, all efforts were made to ensure quality measurements during the non-growing seasons. Maintaining instruments vital for measuring the energy balance and climate can be challenging, with encounters of power-loss, instrument tilt and instrument failure accounting for gaps in temporal data. Examples of observed dips in the evening soil moisture can be attributed to instrument shadow from the tower, which can also cause errors and bias in soil moisture content. Unpredictable weather, ranging from short-term clouds that can limit the amount of solar radiation incident on biofuel crops, to longer-term absences in precipitation that can affect crop vegetative states, can subsequently affect surface albedo.

A second limitation was related to the use of in-situ incoming radiation ($SW_{\downarrow}$). It is important to note that atmospheric transmittance (T_a) and radiative forcing RF are not usually available as an immediately downloadable dataset (Xu et al., 2020). While incident shortwave solar radiation at the TOA and surface can be obtained from historical satellite measurements or climate simulations, this is not the case for T_a. The amount of solar radiation upwelling shortwave radiation exiting a clear sky is usually denoted as a constant averaging 80-85% (i.e., 0.854), but in many regions, climate and weather can play a large determining factor on T_a. As T_a is usually depicted in studies as an annual mean for clear sunny skies, the use of a constant can add up to 30% bias in in accounting for additional atmospheric absorption of $Sw_{\downarrow}$, which can affect Δ_{α} at the surface. Reducing the amount of error in calculations of albedo and radiative forcing is imperative in mitigating changes in climate warming (Chen et al., 2021; Sciusco et al., 2020).

Thirdly, this study focused on the effect of the change of albedo and RF on GWI, but it did not consider other effects that also impact global warming potentials. Other factors include latent and sensible heat, outgoing longwave radiation, surface roughness, agronomic practices such as fertilization and plant management, and plant dynamics that can affect evapotranspiration, soil moisture retention and plant canopy growth. These factors control fluxes of energy, water and aerodynamic movement between the surface and the atmosphere, which subsequently influence climate on local to global scales (Pielke et al., 1998). Hence, there is still a need to account for these factors in a comprehensive manner.

Finally, despite advances in recent research, changes in climate from albedo and radiative forcing relative to carbon dioxide equivalents is not yet comprehensively studied. Results, literature and even the IPCC all agree that effects from radiative forcing due to changes in the landscape may either cool or warm the landscape due to changes in spatial and temporal albedo. Understanding the potential magnitudes of the irradiance can help develop accurate calculations of albedo in future modeling and climate assessments of bioenergy.

Conclusion

This study quantified the differences of albedo to determine albedo-induced GWI in order to understand the potential magnitude of the albedo influence and its effect in future modeling assessments of bioenergy landscapes. When surface reflectivity is maximized, bioenergy systems can have a localized cooling effect when forest is potentially converted to a bioenergy crop. As albedo controls the surface energy balance, even a small change in albedo could significantly impact the physical climate system and its influences on climate and weather. This study inherently shows that surface albedo changes are known to vary with ecosystem dynamics, including the response of vegetation growth to climate change. This can be used to guide mitigation efforts through land cover management (Carrer et al., 2018) or direct modeling efforts in LCA to provide a substantial contribution to the climate impact in relation to GHG emissions (Betts, 2001). The impacts for bioenergy are higher for short-term horizons, and tend to considerably decrease over time, but most modeling endeavors assume that the landscape will not change drastically in order to maximize cooling benefits. Further research is needed to integrate climatic effects of land use on different spatial and temporal scales.

APPENDIX

Table A8: Summary of bioenergy crops used within the study, as well as their abbreviation, ID, and species composition.

Crop	**Abr**	**ID**	**Species**	**Assessment**
Maize	MAI	G1	*Zea mays L.*	Monoculture annual row crop member of the grass family Poaceae
Sorghum	SOR	G2	*Photoperiod insensitive hybrid TAM 17900 variety*	Monoculture annual row crop variety for continuous improvement of yield and adaptation
Switchgrass	SW	G5	*Panicum virgatum L.*	Monoculture perennial Cave-n-Rock perennial variety, consisting of "warm season" (C4) native grass
Miscanthus	MIS	G6	*Miscanthus x giganteus*	Monoculture perennial sterile hybrid crossed between two grasses (*Miscanthus sinensis* and *Miscanthus sacchariflorus*
Native Grasses	NG	G7	A mix of species	Polyculture perennial consisting of Little Bluestem (Schizachyrium scoparium), Big Bluestem (Andropogon gerardii), Indiangrass (Sorghastrum nutans) and Cordgrass (Spartina pectinata)
Early Successional	ES	G9	A mix of species	Polyculture perennial comprised of grasses and forbs which grow naturally following land removed from agriculture use
Restored Prairie	PR	G10	A mix of species	Polyculture perennial North American tallgrass prairie composed of a diverse mix of "cool season" (C3) and "warm season" (C4) plant species

REFERENCES

REFERENCES

Abraha, M., Gelfand, I., Hamilton, S. K., Shao, C., Su, Y. J., Robertson, G. P., & Chen, J. (2016). Ecosystem water-use efficiency of annual corn and perennial grasslands: contributions from land-use history and species composition. *Ecosystems*, *19*(6), 1001-1012. https://doi.org/10.1007/s10021-016-9981-2

Abraha, M., Gelfand, I., Hamilton, S. K., Chen, J., & Robertson, G. P. (2019). Carbon debt of field-scale conservation reserve program grasslands converted to annual and perennial bioenergy crops. *Environmental Research Letters*. https://doi.org/10.1088/1748-9326/aafc10

Akbari, H., Menon, S., & Rosenfeld, A. (2009). Global cooling: increasing world-wide urban albedos to offset CO_2. *Climatic Change*, *94*(3), 275-286. https://doi.org/10.1007/s10584-008-9515-9

Betts, R. A. (2001). Biogeophysical impacts of land use on present-day climate: Near-surface temperature change and radiative forcing. *Atmospheric Science Letters*, 2(1-4), 39-51.

Betts, A. K., Desjardins, R. L., & Worth, D. (2007). Impact of agriculture, forest and cloud feedback on the surface energy budget in BOREAS. *Agricultural and Forest Meteorology*, *142*(2-4), 156-169. https://doi.org/10.1016/j.agrformet.2006.08.020

Blumthaler, M., & Ambach, W. (1988). Solar UVB-albedo of various surfaces. *Photochemistry and Photobiology, 48*(1), 85-88. https://doi.org/10.1111/j.1751-1097.1988.tb02790.x

Bonan, G. (2015). *Ecological Climatology: Concepts and Applications*. Third Edition, Cambridge University Press Cambridge, United Kingdom and Sheridan Books, Inc., USA.

Boussaada, Z., Curea, O., Remaci, A., Camblong, H., & Mrabet Bellaaj, N. (2018). A nonlinear autoregressive exogenous (NARX) neural network model for the prediction of the daily direct solar radiation. *Energies*, *11*(3), 620. https://doi.org/10.3390/en11030620

Bright, R. M., Strømman, A. H., & Peters, G. P. (2011). Radiative forcing impacts of boreal forest biofuels: A scenario study for Norway in light of albedo. *Environmental Science & Technology*, *45*(17), 7570–7580. https://doi.org/10.1021/es201746b

Bright, R. M., Cherubini, F., & Strømman, A. H. (2012). Climate impacts of bioenergy: Inclusion of carbon cycle and albedo dynamics in life cycle impact assessment. *Environmental Impact Assessment Review*, *37*, 2-11.

Bright, R. M., & Kvalevåg, M. M. (2013). Technical Note: Evaluating a simple parameterization of radiative shortwave forcing from surface albedo change. *Atmospheric Chemistry and Physics*, *13*(22), 11169–11174. https://doi.org/10.5194/acp-13-11169-2013

Bright, R. M., Zhao, K., Jackson, R. B., & Cherubini, F. (2015). Quantifying surface albedo and other direct biogeophysical climate forcings of forestry activities. *Global Change Biology*, *21*(9), 3246–3266. https://doi.org/10.1111/gcb.12951

Bright, R. M. (2015). Metrics for biogeophysical climate forcings from land use and land cover changes and their inclusion in life cycle assessment: A critical review. *Environmental Science & Technology*, *49*(6), 3291–3303. https://doi.org/10.1021/es505465t

Burakowski, E., Tawfik, A., Ouimette, A., Lepine, L., Novick, K., Ollinger, S. ... & Bonan, G. (2018). The role of surface roughness, albedo, and Bowen ratio on ecosystem energy balance in the Eastern United States. *Agricultural and Forest Meteorology*, *249*, 367-376. https://doi.org/10.1016/j.agrformet.2017.11.030

Cai, H., Wang, J., Feng, Y., Wang, M., Qin, Z., & Dunn, J. B. (2016). Consideration of land use change-induced surface albedo effects in life-cycle analysis of biofuels. *Energy & Environmental Science*, *9*(9), 2855-2867. DOI: 10.1039/C6EE01728B

Caiazzo, F., Malina, R., Staples, M. D., Wolfe, P. J., Yim, S. H. L., & Barrett, S. R. H. (2014). Quantifying the climate impacts of albedo changes due to biofuel production: A comparison with biogeochemical effects. *Environmental Research Letters*, *9*(2), 024015. https://doi.org/10.1088/1748-9326/9/2/024015

Campbell, G. S., & Norman, J. (2012). Radiation Fluxes in Natural Environments. In *An Introduction to Environmental Biophysics*; Eds. 2; Springer-Verlag: New York, USA, pp. 167–184.

Carrer, D., Pique, G., Ferlicoq, M., Ceamanos, X., & Ceschia, E. (2018). What is the potential of cropland albedo management in the fight against global warming? A case study based on the use of cover crops. *Environmental Research Letters*, *13*(4), 044030. https://doi.org/10.1088/1748-9326/aab650

Cherubini, F., Peters, G. P., Berntsen, T., Strømman, A. H., & Hertwich, E. (2011). CO2 emissions from biomass combustion for bioenergy: Atmospheric decay and contribution to global warming. *Global Change Biology: Bioenergy*, *3*(5), 413-426. https://doi.org/10.1111/j.1757-1707.2011.01102.x

Cherubini, F., Bright, R. M., & Strømman, A. H. (2012). Site-specific global warming potentials of biogenic CO_2 for bioenergy: contributions from carbon fluxes and albedo dynamics. *Environmental Research Letters*, *7*(4), 045902. https://doi.org/10.1088/1748-9326/7/4/045902

Chen, J., Franklin, J. F., & Spies, T. A. (1993). Contrasting microclimates among clearcut, edge, and interior of old-growth Douglas-fir forest. *Agricultural and Forest Meteorology*, *63*(3-4), 219-237. https://doi.org/10.1016/0168-1923(93)90061-L

Chen, J., Franklin, J. F., & Spies, T. A. (1995). Growing-season microclimatic gradients from clearcut edges into old-growth Douglas-fir forests. *Ecological Applications*, *5*(1), 74-86. https://doi.org/10.2307/1942053

Chen, J., Brosofske, K., Noormets, A. (2004). A working framework for quantifying carbon sequestration in disturbed land mosaics. *Environmental Management*, *33*, S210–S221. https://doi.org/10.1007/s00267-003-9131-4

Chen, J., Lei, C., Sciusco, P. (2021). Modeling ecosystem global warming potentials. Chapter 5 in *Biophysical Models and Applications in Ecosystem Analysis*. East Lansing: Michigan State University Press. muse.jhu.edu/book/82816

Crum, J.R., & Collins, H.P. (1995). KBS Soils. Zenodo. http://doi.org/10.5281/zenodo.2581504

Cunnington, W. M., & Rowntree, P. R. (1986). Simulations of the Saharan atmosphere—dependence on moisture and albedo. *Quarterly Journal of the Royal Meteorological Society*, *112*(474), 971-999. https://doi.org/10.1002/qj.49711247405

Davin, E. L., Seneviratne, S. I., Ciais, P., Olioso, A., & Wang, T. (2014). Preferential cooling of hot extremes from cropland albedo management. *Proceedings of the National Academy of Sciences*, 201317323.

Davidson, A., & Wang, S. (2004). The effects of sampling resolution on the surface albedos of dominant land cover types in the North American boreal region. *Remote Sensing of Environment*, *93*(1-2), 211-224.

Don, A., Osborne, B., Hastings, A., Skiba, U., Carter, M. S., Drewer, J. ... & Zenone, T. (2012). Land-use change to bioenergy production in Europe: implications for the greenhouse gas balance and soil carbon. *Global Change Biology: Bioenergy*, *4*(4), 372-391. https://doi.org/10.1111/j.1757-1707.2011.01116.x

Forster, P., Ramaswamy, V., Artaxo, P., Berntsen, T., Betts, R., Fahey, D. W. ... & Van Dorland, R. (2007). Changes in atmospheric constituents and in radiative forcing. In *Climate change 2007. The Physical Science Basis*. Broadway, Cambridge University Press, Cambridge, United Kingdom and Boulder, CO, USA. http://www.ipcc.ch/pdf/assessment-report/ar4/wg1/ar4-wg1-chapter2.pdf

Fu, B., Li, B., Gasser, T., Tao, S., Ciais, P., Piao, S. ... & Xu, J. (2021). The contributions of individual countries and regions to the global radiative forcing. *Proceedings of the National Academy of Sciences*, *118*(15). https://doi.org/10.1073/pnas.2018211118

Georgescu, M., Lobell, D. B., & Field, C. B. (2011). Direct climate effects of perennial bioenergy crops in the United States. *Proceedings of the National Academy of Sciences*, *108*(11), 4307-4312. https://doi.org/10.1073/pnas.1008779108

Heaton, E. A., Dohleman, F. G., & Long, S. P. (2008). Meeting US biofuel goals with less land: the potential of Miscanthus. *Global Change Biology*, *14*(9), 2000-2014. https://doi.org/10.1111/j.1365-2486.2008.01662.x

Henderson-Sellers, A. (1980). Albedo changes—surface surveillance from satellites. *Climatic Change*, *2*(3), 275-281. https://doi.org/10.1007/BF00137991

Henderson-Sellers, A., & Hughes, N. A. (1982). Albedo and its importance in climate theory. *Progress in Physical Geography*, *6*(1), 1-44. https://doi.org/10.1177%2F030913338200600101

Henderson-Sellers, A., & Wilson, M. (1983). Surface albedo data for climatic modeling. *Reviews of Geophysics*, *21*(8), 1743–1778. https://doi.org/10.1029/RG021i008p01743

Hillier, J., Whittaker, C., Dailey, G., Aylott, M., Casella, E., Richter, G. M. ... & Smith, P. (2009). Greenhouse gas emissions from four bioenergy crops in England and Wales: integrating spatial estimates of yield and soil carbon balance in life cycle analyses. *Global Change Biology: Bioenergy*, *1*(4), 267-281. https://doi.org/10.1111/j.1757-1707.2009.01021.x

Ingram, W. J., Wilson, C. A., & Mitchell, J. F. B. (1989). Modeling climate change: An assessment of sea ice and surface albedo feedbacks. *Journal of Geophysical Research: Atmospheres*, *94*(D6), 8609-8622. https://doi.org/10.1029/JD094iD06p08609

Iziomon, M. G., & Mayer, H. (2002). On the variability and modelling of surface albedo and long-wave radiation components. *Agricultural and Forest Meteorology*, *111*(2), 141-152.

Joos, F., Roth, R., Fuglestvedt, J. S., Peters, G. P., Enting, I. G., Bloh, W. V. ... & Weaver, A. J. (2013). Carbon dioxide and climate impulse response functions for the computation of greenhouse gas metrics: a multi-model analysis. *Atmospheric Chemistry and Physics*, *13*(5), 2793-2825. https://doi.org/10.5194/acp-13-2793-2013

Kaye, J. P., & Quemada, M. (2017). Using cover crops to mitigate and adapt to climate change. A review. *Agronomy for Sustainable Development*, *37*(1), 4. https://doi.org/10.1007/s13593-016-0410-x

Landsberg, J., & Sands, P. (2011). *Physiological Ecology of Forest Production: Principles, Processes and Models* (Vol. 4). London: Elsevier/Academic Press. https://doi.org/10.1093/treephys/tpr062

Lei, C., Abraha, M., Chen, J., & Su, Y. J. (2021). Long-term variability of root production in bioenergy crops from ingrowth core measurements. *Journal of Plant Ecology*, *14*(5), 757-770. https://doi.org/10.1093/jpe/rtab018

Lenton, T. M., & Vaughan, N. E. (2009). The radiative forcing potential of different climate geoengineering options. *Atmospheric Chemistry and Physics, 9*(15), 5539-5561. https://doi.org/10.5194/acp-9-5539-2009

Lobell, D. B., & Field, C. B. (2007). Global scale climate–crop yield relationships and the impacts of recent warming. *Environmental Research Letters*, *2*(1), 014002. https://doi.org/10.1088/1748-9326/2/1/014002

Luyssaert, S., Jammet, M., Stoy, P. C., Estel, S., Pongratz, J., Ceschia, E. ... & Gielen, B. (2014). Land management and land-cover change have impacts of similar magnitude on surface temperature. *Nature Climate Change*, *4*(5), 389–393. https://doi.org/10.1038/nclimate2196

Miller, J. N., VanLoocke, A., Gomez-Casanovas, N., & Bernacchi, C. J. (2016). Candidate perennial bioenergy grasses have a higher albedo than annual row crops. *Global Change Biology: Bioenergy*, *8*(4), 818-825. https://doi.org/10.1111/gcbb.12291

Muñoz, I., Campra, P., & Fernández-Alba, A. R. (2010). Including CO_2 emission equivalence of changes in land surface albedo in life cycle assessment. Methodology and case study on greenhouse agriculture. *The International Journal of Life Cycle Assessment*, *15*(7), 672-681. https://doi.org/10.1007/s11367-010-0202-5

Muñoz, J. D., Kravchenko, A. (2011). Soil carbon mapping using on-the-go near infrared spectroscopy, topography and aerial photographs. *Geoderma*, *166*, 102–110.

NOAA. (2005). ESRL Global Monitoring Laboratory - Global Radiation and Aerosols. Earth System Research Laboratories Global Monitoring Laboratory. https://gml.noaa.gov/grad/solcalc/

NCDC (National Climate Data Center). (2013). Summary of Monthly Normal 1981–2010 (MI, USA: Gull Lake Biology Station) (www.ncdc.noaa.gov/cdo-web/search)

Ollinger, S. V., Richardson, A. D., Martin, M. E., Hollinger, D. Y., Frolking, S. E., Reich, P. B., ... Smith, M. L. (2008). Canopy nitrogen, carbon assimilation, and albedo in temperate and boreal forests: Functional relations and potential climate feedbacks. *Proceedings of the National Academy of Sciences*, *105*(49), 19336-19341. https://doi.org/10.1073/pnas.0810021105

Pielke, R. A., Avissar, R., Raupach, M., Dolman, A. J., Zeng, X., & Denning, A. S. (1998). Interactions between the atmosphere and terrestrial ecosystems: influence on weather and climate. *Global Change Biology*, *4*(5), 461-475. https://doi.org/10.1046/j.1365-2486.1998.t01-1-00176.x

Pirazzini, R. (2004). Surface albedo measurements over Antarctic sites in summer. Journal of Geophysical Research: Atmospheres, *109*(D20). https://doi.org/10.1029/2004JD004617

Raupach, M. R. (1994). Simplified expressions for vegetation roughness length and zero-plane displacement as functions of canopy height and area index. *Boundary-Layer Meteorology*, *71*(1), 211-216. https://doi.org/10.1007/BF00709229

R Development Team. (2013). *R foundation for statistical computing*. Vienna, Austria, 3(0).

Robertson, G. P., Dale, V. H., Doering, O. C., Hamburg, S. P., Melillo, J. M., Wander, M. M., ... & Duke, C. S. (2008). Sustainable biofuels redux. *Science*, *322*(5898), 49-50.

Robertson, G. P., Hamilton, S. K., Del Grosso, S. J., & Parton, W. J. (2011). The biogeochemistry of bioenergy landscapes: Carbon, nitrogen, and water considerations. *Ecological Applications*, *21*(4), 1055-1067. https://doi.org/10.1890/09-0456.1

Robertson, G. P., Hamilton, S. K., Barham, B. L., Dale, B. E., Izaurralde, R. C., Jackson, R. D., ... & Tiedje, J. M. (2017). Cellulosic biofuel contributions to a sustainable energy future: Choices and outcomes. *Science*, *356*(6345), http://dx.doi.org/10.1126/science.aal2324

Russel, H.N. (1916). On the albedo of the planets and their satellites. *Proceedings of the National Academy of Sciences*, *2*(2), 74-77. https://doi.org/10.1073/pnas.2.2.7

Sanjuán, M. Á., Morales, Á., & Zaragoza, A. (2021). Effect of precast concrete pavement albedo on the climate change mitigation in Spain. *Sustainability*, *13*(20), 11448. https://doi.org/10.3390/su132011448

Schaeffer, M., Eickhout, B., Hoogwijk, M., Strengers, B., Van Vuuren, D., Leemans, R., & Opsteegh, T. (2006). CO2 and albedo climate impacts of extratropical carbon and biomass plantations. *Global Biogeochemical Cycles*, *20*(2). https://doi.org/10.1029/2005GB002581

Sciusco, P., Chen, J., Abraha, M., Lei, C., Robertson, G. P., Lafortezza, R. ... & John, R. (2020). Spatiotemporal variations of albedo in managed agricultural landscapes: inferences to global warming impacts (GWI). *Landscape Ecology*, *35*(6), 1385-1402. https://doi.org/10.1007/s10980-020-01022-8

Shine, K. P., Derwent, R. G., Wuebbles, D. J., & Morcrette, J. J. (1990). Radiative forcing of climate. *Climate change: The IPCC Scientific Assessment*, 41-68. https://core.ac.uk/download/pdf/42811043.pdf

Sieber, P., Ericsson, N., Hammar, T., & Hansson, P. A. (2022). Albedo impacts of current agricultural land use: Crop-specific albedo from MODIS data and inclusion in LCA of crop production. *Science of the Total Environment*, 835, 155455. https://doi.org/10.1016/j.scitotenv.2022.155455

Sieber, P., Ericsson, N., Hammar, T., & Hansson, P. A. (2020). Including albedo in time-dependent LCA of bioenergy. *Global Change Biology: Bioenergy*, *12*(6), 410-425. https://doi.org/10.1111/gcbb.12682

Sieber, P., Ericsson, N., & Hansson, P. A. (2019). Climate impact of surface albedo change in Life Cycle Assessment: Implications of site and time dependence. *Environmental Impact Assessment Review*, *77*, 191-200. https://doi.org/10.1016/j.eiar.2019.04.003

Smith, P., Clark, H., Dong, H., Elsiddig, E.A., Haberl, H., Harper, R., House, J., Jafari, M., et al. (2014). Chapter 11 - Agriculture, forestry and other land use (AFOLU). In: *Climate Change 2014: Mitigation of Climate Change.* IPCC Working Group III Contribution to AR5. Cambridge University Press, Cambridge, United Kingdom. https://pure.iiasa.ac.at/id/eprint/11115/

Tilman, D., Hill, J., & Lehman, C. (2006). Carbon-negative biofuels from low-input high-diversity grassland biomass. *Science*, *314*(5805), 1598-1600. https://doi.org/10.1126/science.1133306

Thoen, G. F. (1990). *Soil Survey of Barry County, Michigan*. (USDA Soil Conservation Service, Michigan Agricultural Experiment Station, and Michigan Technological University, Washington DC), pp. 187, 286.

Wang, S., & Davidson, A. (2007). Impact of climate variations on surface albedo of a temperate grassland. *Agricultural and Forest Meteorology*, *142*(2-4), 133-142. https://doi.org/10.1016/j.agrformet.2006.03.027

Williams, M. (1992). *Americans and Their Forests: A Historical Geography*. Cambridge University Press, Cambridge, United Kingdom and New York, NY, USA.

Xu, X., Swei, O., Xu, L., Schlosser, C. A., Gregory, J., & Kirchain, R. (2020). Quantifying location-specific impacts of pavement albedo on radiative forcing using an Analytical approach. *Environmental science & Technology*, *54*(4), 2411-2421. https://doi.org/10.1021/acs.est.9b04556

Zeri, M., Anderson-Teixeira, K., Hickman, G., Masters, M., DeLucia, E., & Bernacchi, C. J. (2011). Carbon exchange by establishing biofuel crops in Central Illinois. *Agriculture, Ecosystems & Environment*, *144*(1), 319-329. https://doi.org/10.1016/j.agee.2011.09.006

CHAPTER 5. CONCLUSIONS

This dissertation offers a collection of works that focus on different aspects of bioenergy crops, using multiple types of scientific observations and modeling, in order to increase understand of surface induced albedo and global warming impacts on the landscape.

Major Discoveries

This study outlined potential land management strategies which can be combined with continued climate modeling in order to fully guide future climate science. Perennial grasses are not only a way to increase ecosystem diversity, but provide a sustainable form of climate mitigation, and are proven against droughts and temperature swings to provide greater carbon sequestration and reflect more radiation back into the atmosphere. The use of continuous climate measurements to instantaneous field measurements gathered from the Kellogg Biological Station Biofuel Cropping System over three years identified gaps on how surface reflectivity on biofuel crops can lead to warming or cooling of the climate. My study investigated how land use change affects surface reflectivity and subsequently climate cooling potential of biofuel ecosystems and showed that albedo is highly dependent on landscape and climate. Several modeling studies have been completed within the last decade to analyze the climate impact of altering albedo between perennial and annual croplands in certain landscapes (Davis et al., 2009; Georgescu et al., 2009; Miller et al., 2014; Sciusco et al., 2020, 2022), which have successfully noted conversions from annual cropland and forest to bioenergy crops resulting in a cooling effect upon the landscape.

Major findings in Chapter 2 revealed that observation-based continuous measurements of albedo are an invaluable tool in order to calculate and improve climate models and understanding how land use and land cover affects albedo and climate cooling. Findings also uncovered that lower albedo observed during the summer months and higher during winter months is highly dependent on factors including crop height, species composition, planting density, and canopy cover, and these variables change over the course of season, depending on agronomic management practices, local geology, climate and the environment dynamics. Vegetation was found to affect albedo by reducing the amount of solar radiation that is absorbed by the surface. Local weather conditions of solar radiation, humidity and temperature were also clear indicators temporally. This is important as reflectance can be highly beneficial in regions where plant phenology changes from large green leaves in early summer, to brown landscapes in late fall. Thus, as the landscape changes in the winter to summer, albedo can have a significant effect on global warming/cooling.

Major discoveries in Chapter 3 identified correlations between albedo and vegetation dynamics where temporal variability occurs due to changes in vegetation during the growing season. These responses by different vegetation to changes in climate as well as agronomic practices could affect seasonal and inter-annual albedo differently. Positive impacts of reducing the amount of fertilizer input needed for sustainable agricultural management were also found. This can be beneficial when looking to the future for expanding biofuel croplands into marginal regions: sites where the agricultural land has been abandoned, is not being used to its full potential, is degraded from soil erosion or flooding, or is on a drought-prone region. As perennials here in this study can succeed without large effects of fertilizer, planting perennials on marginal lands would avoid competition with regions in the Midwest being used for food growth, while still providing sustainable ecosystem services. As many of the study's biofuel crops are native to the Midwest, crops such as switchgrass, restored prairie and native grasses have shown great promise at suitability for large-scale cultivation within the United States, most importantly- with or without irrigation.

Major findings in Chapter 4 indicate that accurately measuring albedo at the ground surface can provide a means of calculating the energy transfer between the ground, biofuel crop and atmosphere, in order to determine high cooling potentials for different types of bioenergy ecosystems. Although much research on potential climate cooling have focused on only switchgrass and maize, the inclusion of climate modeling for native species (i.e., switchgrass, native grasses, restored prairie), genetically modified perennials (e.g., miscanthus), forest conversion in different stages (e.g., old growth forest, early successional), and other types of annual row crops (e.g., maize, sorghum) will provide a breakthrough in the current research on the dynamics of climate mitigation from other types of sustainable biofuel ecosystems.

Future Research

Calculations in recent years have been become significantly improved using in-situ measurements, satellite measurements including Advanced Very High-Resolution Radiometer (AVHRR) and Moderate Resolution Imaging Spectroradiometer (MODIS) (Carrer et al., 2014; Schaaf et al., 2002), drone measurements, and statistical analyses which relate albedo to climate warming metrics such as global warming impact (GWI) (Bright, 2015; O'Hare et al., 2009). However, more comprehensive assessments (e.g., drone, low aircraft, broadening the application of micrometeorological towers) are needed to fully understand and integrate albedo into modeling, policy, and land management policies.

The improved integration of surface albedo data into climate modeling products is necessary for better predictive power and complexity. In order to provide a more accurate illustration of the full impacts of surface-induced albedo on climate cooling, the social components need to be fully adopted. As part on ongoing research, the dissemination of information to farmers, the public, and the scientific community is necessary to fully realize the benefits of planting bioenergy crops sustainably and productively.